ALPHA FOUNDATION FOR THE IMPROVEMENT OF MINE SAFETY AND HEALTH

Final Technical Report

Project Title: The effect of coal and mine respirable dust size on lung cells and exposure assessment
Grant Number: AFC820-43, Alpha Foundation on Projects in Mining Safety and Health Research AFC820

Organization: Colorado State University 9/1/2019 - 11/6/2020
University of California Los Angeles 9/1/2021 – 8/31/2023

Principal Investigator: Dr. Su-Jung (Candace) Tsai, Associate Professor
Contact Information:
Organization Name: University of California Los Angeles
Department: Environmental Health Sciences
Mailing Address: 650 Charles E. Young Drive S., MC 177220
Los Angeles, California 90095-1735
Phone: 310-206-5296 (Department Office); 310-206-9258 (Tsai)
PI Email: candacetsai@ucla.edu

Period of Performance: 9/1/2019 - 08/31/2023

Co-PI: Dr. Jared Brown, Professor of Toxicology, University of Colorado Anschutz Medical Campus
Co-PI: Dr. Jürgen Brune, Professor, Colorado School of Mines

Acknowledgement/Disclaimer: Final Report must include the following disclaimer language: "This study was sponsored by the Alpha Foundation for the Improvement of Mine Safety and Health, Inc. (ALPHA FOUNDATION). The views, opinions and recommendations expressed herein are solely those of the authors and do not imply any endorsement by the ALPHA FOUNDATION, its Directors and staff."

Table of Contents

1.0 Executive Summary

Problem Statement: Exposure to mine dusts has been recognized as a hazard for decades, and studies have shown that exposure can exceed permissible exposure limits (PEL) in some underground tasks (Glover and Cram 1997, Tomb, Peluso et al. 1998, Naidoo, Seixas et al. 2006, (NIOSH) 2011, Grove, Van Dyk et al. 2014). Inhalation of fine airborne dust particles, such as coal or silica dust, can cause various types of occupational lung disease, including coal workers' pneumoconiosis (CWP), progressive massive fibrosis (PMF), chronic obstructive pulmonary disease (COPD) and silicosis. Submicrometer particles have been reported in the mining environment since the 1950s (Brown, Cook et al. 1950), and the general dangers of exposure to small dust particles were known even earlier (Drinker and Hatch 1936). Modern mining uses larger and more powerful mining equipment, which is more efficient and increases the volume and speed of coal loading and transportation and thus increases the productivity of coal mine extraction. However, an increased amount of total dust is generated from highly productive equipment, and the dust can contain a high proportion of very small particles. The coal mining process, which includes roof bolting, continuous mining, rock dusting, shuttle car driving, bracing and other activities, creates and *exposes miners to a mixture of small particles of respirable size*.

Coal dust of submicron size or smaller is constantly generated and inhaled by miners during normal operations at the face area, along with billions of other particles. These very small particles are deposited in the respiratory tract system, specifically in the alveoli region (ICRP 1994), and have much larger surface area per unit volume than larger-sized particles, thus leading to much more biologically active (toxic) interactions (ICRP 1994, Oberdorster, Maynard et al. 2005, Elsaesser and Howard 2012). The prevalence of PMF reached historic lows in the 1990s, but a new outbreak has occurred in recent years, with a sharp increase in 2015-2016 (Blackley, Crum et al. 2016). A report published by the National Academies in 2018 clearly stated the concerns regarding exposure to submicrometer and micrometer particles in the mining environment, along with the need to investigate and evaluate in a timely manner those particles associated with coal production, rock dust use and diesel engine emissions (National Academies 2018). These submicrometer- and nanometer-sized particles are greatly underestimated with regard to miner exposure due to their very low mass and inability to be measured using the traditional gravimetric method. This issue represents a potentially serious but largely unstudied exposure risk in the mining environment.

Research Approach: We characterized a range of micrometer- to nanometer-sized coal and rock dust gathered from working coal mines using a different metric, particle number count, in addition to mass. We studied toxicity markers indicative of pulmonary disease development for fractions of coal and rock dust of different sizes, including particles in the nano-size range (less than 100 nm). For toxicity assessments, we originally proposed primary human bronchial epithelial cells cultured at the air-liquid interface as a 3D cell model representing both the structural and functional aspects of human lung airways. Due to unexpected challenges in operating aerosol exposure in a stable concentration and obtaining exposed dosage scientifically, we have revised to use 2D cell models with aerosol characterizations to study relevant toxicity endpoints including cytotoxicity, oxidative stress, inflammation, cellular uptake of particles and dose dependency of the effects associated with the different fractionated particle sizes. For

dust preparation and evaluation, we used coal dust bulk materials from an underground coal mine and rock dust to prepare size-fractionated dust samples for the cellular studies. Coal and rock dust were also characterized, measured and collected on-site at an underground coal mine to evaluate exposure levels and dust constituents in order to correlate exposure levels with the *in vitro* cell studies. We will use two types of sampling techniques including 1) methods available for regulatory compliance such as the personal dust monitor (PDM) and other dust sampling, and 2) nanoparticle sampling methods capable of analyzing submicrometer (including nanometer) and micrometer particles using electron microscopy following collection.

Accomplishments and Expected Impact on Mining Health and Safety: At completion of this work, we provide new information on the most harmful particle sizes within the respirable size range, such as those less than 100 nm or 500 nm. We are able to correlate the cellular response effect with dust concentration and size. Based on various endpoints, our data suggest that major factors such as dust concentration and size are important considerations in that induce relevant pulmonary diseases such as CWP, as well as other chronic obstructive pulmonary diseases, including asthma and silicosis. In addition, our assessment of airborne coal and rock dust released from practical operations on-site at an underground coal mine provide novel information on very small-sized particles (including those of nanometer size), such as typical concentrations and elemental composition. Using the results from our on-site assessments, coal/rock dust characterization and the dose-response effect data, we suggest appropriate methods should consider particle size and number measurement and analyzing physio-chemical properties of exposed particles for measuring the most harmful portions of respirable coal/rock dust and reducing miner exposure to this toxic dust. Our results also provide data based on endpoints and dose response to aid in future work for estimating no-observed-adverse-effect-level (NOAEL) and lowest-observed-adverse-effect-level (LOAEL) values for exposure to the small-sized dust portion. The generated knowledge concerning hazardous levels of exposure, particularly for nanometer-sized particles, can be used to protect miners and reduce the prevalence of respiratory disease in this population.

2.0 Problem Statement and Objective

Focus Area and Problem Statement: This project falls under the focus area of Injury and Disease Exposure and Risk Factors, with especial relevance for item C, "Respiratory Disease: Understand the reasons for elevated occurrence of CWP and other chronic obstructive pulmonary disease, including asthma, and silicosis in miners and develop prevention measures to mitigate them". One in ten underground coal miners who have worked in mines for at least 25 years were identified as having black lung according to a recent report published by NIOSH[1]. It has been recognized in the mining industry that an increased amount of dust and various dust components are generated by modern mining equipment. Billions of submicron- or smaller-sized coal dust particles and other dust types such as rock dust are generated and constantly inhaled by miners during the production process. These very small particles have a much larger surface area per unit volume and are much more biologically active (toxic) than their larger counterparts. The recent and unexpected increase in new cases of severe coal mine dust disease could be associated with exposure to a large number of submicrometer and nanometer sized particles with a low mass. Therefore, there is an urgent need to understand exposure to these very small particles in the mining industry, including the characteristics and biological effects that may significantly contribute to lung disease.

Justification and Relevance to the Alpha Foundation Mission: This project investigated the characteristics of respirable particles including the portion of coal dust in the submicrometer-to-nanometer size range in order to address whether these smaller-size particles are contributing to the aggressive development of miners' lung diseases. Under current mine operation restrictions, a study evaluating actual exposures in an underground mine at the production area such as face area is nearly impossible due to the many challenges and limitations of such an effort, including the difficulty of gaining access to mine workers, equipment use approval, as well as substantial variation in mining operations and geographic factors. To study exposure and effect, these challenges can be addressed by conducting a laboratory exposure study and performing measurements in various locations of a coal mine, such as the belt area, to generate correlations with the exposure assessment using cell models, as described below. To study the physical characteristics and health effects of coal and rock dust, we utilized two high relevant 2D cell models (primary human bronchial epithelial cells and human macrophages) to determine the effects of exposure to these submicron-sized particles. At the completion of this research, our results provide important scientific conclusions for determining the severity of exposure to submicron-sized dust particles and generate evidence supporting the necessary regulatory changes for monitoring submicron- or nanometer-sized particles for mine worker protection.

Significance: Exposure to respirable coal mine dust (RCMD) containing particles less than 2.5 μm in aerodynamic diameter has been found to be more harmful to the respiratory tract than the larger-sized portion of RCMD and may increase miners' risk for cardiovascular disease. Our research focus on the small-size portion of RCMD, including a comparison of submicron- and nanometer-sized particles to the

[1] https://www.cdc.gov/niosh/updates/upd-07-20-18.html

larger respirable particles, with the ultimate goal of improving miner exposure monitoring and mine safety as well as understanding the mechanisms of toxicity and identifying biomarkers of exposure. Our results address important outstanding scientific questions as to whether the very high numbers of submicron- or nanometer-sized particles in coal dust and rock dust generated from mining operations represent a major problem contributing to the development of pulmonary diseases. More importantly, the dose-response effect of various endpoints is presented using a different metric, particle number concentration, in addition to mass concentration. The current gravimetric measurement method and determinations of the mass of exposed dust are not sufficient and cannot determine the exposure quantity of particles smaller than a few micrometers in size. Our results confirm the importance of characterizing miners' exposure to dust from a different perspective: the size, composition and number concentration of particles. Using these outcomes, we suggest methods to address the pulmonary effects, as well as to increase protection for miners and develop controls to reduce exposure to these small particles.

Project Goals and Specific Aims:

Aim 1: Determine the major factors, including coal/rock particle sizes, that contribute to pulmonary disease using an *in-vitro* cell model.
This aim was achieved by examining the effects of fractionated coal/rock particles on lung cell models to predict toxicity. We examined particle deposition, cytotoxicity, oxidative stress and inflammatory responses across several exposure variables including particle type, size, shape, constituents and concentration.

Aim 2: Estimate a safer level of mine dust exposure to reduce the prevalence of respiratory diseases among miners and suggest improved measurement methods.
This aim was achieved through 1) the evaluation of airborne coal and rock dust on-site at an underground coal mine, 2) detailed characterizations of coal and rock dust from on-site sampling and laboratory processing of the bulk dust, and 3) analysis of corresponding dose-response effects of the characterized dust.

Objectives:

1. To correlate the size and concentration of coal/rock particles with cellular responses in human bronchial epithelial cell culture models.
2. To begin identifying particle size-dependent mechanisms and biomarkers that could be used to predict adverse outcomes in coal mine workers.
3. To suggest a safer level of mine dust exposure based on particle size in order to reduce the prevalence of respiratory diseases.

3.0 Research Approach

This proposed research will determine whether the small (nano-) size fraction of coal and rock dust significantly contributes to disease development as compared to the larger size fraction. If confirmed, these data will fill the knowledge gap regarding the effect of particle size on pulmonary diseases. Furthermore, fundamental evidence will be obtained regarding the proper controls required to eliminate such exposure and promote the regulation of mine dust exposure based on particle number and size.

Research tasks:

Based on each objective, researchers performed the tasks listed here to complete the proposed project.

For Objective 1: To correlate the size and concentration of coal/rock particles with cellular responses in human bronchial epithelial cell culture models.

Task 1: Prepare coal and rock dust to select for specific size groups.

Task 2: Grow primary human bronchial epithelial cells and perform toxicity tests.

Task 3: Analyze and characterize the aerosolized coal and rock dust for cellular tests.

Task 4: Perform cell uptake studies of coal and rock dust in the cell and animal model.

For Objective 2: To begin identifying particle size-dependent mechanisms and biomarkers that could be used to predict adverse outcomes in coal mine workers.

Task 5: Evaluate cytotoxicity and oxidative stress in the cell model.

Task 6: Examine markers of inflammation in the ALI model.

Task 7: Conduct field sampling at a coal mine and analyze the composition and characteristics of field dust.

For Objective 3: To suggest a safer level of mine dust exposure to reduce the prevalence of respiratory diseases.

Task 8: Suggest the NOAEL and LOAEL values and their association with particle metrics and characteristics.

Task 9: Reporting and publishing the findings.

The research approach details and methods applied to perform tasks and achieve objectives are categorized into five sections:

A. **Underground coal mine field study: Dust sampling and measurement**
B. **Cellular uptake studies and animal cellular uptake studies**
C. **Cytotoxicity and oxidative stress:**
D. **Inflammation measurements:**
E. **Dust characterization and dose-response effect analysis: including animal study**

A. Underground coal mine field study: Dust sampling and measurement

We have assessed the mine dust particle exposure and collected mine dust using multiple samplers at an underground mine in Colorado. The field study was completed during July 25-27, 2022. PI Tsai and Dr. Brune with 3 graduate students (see photo) have collected data at the underground coal mine, included area and personal sampling.

Direct reading instrument measurements: Direct reading real-time instruments (RTIs) were used for this study to measure area real-time particle number concentrations, including a NanoScan scanning mobility particle spectrometer (SMPS), an optical particle sizer (OPS), and a PDM. Belt area, mine entrance, and office building were measured using SMPS and OPS to assess particle exposure in different work locations. Personal dust monitor (PDM) was worn by the researcher when riding the vehicle from the office building to the belt area and during the entire period walking at the belt area to measure respirable sized particles mass concentration.

Gravimetric filter sampling: Airborne mine particles were collected using three different samplers: (1) a 37mm cassette with PVC filter according to the NIOSH 500 sampling method (Fig. 1A), (2) a 10mm Nylon cyclone with 37mm Zefon cassette and PVC filter approved by MSHA (Fig. 1B), and (3) a Tsai diffusion sampler (TDS) (Fig. 1C). The collection includes three area samples (belt area, building office, and mine entrance) and two personal samples each attached onto the research team members. Research scientists were divided into two groups, walking at front and back, to evaluate the difference of particle exposure through disturbing the settled mine dust on the ground.

(A) 37mm cassette **(B) Nylon cyclone** **(C) Tsai diffusion sampler (TDS)**

Figure 1. Samplers used in coal mine field. (A) 37mm cassette with PVC filter, (B) 10mm Nylon cyclone with 37mm Zefon cassette and PVC filter, and (C) TDS.

B. Cellular uptake studies and animal cellular uptake studies

We originally proposed to use human bronchial epithelial cells grown at the air liquid interface (ALI) to provide a highly relevant 3D tissue culture model that represents human airways. The aerosolized coal and rock dust have been monitored, sampled, measured and characterized at the beginning stage of this project. As noted in the Deviations and Corrective Actions in the progress report submitted on Feb. 1, 2022, we proposed using human bronchial epithelial cells and human macrophages in a 2D cell culture system. This approach was supported with an aerosol calibration profile to be established in response to the aerosol exposure simulating for 3D culture condition and the 2D cell culture exposure concentration. This alternative was initially discussed in the progress report issued on August 28, 2020, in Task 2. Therefore, we used a 2D culture model to conduct all relevant cell experiments (Tasks 4,5 and 6).

In summary from our previous report, the 3D culture model takes about a month to differentiate the bronchial epithelial cells to an air-liquid interface, so the throughput of these experiments is extremely low. In addition, we are not able to analyze as many endpoints due to both the nature of the 3D model and the low throughput. Considering the disadvantage of 3D culture, after approval of previous report for this alternative, our group continues the study performing on a 2D cell culture. The advantage of 2D cell culture also included in the previous report: 1) reproducibility (i.e. we can control the seeding and number of cells much more consistently); 2) speed at which we can collect data as the cells grow much faster in a submerged culture; 3) we can do more experiments and analyze more endpoints than a 3D culture would allow due to the simplicity and speed of the 2D model.

The dust uptake of cells was proposed to determine by three methodologies: 1) The optical absorption spectra of the cell were measured in the wavelength at 500nm on the microplate reader, 2) ICP-MS and 3) bio-TEM analysis.

The pilot study results of 1) the optical absorption method, (Fig 2) showed the light-wave absorption level of THP-1 cells after the coal mine dusts treatment in 10, 100, 500 μg/mL concentration. It indicated a clear dose-response trend in both coal and rock treatments. However, compared to the no treatment cells (labeled as "Neg" in Fig. 2), the results were not different indicating that the optical spectra had a limitation to distinguish the dust outside the cellular or the particle in the medium. Also, we could not observe the difference between the absorption level between the coal and rock dust, indicating the limitation for using the absorption approach to determine the cellular uptake.

For 2) the ICP-MS method, we were able to clearly detect the elemental compositions in the raw coal and rock dust. Titanium and aluminum were two elements that we targeted to determine the cellular uptake. However, we could not identify a significant difference between the no-treatment cells and the exposed cells in our pilot study. The level of, which titanium and aluminum detected would be the baseline naturally carried in cells. Based on our pilot results of methods 1) and 2), we concluded that the high-resolution bio-TEM analysis is a more suitable method for analyzing uptakes of mine dust exposed cells . Bio-TEM has been shown to be a widely accepted approach to illustrate the cellular uptake which could identify the particle cellular localization as well as uptake.

The 3) bio-TEM analysis method is described below. Cells were fixed in 2.5% glutaraldehyde and 2% formaldehyde in 0.1 M sodium cacodylate buffer for 1hr. After wash, samples were embedded in 4% agarose gel and post-fixed in 1% osmium tetroxide. After wash, samples were dehydrated through a

graded series of ethanol concentrations and Propylene Oxide. After infiltration with Eponate 12 resin, the samples were embedded in fresh Eponate 12 resin and polymerized at 60°C for 48 hours. Ultrathin sections of 70 nm thickness were prepared and placed on formvar carbon coated copper grids and stained with uranyl acetate and lead citrate. The grids were examined using a JEOL 100CX transmission electron microscope at 60 kV and images were captured by an AMT digital camera (Advanced Microscopy Techniques Corporation, model XR611) (Electron Microscopy Core Facility, UCLA Brain Research Institute).

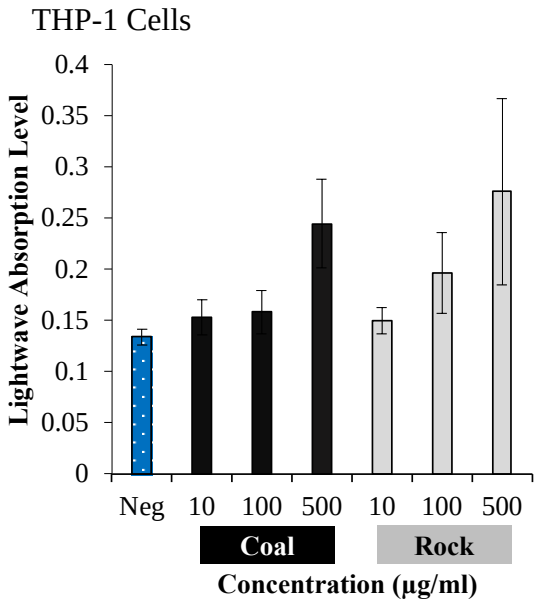

Figure 2. The light-wave absorption level of THP-1 cell after various mine dust concentration treatment.

We have performed dose- and time-response toxicity assessments using different sizes of coal and rock dust mostly with 2D cell models.

Method to conduct cell culture studies are described in detail here. The in-vitro studies were conducted with two cell lines, human THP-1 and HBEC, modeled macrophage reaction and epithelial damage following methods below.

Primary bronchial tracheal epithelial cells (HBECs)

a. Cell Culture –

Human bronchial epithelial cells (HBECs), obtained from the American Type Culture Collection (ATCC, Manassas, VA), were cultured in supplemented BronchiaLife epithelial airway media as described in lifeline technologies (Lifeline Cell Technology, Frederick, MD). The cells were grown in 5% CO_2 to >90% confluency prior to any treatment.

b. ALI Cell Culture –

This method was used originally for testing. Twelve well transwell insert plates (Costar) were prepared with 1ml Stemcell Technologies PneumaCult-Ex Plus media in the basal chamber. Seventy thousand

Primary bronchial tracheal epithelial cells (HBECs) per well in 500µl media were placed on the apical side of the transwell insert. Media was changed every two days. Once cells were confluent 1ml Pneumocult-ALI media was added to the basal chamber and all media was removed from the apical side of the transwell insert. ALI media was changed every two days and every week cells were rinsed with PBS to remove mucous. After 5 weeks the cultures were considered fully grown and ready for use in experimentation. Samples were submitted to the Research Histology Core at CU Anschutz for Hematoxylin and Eosin (H&E) staining to look at cilia and general morphology and Periodic Acid-Schiff (PAS) staining to determine degree of differentiation.

c. Dusting of cells –

This method was used originally for experiments. Cells were grown in ALI cell culture and allowed to grow for at least 4 weeks post ALI lifting before coal exposure. Transwells were taken out of their original plate and put into a new sterile plate for dusting. Plates were placed in the duster as illustrated below.

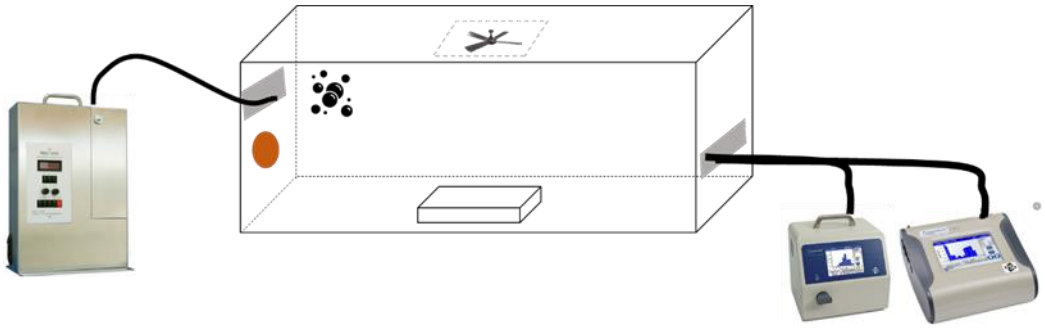

First, we start the SMPS and OPS for monitoring the pre-experiment condition (10 min). At sample number 11, we begin to generate the dust depending on the size needed. We slowly increase the compressed air pressure to reach the pressure approximately 20-25 psi. The level of psi will set the pressure gauge at 1 bar on dust generator. The proportion of the different particle size is changed with the feeding rate ranging from 5 mm/hr to 100 mm/hour. The particle generator is operated at 1200 rpm (max) for all feeding rates. For generating high number of small sized particles, a feeding rate of 100 mm/hr is required. For generating larger particles than small ones, a feeding rate of 5 mm/hr is required. We turn the fan on to the scale at where it is marked (Mark is set based on the flowrate needed for the air circulation). We exposed the cells to the dust for various amounts of time. To shut down the dust generator, we turn off the compressed air first then stop the dust generator. Pictures were taken using brightfield microscope at 40× magnification. We also used dark field microscopy to look at one of the bright field imaged spots. Coal shows up surrounded by white.

THP-1 cells

a. Cell Culture –

Human THP-1 cells from ATCC (Manassas, VA, USA) were grown in RPMI-1640 media with 10% fetal bovine serum (FBS), 100 U/100 µg per mL of penicillin-streptomycin, and 50× 10^{-6} mol/L beta-mercaptoethanol.

b. Particle Exposure–

Coal and rock dust particulates from the top, middle and bottom separations were weighed out and resuspended in culture media to a concentration of 10, 100, and 500µg/mL. THP-1 cells were plated at 3-5 × 10^4 cells per well and HBECs were plated at 1.1 × 10^4 cells per well into 96 well plates. After incubating overnight at 37°C in a 5% CO_2 incubator, cells were treated with various coal or rock samples for 24 hours.

C. Cytotoxicity and oxidative stress:

We analyzed the following endpoints a) MTS assay for cell viability analysis, b) Annexin/PI staining by flow cytometry to determine apoptosis/necrosis, c) Formation of reactive oxygen species as measured by CellRox assay, d) determination of oxidative stress by measuring reduced and oxidized levels of glutathione and cysteine.

With the revision on cell models, we have analyzed all proposed endpoints based on 2D cell culture studies with results published. With raising interests in health effect of "mixture" of mining dust, we have further used dusts from the field study site for 2D cell studies, analyzed MTS and ATP endpoints of mining dust collected from different locations at mine site. Further cytotoxicity and endpoints were analyzed.

We have performed Seahorse assays to further understand these endpoints. With Seahorse assays, we analyzed the following endpoints a) MTS assay for cell viability analysis, b) Annexin/PI staining by flow cytometry to determine apoptosis/necrosis, c) Formation of reactive oxygen species as measured by CellRox assay, d) determination of oxidative stress by measuring reduced and oxidized levels of glutathione and cysteine.

Cells were treated at a concentration of 10,100 and 500 µg/mL for up to 24 hours with coal dust or rock dust separately, experimental details are described below.

a. MTS Assays –

Human primary bronchial epithelial cells (HBECs) were cultured on a 96 - well pate at a seeding density of 11,000 cells/well. Coal dust particulates at 400 mesh, stage 1 with 5.8-9 µm mass median aerodynamic diameter (MMAD) and stage 5 with 1.1-2.1 µm MMAD collected from impactor, were weighed out and resuspended in culture media to a concentration of 1mg/ml. Using a hand sonicator (Heischer Ultrasound Technology, model UP100H ultrasonic processor), particles were sonicated at an amplification of 99% for 180 seconds. Cells were treated with various coal or rock dust types, sizes and concentrations (see section 4.0). After cells were incubated for 1,3, or 24 hrs, they were then treated with 3-(4,5-dimethylthiazol- 2-yl)-5-(3-carboxymethoxyphenyl)-2-(4-sulfophenyl)-2H-tetrazolium (inner salt; MTS) according to the manufacturer's protocol (Promega, Madison, WI). To determine mitochondrial activity, MTS dye (CellTiter96proliferation assay, Promega) was added (20 µl) to the culture medium (100 µl) and incubated for 1h at 37 °C. Absorbance was measured using our fluorescent spectrophotometer at 490 nm (BioTek Synergy HT, BioTek, Winooski, VT; software: Gen5 2.04).

b. LDH Assays –

HBEC's were cultured on a 96 - well plate at a seeding density of 11,000 cells/ well. CytoTox 96® Non-Radioactive Cytotoxicity Assay was used to measure lactate dehydrogenase (LDH) which is a stable cytosolic enzyme that is released upon cell lysis (CytoTox 96® Non-Radioactive Cytotoxicity Assay, Promega). Coal dust samples were weighed out and resuspended in double distilled water to a concentration of 1 mg/mL. Using a handheld probe sonicator (Heischer Ultrasound Technology, model UP100H ultrasonic processor), particles were sonicated at an amplification of 99% for 180 seconds. Cells were treated at with various concentrations of coal dust separately. Cells were incubated for 1,3, and 24 hrs and then spun down to remove the supernatant to measure LDH release. The protocol provided by Promega was followed after obtaining supernatant and the absorbance was measured using a fluorescent spectrophotometer at 490 nm (BioTek Synergy HT, BioTek, Winooski, VT; software: Gen5 2.04).

c. Seahorse Assays –

Seahorse assays were used to measure the oxygen consumption rate (OCR) and extracellular acidification rate (ECAR) of live HBEC cells on 96-well plates following exposure to coal and rock dust. OCR and ECAR rates are key indicators of mitochondrial respiration and glycolysis as well as ATP production rate. Together these measurements provide a systems-level view of cellular metabolic function in cells. Parameters measured in the assay include basal respiration, ATP production, proton leak, maximal respiration, spare respiratory capacity, nonmitochondrial respiration and coupling efficiency. Preliminary tests were performed to determine HBEC cell seeding density and find the optimal Carbonyl cyanide p-trifluoro-methoxyphenyl hydrazone (FCCP) addition for maximal response. Once conditions were optimized, 3 seahorse plates were seeded with 25,000 HBEC cells per well. After incubating for 48 hours at 5% CO2 HBEC media was changed and four treatment groups. Agilent Seahorse assay basal media (BAM) was prepared and supplemented with glucose, glutamine, and pyruvate to match the usual HBEC media. After 24 hours incubating at 5% CO2, the normal HBEC media was removed from the wells and cells were washed twice with BAM and left in BAM media. Assay ports were loaded with oligomycin, FCCP and Reotenone/antimycin A. While the sensor cartridge was running on the Seahorse XFe96 Analyzer (Agilent, Santa Clara, California, USA) the treated cells were counted using a Cytation cell imaging multimode reader (Biotek, Winooski, VT, USA). The treated plates were then read on XFe96.

d. ATP Light Assays -

The effects of coal/rock treatment, after 24 hours exposure, on ATP levels in HBEC cells were assessed using the ATPlite assay. HBEC's were cultured on a 96-well plates at a seeding density of 11,000 cells/well. The ATPlite Assay was used to measure ATP which is a marker for cell viability because it is present in all metabolically active cells. Because ATP concentration declines rapidly when cells undergo necrosis or apoptosis, monitoring ATP is a good indicator of cytocidal, cytostatic and proliferation effects. Coal and Rock dust particulates from the Top, Middle and Bottom separations were weighed out and resuspended in culture media to a concentration of 0.1mg/ml, 1mg/ml and 10mg/ml. Using a water bath sonicater, particles were sonicated at an amplification of 99% for 5 minutes. Cells were treated at a concentration of 10,100 and 500 µg/mL with coal dust or rock dust separately. Cells were incubated for 24 hrs and then spun down to remove the supernatant from the cells. The protocol provided by Perkin

Elmer was followed after obtaining cells and the luminescence was measured using a BioTek Synergy HT.

D. Inflammation measurements:

We utilized a) a PCR array to examine 84 inflammatory cytokines in the ALI cell model following exposure to coal and rock dust and b) ELISA to confirm protein levels of select genes based on the PCR data.

a. Cytokine PCR Assays -

Rock/Coal Exposure Experiments for cytokine analysis. HBEC's were cultured on 6 - well plates at a seeding density of 50,000 cells/well. Cells were exposed to Rock and Coal, Top, Middle, and Bottom samples at 1, 10, 100 and 500 μg/ml for 24 hours. After 1ml supernatant (media) was removed, cells were rinsed twice with 1×PBS, and then cells were removed after TRI Reagent exposure and frozen at -80 overnight. Cells were thawed and processed to remove RNA using the standard procedure for the Direct-zol RNA Miniprep Plus Kit (Zymo Research) and then cDNA was made using the standard procedure for the iScript cDNA Synthesis Kit (BioRad). The SsoAdvanced Universal SYBR Green Supermix (BioRad) was then used to perform SYBR Green PCR to determine fold change from the no treatment control for Tumor Necrosis Factor (TNF), Interleukin 1 Beta (IL-1B) and Interleukin 6 (IL-6).

b. Endotoxin Testing –

The Thermo Scientific™ Pierce™ Chromogenic Endotoxin Quant Kit was used to investigate possible endotoxin contamination in the assay media, 400 mesh and less processed Pittsburg coal samples. Endotoxin removal methodologies using ultraviolet light (UV) and heat exposure at 360 degrees Fahrenheit for 3 hours and 480 degrees Fahrenheit for 30 minutes were investigated.

c. Cytokine ELISA Assays –

Cytokine expression of TNF-α, IL-1β, and IL-6 in cell culture, which reflects inflammatory response, was examined after various rock and coal dust exposure by enzyme-linked immunosorbent assay (ELISA). The commercial kits for ELISA were performed following the manufacturer's protocols (Thermo Fisher Scientific, Inc., Waltham, MA, USA)(IL-6 Human IL-6 DuoSet ELISA, R&D Systems, Minneapolis, MN, USA).

E. Dust characterization and dose-response effect analysis: including animal study

Coal and rock dust were obtained and then sieved to prepare size separated particles. We originally set up and constructed a small enclosure for aerosol generation and ALI cell model. Later this set up was revised to use 2D cell model as described in previous section. We also adopted a novel separation method collaborating with colleagues at UCLA medical school using the centrifugation method that successfully separated particles sizes as planned.

We analyzed data obtained from the previous tasks to establish the dose-response profile associated with the variables studied in this project. We discussed the biological endpoints and the association with practical exposure at the mine site. We determined the concentration of exposed coal and rock dust and the toxicity responses at different sizes. The dust components at different sizes were analyzed and discussed if specific constituents show significant effects upon exposure to the human lung cells. Furthermore, these analyses will inform suggestions of NOAEL and LOAEL exposure values for the small-sized portion of coal and rock dust and for each studied endpoint. In addition, proper measurement metrics will be suggested.

To further support the development of NOAEL and LOAEL values as proposed in this task, we added a small-scale animal study as an alternative approach to provide us additional data for this Task, as noted in June report of 2023 in 2.0 Derivations and Corrective Actions. The Anschutz IACUC has approved studies on Black Six mice. These studies include an initial study involving oropharyngeal aspiration of 0, 10, 50, and 100μg of Colorado 400mesh coal into groups of 5 mice each to determine dosing for later experiments. Once dosing is determined we dose groups of 6 mice with two different doses of each of our 6 coal and rock size groups (Top, Middle and Bottom Groups).

a. DLS Sizing of Coal and Rock Particles -

Dynamic light scattering (DLS) was used to measure the size and agglomeration of particles suspended in cell culture media. Coal dust was separated by Anderson cascade impactor into 7 stages. Stages 1, 3, 4 and 5 were suspended in media following the same procedure as preparing the particle suspension for cell exposure. We also suspended 400 mesh, ball milled and less processed coal dust particles from Colorado and Pittsburg mines in media for particle size measurements. All samples were prepared with dilution ratios of 1:100 and the measurements by DLS included 3 runs with 5 reading in each run. To address the agglomeration issue and make the coal particle preparation cleaner, we looked at water sonicating the samples for 5, 10, 15 and 30 minutes.

b. Animal Experiment (Murine) –

Mouse experiments were approved by the University of Colorado Anschutz Institutional Animal Care and Use Committee (Protocol # - 01311). Eight-Week-old C57BL/6 mice were ordered from Jackson Laboratories for each experiment. In the initial experiments, multiples of 5 mice were treated with 0, 10, 50 or 100 ug 400 Mesh coal via intratracheal instillation to determine coal toxicity. First, mice were given 4.0L/min isoflurane until the animals were deeply anesthetized. Next, the dose was reduced to 2.5L/min which was the maintenance dose. Anesthetized mice were hung by their teeth on the instillation device. The mice tongues were pulled to the left with tweezers and 50ul of PBS or treatments in PBS were injected into their mouths. When the mice gasped for breath, the treatment was delivered to their lungs. In the final experiment, sets of four mice were treated with PBS, 100ug of Top Coal, Bottom Coal, Top Rock or Bottom Rock using the method above. Three days post treatment the mice were euthanized with carbon dioxide, blood was collected via intra cardiac stick, and cells were collected from their lungs via bronchioalveolar lavage (BAL). Briefly, the mouse was dissected to access the trachea. A small slit was cut in the trachea and the lavage needle was inserted into the trachea towards the lungs and the lavage

needle was tied in with suture. 1ml of PBS with 0.5M EDTA was injected into the lungs and then retrieved after 10 seconds and put into a 1.5ml microcentrifuge tube (tube 1). Two more lavages were performed on the same mice with 0.5ml PBS with 0.5M EDTA and the fluid was stored in a second tube (tube 2). Blood was spun down at 1200 x g to obtain serum and serum was stored in a -80 Celsius freezer. Lavage tube 1 and 2 were spun down at 1200RPM for 5 minutes, the tube 1 BAL fluid was saved for future cytokine analysis and the tube 2 BAL fluid was discarded. Cells were combined in one tube, resuspended in 1ml PBS/1%BSA, counted and then resuspended in 500ul of the lavage fluid. 125ul of this fluid was centrifuged in a Thermo Scientific Cytospin 4 Centrifuge to get the cells on slides for cell counting. After the cytospin slides dried overnight they were stained using the Hema 3 staining system and then manually counted.

c. Centrifugation size separation-

Density gradient centrifugation was performed using solutions of 10, 20 and 40% w/v polyethylene glycol (PEG, 20K) dissolved in water. Aliquots of 10 mL of 20% w/v PEG solution were carefully layered on the top of the 40% w/v PEG solution within a 50 mL centrifuge tube for coal samples. 10 mL of 10% w/v PEG solution was layered on top of rock samples. Then, 10 mL of the solution containing 18 mg/mL coal or 50 mg/mL rock dust were dropped at the top of the PEG layers. Avoid mixing between the layers during this process. The coal tube was centrifuged at 100 RCF for 1 min, resulting in 2 distinct layers. The rock tube was allowed to deposit for 10 minutes, resulting in 3 distinct layers. After centrifugation or deposition, 1 mL of solution from top and bottom layers was collected. The dust in PEG solution was washed twice with water to remove PEG (10,000 RCF, 20 min). All samples were dried overnight in a vacuum oven at 50°C. Size was measured after washing and drying to account for potential loss of small particles in the washing process. Finally, the dry samples were weighed and analyzed by Dynamic Light Scattering (DLS) and Transmission Electron Microscopy (TEM) in 2 mg/mL ethanol solution.

d. Physico-Chemical Characterizations of Coal and Rock Particles-

Contact angle and IR methods for hydrophobicity measurement: Samples were dried in a vacuum oven at 50 °C for 24 hours. Samples were packed into a hydraulic pellet press to make a surface for contact angle measurement. 300 mg of dust sample were pressed at 7000 psi for 3 minutes. Immediate contact angle with water was taken within 1 second and averaged for 3 pellets.

*Functional groups were determined using FTIR (Agilent Technologies):*A background reference was obtained with an empty cartridge. 2 mg of sample and 200 mg of KBr were mixed and ground, packed into a pellet press and pressed at 10,000 psi for 10 minutes. The spectral range was 4000–400 cm−1, the resolution was 4 cm−1, and each sample was scanned 64 times. Spectra of transmittance to wavenumber were deconvoluted. Hydroxyl structures were noted in the 3800–3000 cm−1 region, aliphatic structures in 3000–2800 cm−1, oxygen-containing functional groups in 1800–1000 cm−1 and the aromatic structures in 900–700 cm−1 (Zhao et al., 2018) from spectra (Lin et al., 2019).

Surface charge method: Zeta potential was measured using the ZetaPALS (Brookhaven Instruments) analyzer for each coal and rock size.

Elemental composition method: Dust suspensions of 2 mg/mL concentration were vortexed and sonicated for 15 seconds, then a drop of the suspension was put on a Quantifoil TM R 2/1 on a 200 copper mesh TEM grid and dried. STEM w/ EDX (FEI Titan S/TEM electron microscope, Oxford X-Max TEM EDS system, 80kV) detected the elemental composition of the sample on the TEM grid.

e. Aerosolization of mining dust

To correlate the 2D cell culture and real-work exposure, coal and rock dusts were aerosolized in the lab chamber as shown in Fig. 3. Dust powder was placed in a glass beaker at a certain height to ensure the powder disperser can homogeneously stir the dust powder and produce the aerosol. 10 mins stirring after, we collected the aerosolized particles by TDS in 90 mins. SMPS and OPS were placed inside the chamber to monitor the real-time number concentration. The mass concentration was determined by the difference between pre- and post- filter weight. The grid on TDS filter were imaged by TEM to determine the morphology and size range. Filter from TDS was infiltrated into a 50 ml tube with D.I water and sonicated in the bath 60 mins to release the collected particles. The suspension containing aerosolized mine dust particles were measured via DLS to determine the size ranges.

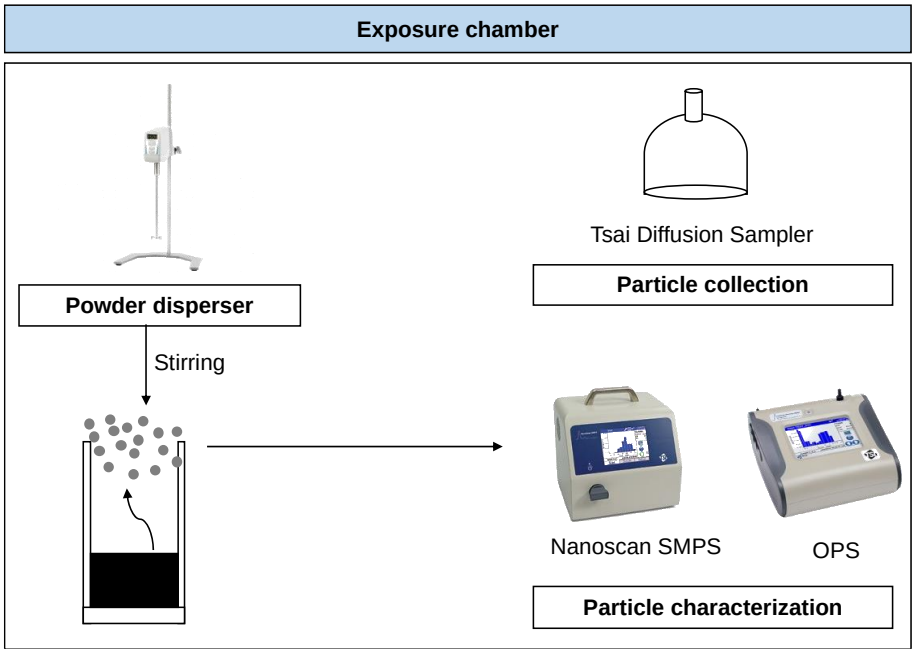

Figure 3. The study design for aerosolization of the coal and rock dusts in a lab exposure chamber. TDS was used to collect the particles for concentration determination and TEM analysis. SMPS and OPS were included in this experiment to monitor the real-time number concentration.

4.0 Research Findings and Accomplishments

A. Underground coal mine field study: Dust sampling and measurement

Exposure Level Investigation

Real time direct instruments:

A NanoScan scanning mobility particle spectrometers (SMPSs) and an optical particle sizer (OPS) measured particle number concentrations at belt area, mine entrance, and office building of the underground mine to investigate the particle exposure at different location involving different activity. Personal dust monitor (PDM) was worn by the researcher when riding the vehicle from the office building to the belt area and during the entire period walking at the belt area to measure respirable sized particles mass concentration.

Table 1 summarizes the measurement, sampling, and analysis for the underground mine dust particles in this field study. The sampling time at each location varies relating to equipment availability and limitations (Table 1). Fig. 4 presents the total number concentration by SMPS and OPS in the belt area, building office, and mine entrance of an underground mine site. Belt area (34670 ± 56320 particles/cm^3) had a significantly higher total particle number concentration than the mine entrance (4184 ± 12280 particles/cm^3) and building office (4634 ± 3832 particles/cm^3). Compared to the relatively stable office environment, the fluctuation of concentration revealed that particle exposure in the mine entrance is dependent on human activities, like miner walking or vehicle transportation (Fig. 4A). OPS data showed a similar finding that measurements in the belt area (167100 ± 57710 particles/cm^3) had higher level of exposure to mine dust particles compared to those in the building office (10180 ± 1958 particles/cm^3) and mine entrance (16140 ± 4761 particles/cm^3), seen in Figure 1B. SMPS and OPS both indicated an elevated peak concentration around 80 mins and dropped to usual level after 15 mins (Fig. 4). The unexpected concentration increase may relate to the coal transporting on the conveyor. The conveyor was activated around the time where the peak concentration appeared during measurements.

A higher particle count concentration was measured by OPS than SMPS indicating more larger particles were detected (Fig. 4) and the size fraction data supported this finding as shown in Fig. 5. Figure 2 showed a significantly higher particle number concentration of micron sized particles measured by OPS. Given example, in the belt area the average concentration of micron sized particles (300 nm-10,000 nm) was 9830 particles/cm^3, the submicron sized particles (10-420nm) were found to be in a much lower concentration of 2667 particles/cm^3. The difference of exposure levels between large and small size ranges in the building office and at the front of the mine entrance were not as obvious as in the belt area. The concentration data showed that the belt area not only exhibited the highest total particle number concentration of the areas that were measured, but also had distinct particle size distribution from coarse to fine range through the SMPS and OPS observation. Remarkably, the small submicron sized particles detection by SMPS demonstrated the emission of finer particles in the belt area, and it was 7.5 times higher than the concentrations in the building office and 8.3 times higher than at the mine entrance, especially in the size range between 36.5 nm to 205.4 nm, the nanoparticles. The belt area's highest concentration 8533 particles/cm^3 peaked at 86.6nm while both the building office (898 particles/cm^3) and mine entrance peaked at 27.4nm (737 particles/cm^3).

The results clearly showed that the belt area exhibited the highest concentration across all size fractions compared to the building office and entrance, and significantly higher concentration of submicron and nanoparticles were found.

PDMs were used to monitor the personal dust exposure level in the mine together with the gravimetric samplers. Fig. 4B showed the mass concentration monitored throughout the entire period of measurement, which could represent a daily routine of miners performing similar activities. The high level of fluctuation of particle concentration during the period transporting underground into the mine entrance was caused by the vibration during transition by vehicles. The level was dropped and remained at a more stable lower level when reaching the entrance and during the walk to the belt area. The average mass concentration measured by PDM in the belt area was 0.178± 0.02 mg/m^3 and the level increased to 0.22 mg/m^3 at the end of sampling.

Samplers:

The measurement, sampling and analysis by three samplers to collect airborne mine particles were summarized in Table 1. The measured mass concentrations clearly showed that more mine dust was collected in the belt area than in the building office and mine entrance (Table 1), which is consistent to our real-time particle measurement results (Fig. 4 and 5). The NIOSH 500 method (with 37 mm cassette) and cyclone were designed to sample respirable dust particles, and TDS was used for collecting particles in both the nanometer and respirable size range. The NIOSH 500 and cyclone methods found that the belt area has the highest respirable particle level, followed by the mine entrance then the office.

Table 1a. Summary of RTIs detection for the measurement and analysis of underground mine dust particles.

Instrument	**Locations**	**Sampling time (mins)**	**Sample analysis (outcomes)**
SMPS and OPS	Office	926	Number concentration, size-fraction number concentration
	Belt area	149	
	Mine entrance	29	
PDM	Office	95	Mass concentration
	Belt area	170	
	Mine entrance	18	

Table 1b. Summary of filter sampling for the measurement and analysis of underground mine dust particles.

Sampler	Locations	Sampling time (mins)	Dust weight (mg)	Volume (m^3)	Concentration (mg/m^3)
37mm cassette	Building office	525	0.02	0.525	0.02±0.02
	Belt area	147	0.77	0.148	5.18
	Mine entrance	210	0.03	0.210	0.12±0.01
	Personal	62	0.07	0.062	1.10±0.18
TDS	Building office	407	0.05	0.407	0.16±0.08
	Belt area	147	0.18	0.148	1.23±1.04
	Mine entrance	210	0.02	0.210	0.09±0.10
	Personal	62	0.03	0.062	0.54±0.03
Cyclone	Building office	527	0.12	0.53	0.42±0.33
	Belt area	147	0.20	0.15	1.35±0.30
	Mine entrance	210	0.14	0.21	0.67±0.41
	Personal	62	0.09	0.06	1.55±2.18

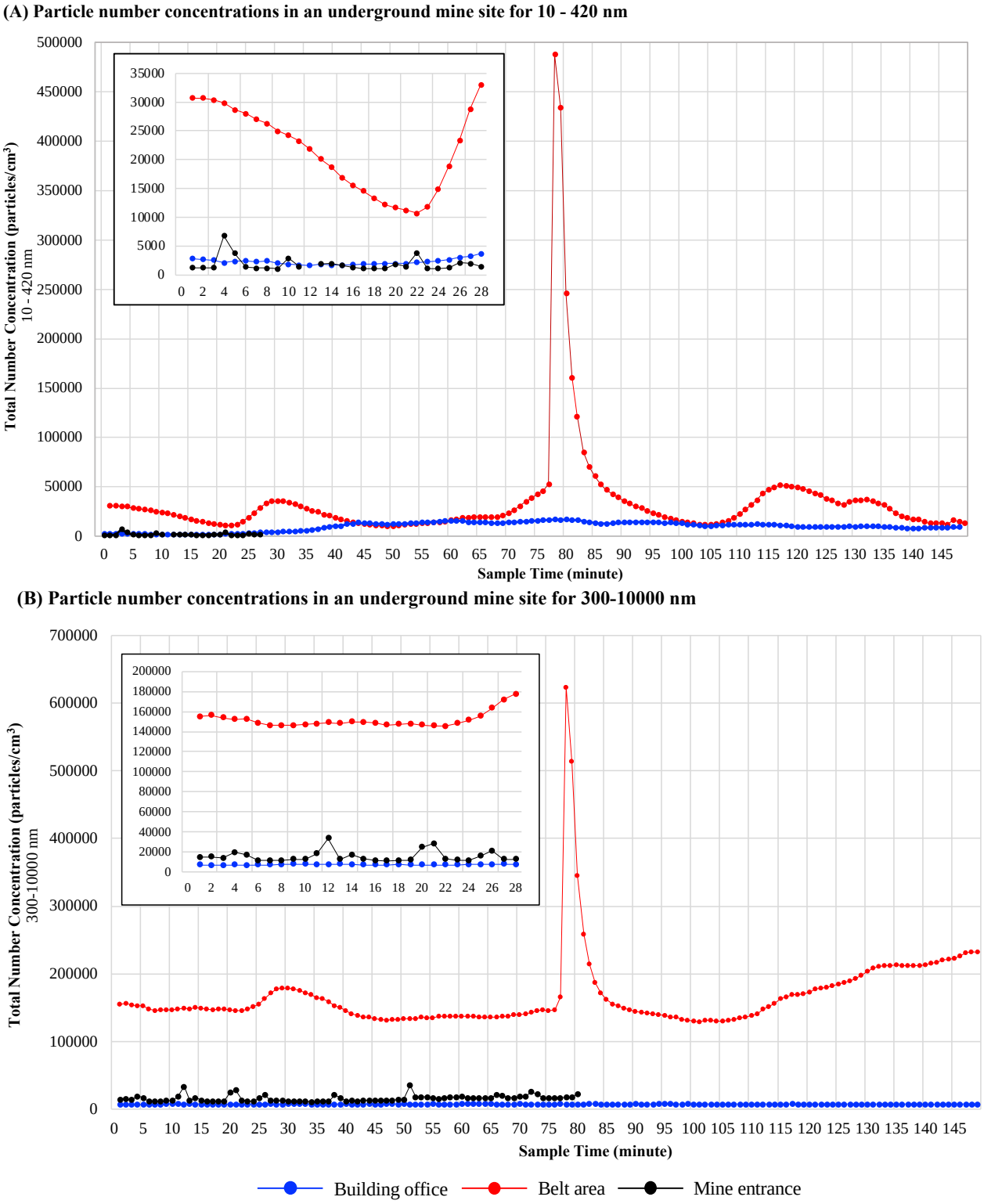

Figure 4. Area particle measurements in an underground mine site including the building office, belt area, and mine entrance by (A) SMPS and (B) OPS.

(A) Size-fractioned particle number concentrations in an underground mine site for 10-420 nm

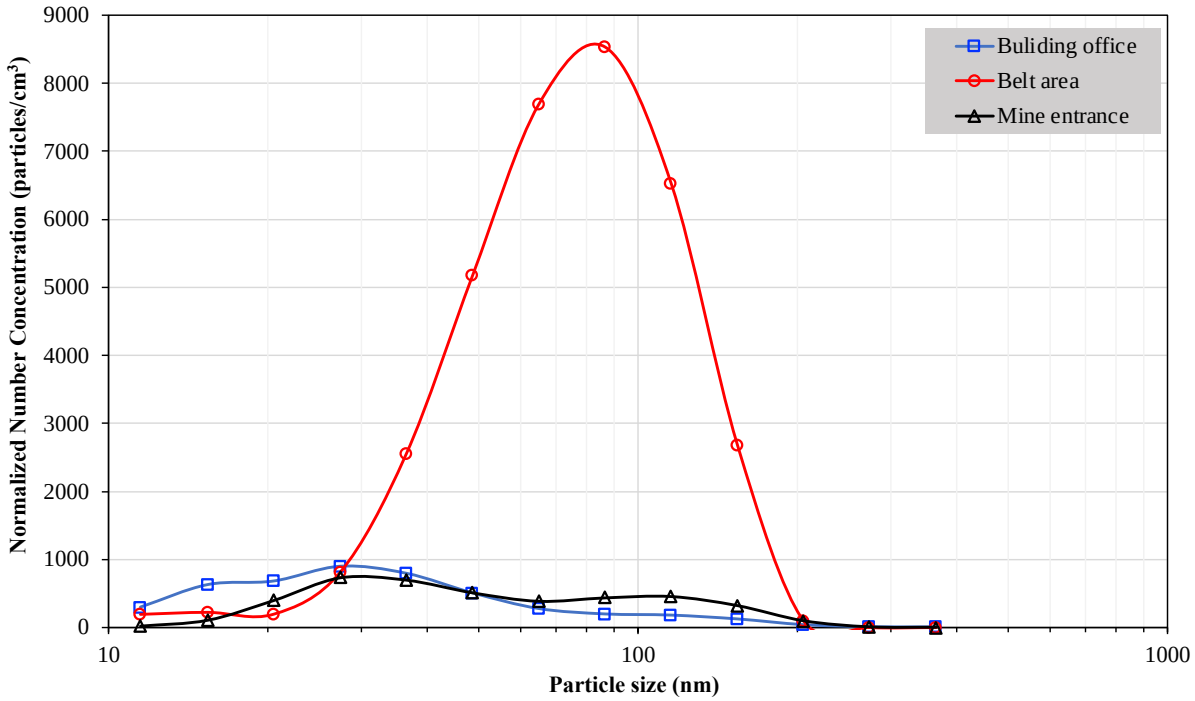

(B) Size-fractioned particle number concentrations in an underground mine site for 300-10000 nm

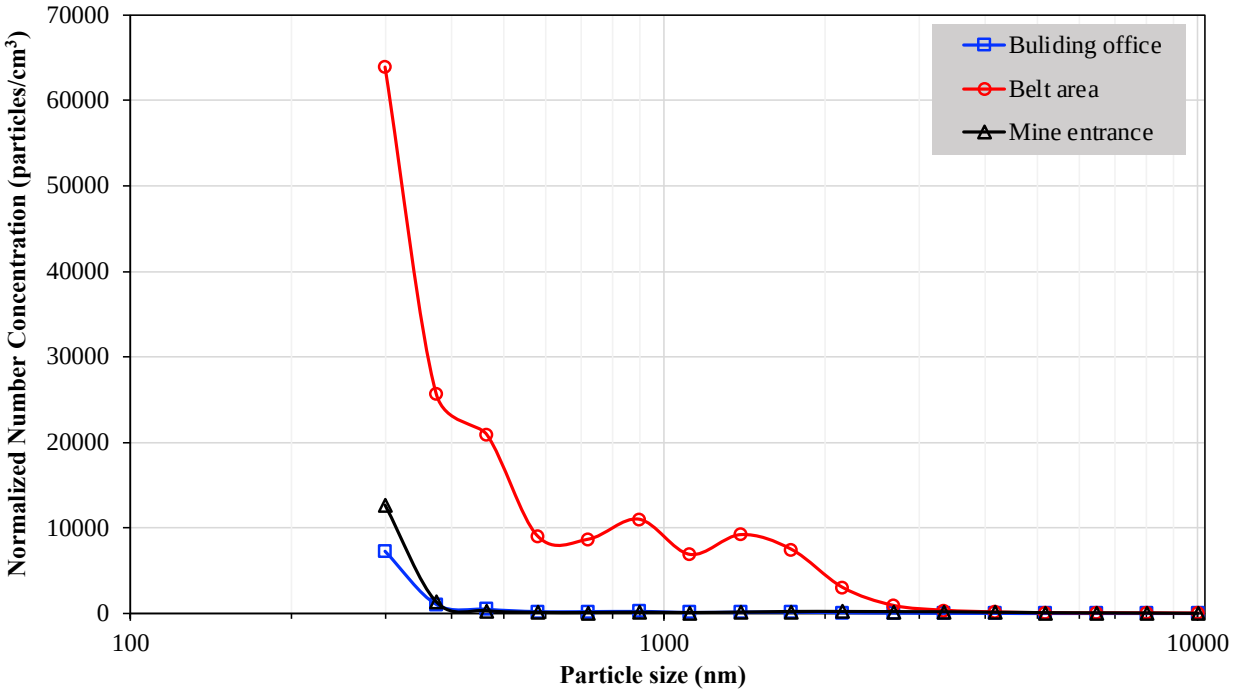

Figure 5. Size-fractioned particle number concentrations in an underground mine site including locations in the building office, at belt area, and mine entrance by (A) SMPS and (B) OPS.

The TDS sampler found that in the nanometer size range, the belt area showed the highest nanoparticle exposure. Surprisingly, we found that the building office had 1.8 times higher particle mass concentration than the mine entrance in the respirable size fraction by TDS and also had 1.1 higher particle number concentration in the submicron size fraction by SMPS. Personal sampling mass concentration by cyclone shows that the group of team members walking behind were exposed to more respirable particles than the front group, likely due to dust kicked off from the ground by the front group.

Mass concentrations calculated to compare with ACGIH TLV and MSHA PEL was displayed in Fig. 6A. The particle mass concentrations at belt area were found to be different with different sampling methods, i.e., 5.18 mg/m^3 by cassette, 1.23 mg/m^3 by TDS, and 1.35 mg/m^3 by cyclone. As a result, three types of personal samplers sampled at the belt area all have a significantly higher exposure to mine dust particles of respirable size than the office (0.02, 0.16, 0.42 mg/m^3) and mine entrance (0.12, 0.09, 0.67 mg/m^3). It is also concluded that the scientists walked behind the others expose to a significantly higher concentration of mine dust particles than the group walking in front of them based on cassette with NIOSH500 method and cyclone samplers' results. However, we found that the TDS sampling results presenting submicron and respirable sized particles had similar mass concentrations collected on both front and back groups. TDS sampled concentrations showed that the team walked behind and at front exposed the level of 0.52 mg/m^3 and 0.56 mg/m^3 respectively.

Referring to the ACGIH TLV-TWA (0.9 mg/m^3) for respirable bituminous coal dust and MSHA PEL (1.5 mg/m^3) at underground and surface coal mines, the dust exposure levels found in belt area is more of a concern and potential exposure to the workers walking behind others required more attention on the possible elevated exposure level.

In addition, PDMs are used to monitor the personal dust exposure level in the mine together with the gravimetric samplers. Fig. 6B showed the mass concentration monitored throughout the entire period of measurement, which could represent a daily routine of miners performing similar activities. The high level of fluctuation of particle concentration during the period transporting underground into the mine entrance was caused by the vibration during transition by vehicles. The level was dropped and remained at a more stable lower level when reaching the entrance and during the walk to the belt area. The average mass concentration measured by PDM in the belt area was 0.178± 0.02 mg/m^3 and the level increased to 0.22 mg/m^3 at the end of sampling.

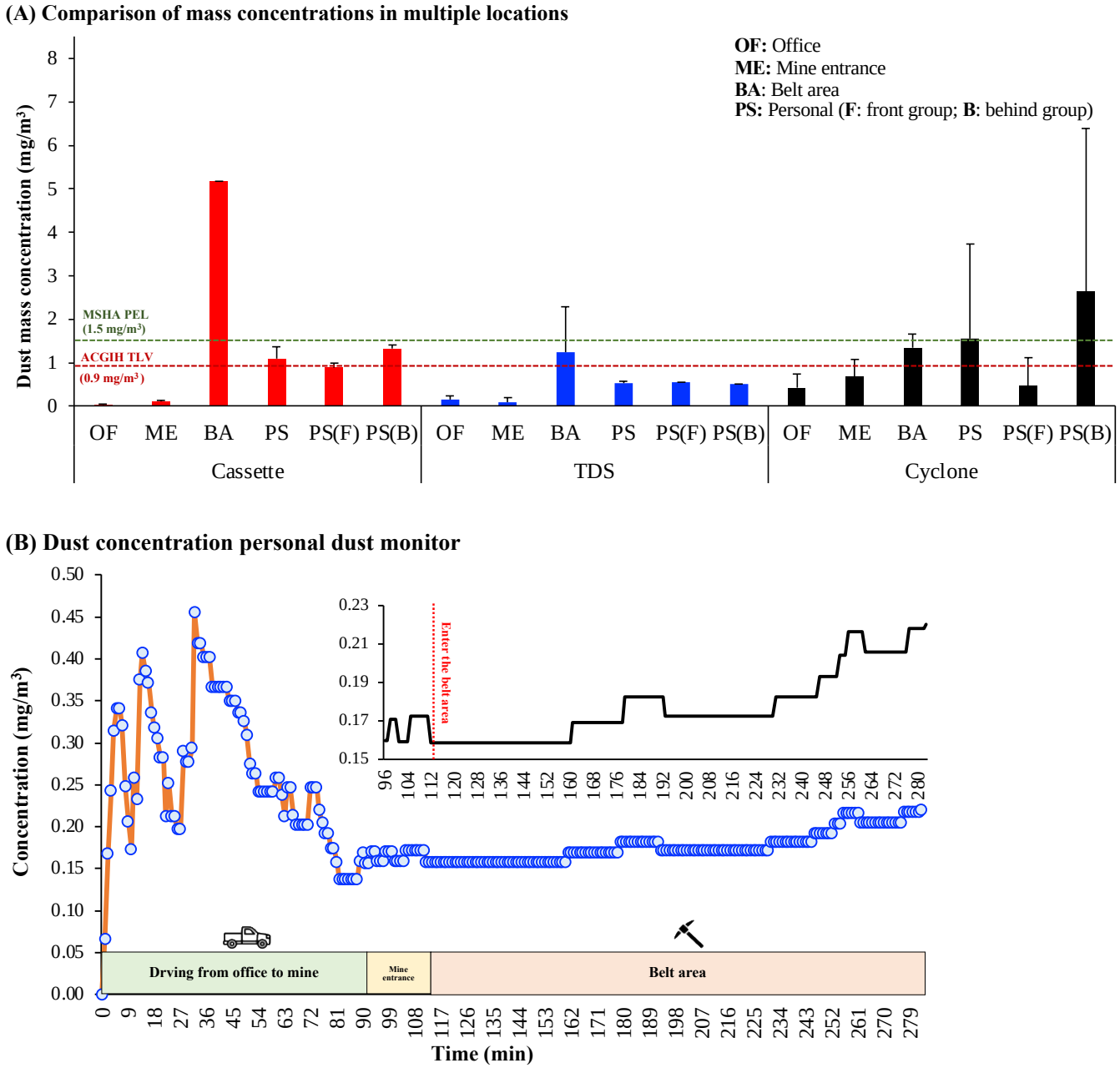

Figure 6. Mass concentrations of the dust particle exposure in the mine industry at multiple locations (belt area, building office, and mine entrance). (A) Concentrations of three samplers collected at multiple locations. Results showed that the belt area has a significantly higher amount of respirable dust particles than other locations. (B) The PDM mass concentration monitored during the entire activity period.

Characteristics of particles

Morphology:

Surface features and morphology of dust particles collected by the samplers were analyzed by electron microscope, i.e., scanning electron microscopy (SEM) and transmission electron microscopy (TEM). The SEM images present the morphology of particles which differ at various sampling locations. In the office, the particles were relatively big (> 2 μm), and coal particles were observed indicating the office was contaminated with mine dust particles which could be carried by personnels accessing the mine (Fig. 7A).

At the entrance to the underground tunnel of mine, we found that the sampled particle by TDS sizes were relatively small compared to the particles collected in office and the morphology was monotonous (Fig. 7B). The SEM images remarkably presented extremely dense particle deposition on the TDS filter collected at the belt area (Fig. 7C) and personal samples walking along the belt area (Fig. 7D). At the belt area, mine dust particles were agglomerated together as spherical shape acclimating on the filters. The size ranges approximately from 400 nm to 1 μm (Fig. 7C). Differing from solid structure of particles at the belt area, the surface of agglomerated particles were loose and more fiber-shape particulates were noticed in the personal samples, with size finer than 200 nm (Fig. 7D).

Fig. 8 presents the TEM images and supports the finding from SEM observations. The office particles were large and likely were associated with contamination carried in through human activities. Mine dust and general dirt particles were both noticed on the samples collected at the mine entrance (Fig 8B). As a result, area and personal samples collected at the belt area were observed with a high amount of mine dust particles, including very small nanoparticles down to even smaller than 50 nm.

(A) Office

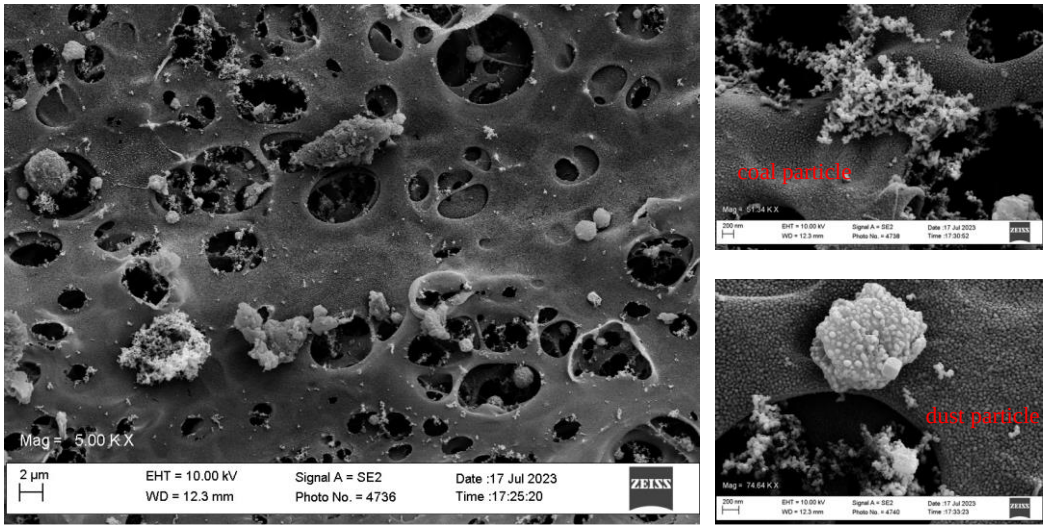

(B) Mine entrance

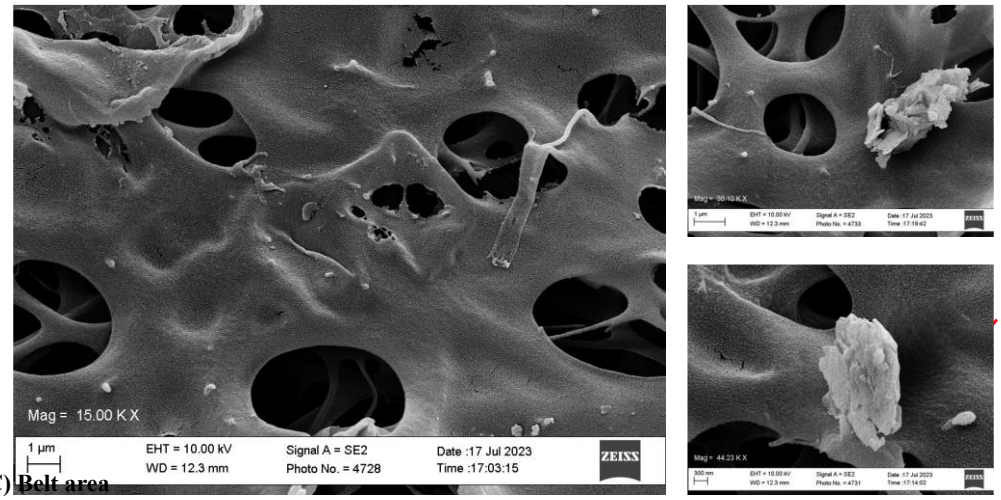

(C) Belt area

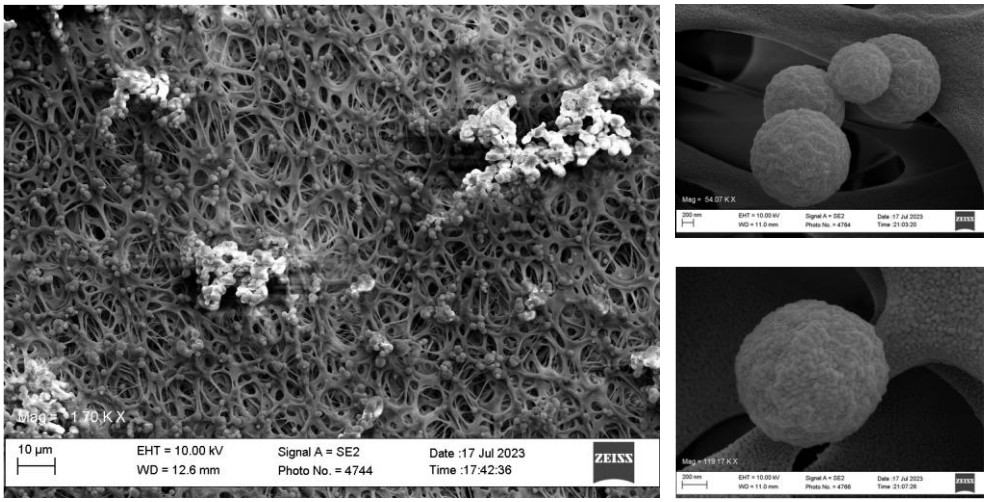

(D) Personal

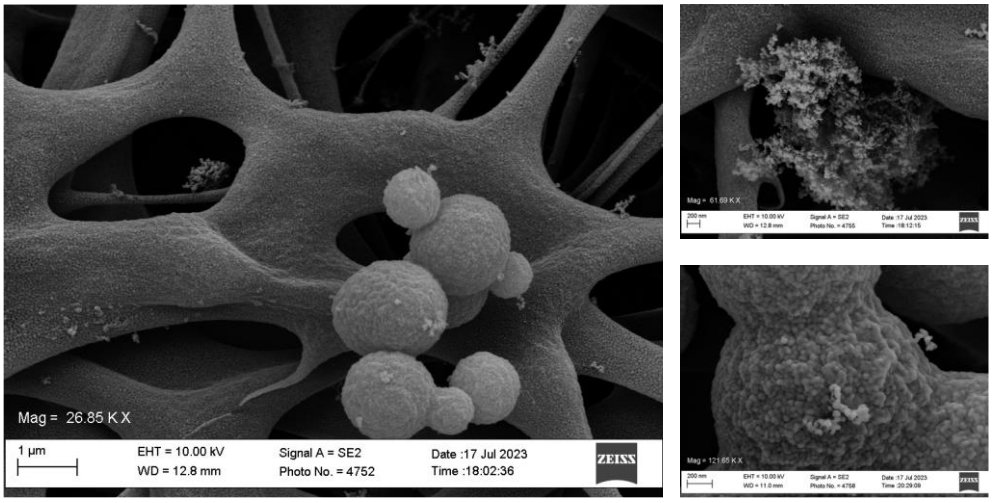

Figure 7. Scanning electron microscope images of particles sampled by NIOSH 500 method with PVC filters from the underground mine showing particles deposited on the filter and their particulate morphology collected at multiple locations. (A) Office; (B) Mne entrance; (C) Area sample at the belt area; (D) Personal sample at the belt area.

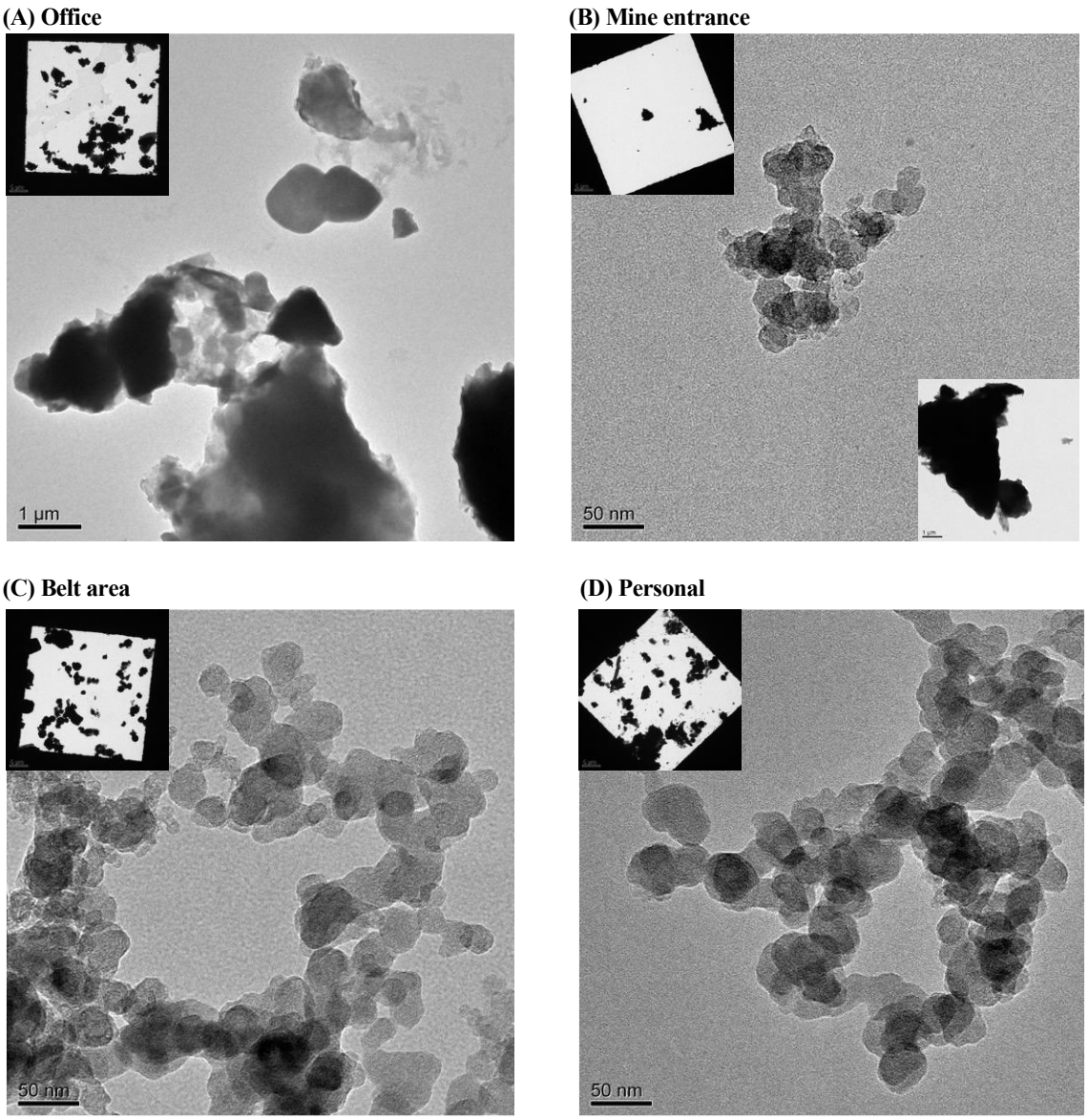

Figure 8. Transmission electron microscopy images of dust particles deposited onto TEM grids sampled by TDS at the underground mine showing the particulate morphology at multiple locations. (A) Office; (B) Mine entrance; (C) Area sample at the belt area; (D) Personal sample at belt area.

Elemental Composition:

Elemental composition of collected samples was examined by SEM/TEM with EDS. The results were shown on Fig. 9 with the spectrum map and element percentages. The elemental composition of particles in the office confirmed the sources of particle which likely were from natural sources based on the appears of calcium, an abundant metal in the earth's crust. The absence of carbon, a major element in coal mine, supported the TEM finding (Fig. 7A and Fig. 8A), showing the particle sources in the office environment were majority from the ambient environment and general dust carried by employees. The inorganic components are the majority of elements found in office samples, including Ca (52.6%) following with Cu (35.4%), Si (4.4%), Al (3.3%), Fe (3.2%), and Co (1.2%), which is similar to soil or earth crust

(Yaroshevsky 2006). The compositions of particles at the mine entrance were similar to the office with Cu (87.0%) followed with Si (7.7%), Al (2.5%), Ca (1.2%), Fe, Cl, and K. The elements founds on the area and personal samples at the belt area were comparable, mostly consist with C, Cu, and O. According to our group publication and results of this project presenting the elemental compositions of coal and rock particles crushed from bulk coal and bulk rock (Chen, Nguyen et al. 2023), coal and rock particles were found on the samples collected in the belt area, and in the personal breathing zone samples. Particles found in the personal samples carry more metal elements, including Pt (1.6%), Co (1.1%), Mg (0.5%), Na (0.4%), and Ni (0.2%), with most were toxic leading to a potential risk of adverse respiratory effect after inhalation

(A) Office

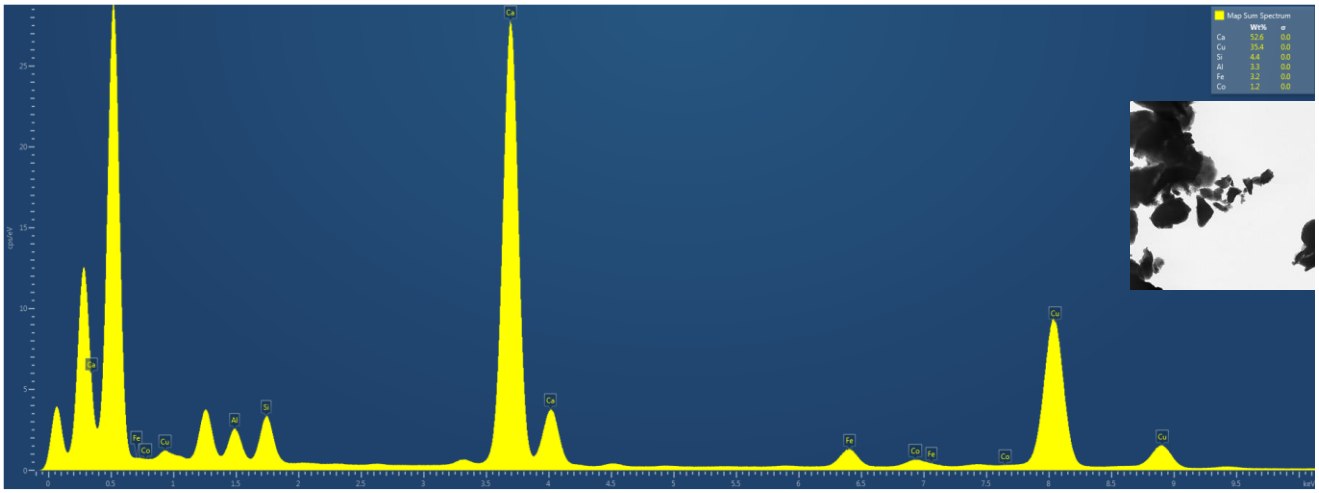

(B) Mine entrance

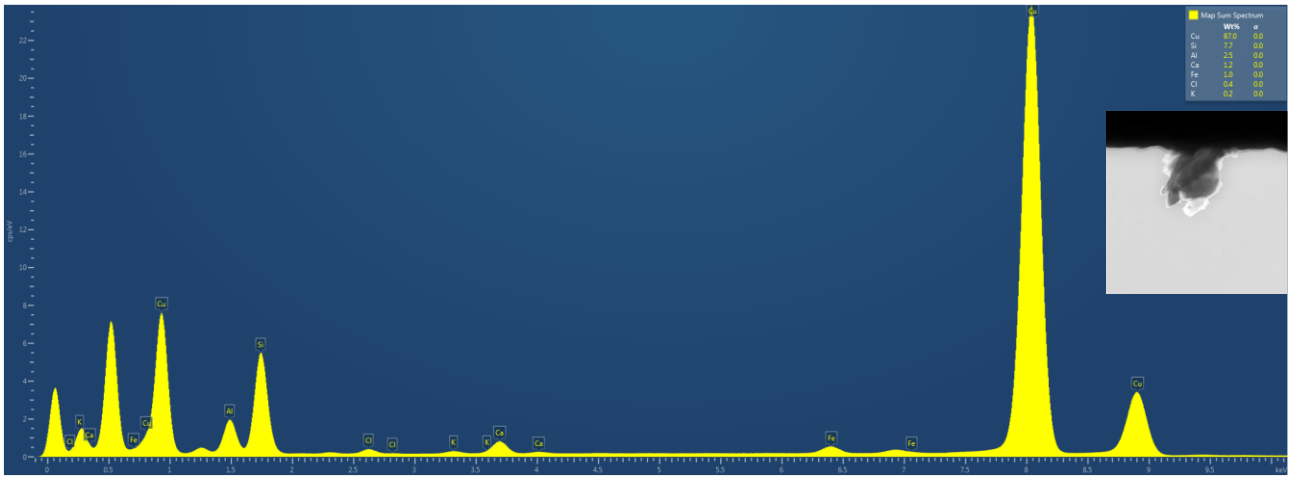

(C) Belt area

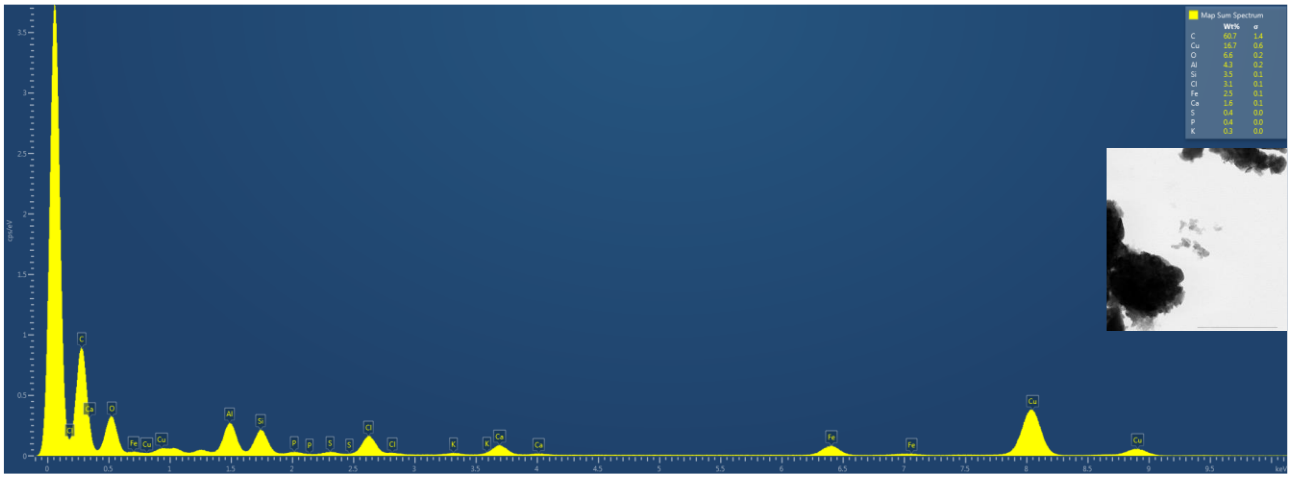

(D) Personal

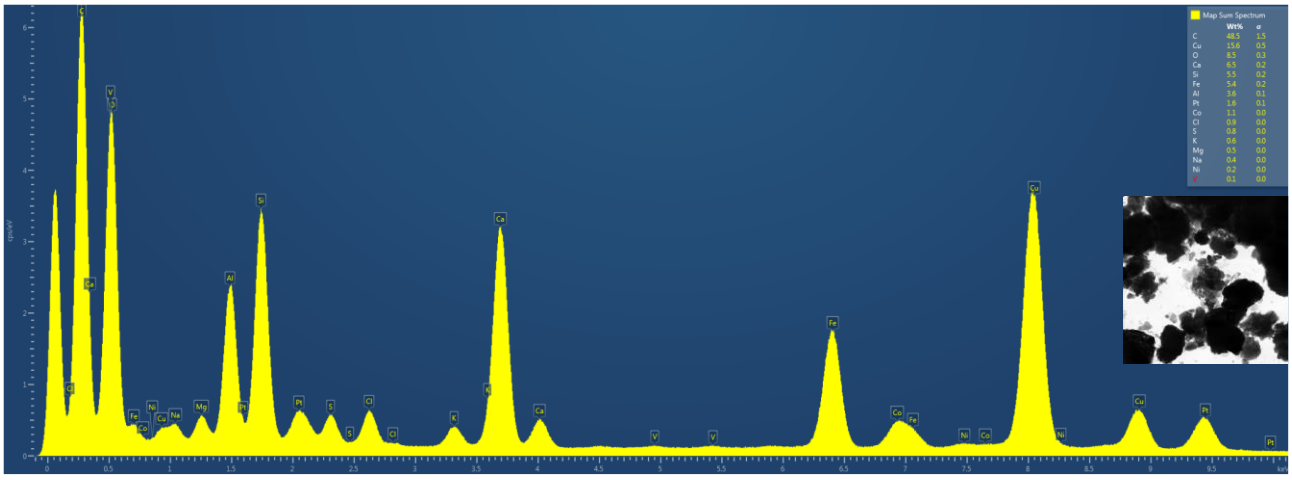

Figure 9. Elemental compositions of dust particles sampled from the underground mine in multiple locations by STEM with EDS. (A) Office; (B) Mine entrance; (C) Belt area; (D) Personal sample at the belt area

Finding summary: The results clearly showed that the belt area exhibited the highest concentration across all size fraction compared to the building office and entrance, and significantly higher concentration of submicron and nanoparticles were found. Mass concentrations obtained from sampling showed a few samples exceed the current PEL of 1.5 mg/m^3. Coal and rock particles were found on the samples collected in the belt area, and more importantly in the personal breathing zone samples. The particles found in the personal samples carry more metal elements, including Pt (1.6%), Co (1.1%), Mg (0.5%), Na (0.4%), and Ni (0.2%), leading to a potential risk to stimulate toxicity after entering organism.

B. Cellular uptake studies and animal cellular uptake studies

a. Cell Culture –

Human bronchial epithelial cells (HBECs), obtained from the American Type Culture Collection (ATCC, Manassas, VA), cultured in supplemented BronchiaLife epithelial airway media, grew well up to the 9th pass.

Finding summary: HBEC cells grew well and showed no signs of transformation for 9 passes. We did not use the HBEC cells after passage 9.

b. ALI Cell Culture –

After 5 weeks of growth in ALI culture the membranes were cut out and submitted to the Research Histology Core at CU Anschutz for Hematoxylin and Eosin (H&E) staining to look at cilia and general morphology and Periodic Acid-Schiff (PAS) staining to determine degree of differentiation. Fig. 10 shows the results of this staining. This experiment proved that we could grow HBECs on the transwell plates (ALI culture) and that proper differentiation had occurred after initial growth.

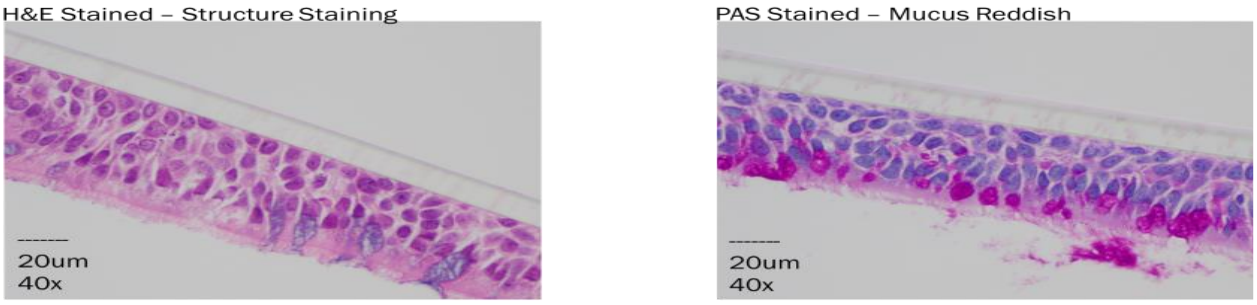

Figure 10. Images of cells grown and differentiated using ALI culture on Transwell plates.

Finding summary: cell culture worked very well in our hands. Differentiation and mucus were clear in images of HBEC cells grown on transwell membranes.

c. Dusting of cells –

In experiment one cells which were exposed for 30 minutes were killed and no results were obtained. The cells dusted for 15 minutes did survive and large coal agglomerations can occasionally be seen on their surface but not inside the cells. Representative samples are shown in Fig. 11. Changes were made in experiment two to try and get smaller particles onto the surface of the cells. The exposure chamber was modified with un upside down funnel to disperse the dust directly over the cells (where the fan is shown in the picture above in section 3.08). Cells were exposed for 0, 10, 15 20 and 30 minutes. Also, some samples were washed before cutting out the membrane for staining and others were not washed before cutting. Results looked like experiment one with most areas not having noticeable coal exposure while other areas had coal on the surface. 30 minutes of exposure did not kill the cells in experiment two. Fig. 12 shows the brightfield microscope 40× picture next to a darkfield microscopy picture of the same spot which shows the coal surrounded by white. In the following task period, we will use high resolution TEM to analyze exposed cells and identify small coal/rock particles.

Finding summary: While we were able to expose cells to coal dust and have pictures of dust on cells, we had difficulty standardizing the size of the coal particles that were generated and exposed on the HBEC cells. We were able to do dark field and bright field microscopy and found coal deposits on the outside of the cells but were never able to determine that coal was taken up by the HBEC cells.

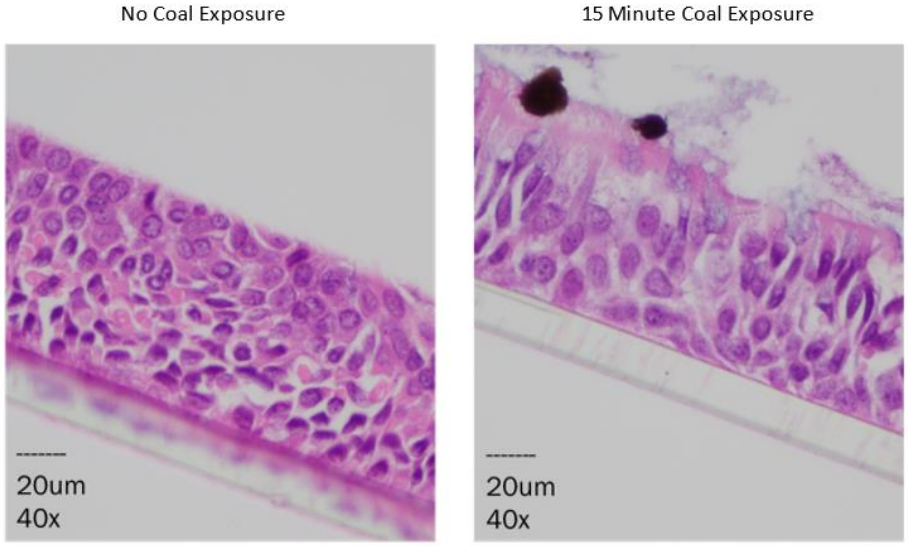

Figure 11. Cell images showing coal particle deposition onto cells grown in ALI culture.

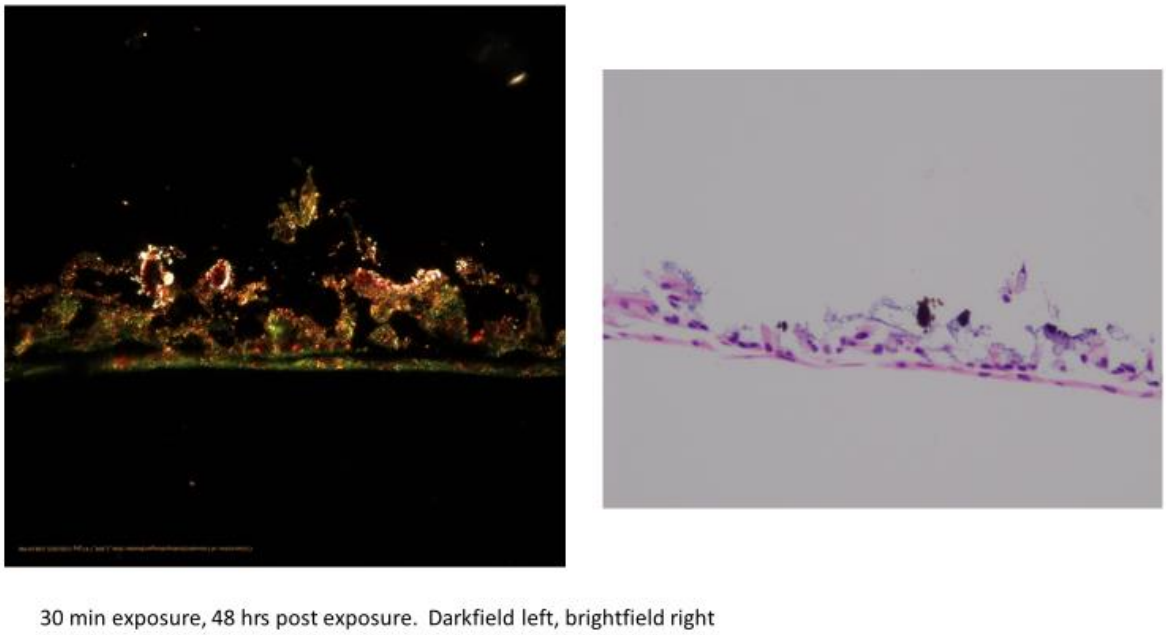

Figure 12. Microscope images of the same location with cells and coal particles using a darkfield and lightfield microscope.

d. Cell uptake analysis using bio-TEM

TEM with an AMT digital camera was used to observe the cell uptake of mine dust treatments on THP-1cells and mice primary bronchial tracheal epithelial cells (MBECs). Fig. 13 showed the morphological and phenotypic cell structure changes which responded to the dust particle stimulations. Fig. 13A and 13D presented the THP-1 cell and MBECs under normal condition, respectively. The vacuum shown on Fig. 13B, 13E, 13C, and 13F occurred after the cells could intake the particles. The coal mine particle treatment significantly contributed to a different level of cellular damage (Fig 13B, 13E, 13C, 13F). Two cell lines exposed to the rock particle both showed observable nuclear swelling. The morphology change represented the mechanical activation for inflammatory lipid signaling. The cell was damaged at a more serious level under coal treatment than rock in both cell lines. For THP-1 cell, the cell exposed to coal dust was on the apoptotic stage already, as seen in Fig. 13C that the cell was collapsing into debris. The coal particles resulted in a similar level impact on the MBECs as seen in Fig. 13F that showed a significantly different structure between rock- and coal-treated MBECs, presenting on the membrane stretching, more vacuums, and greatly nuclear swelling.

(A) THP-1 cell

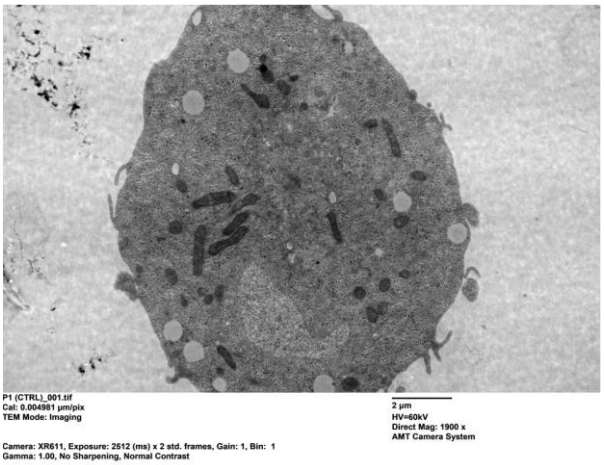

(D) MBECs

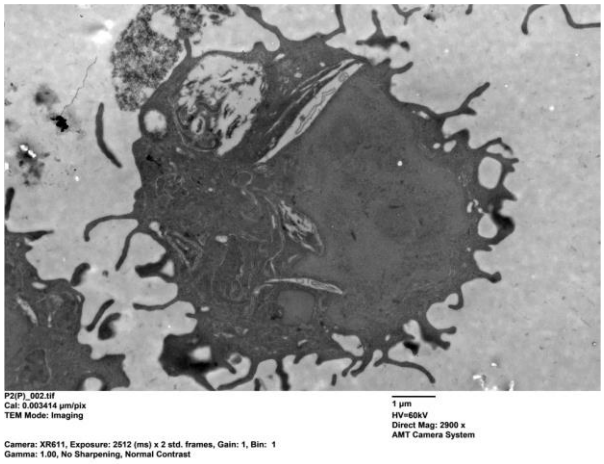

(B) THP-1 treated with rock

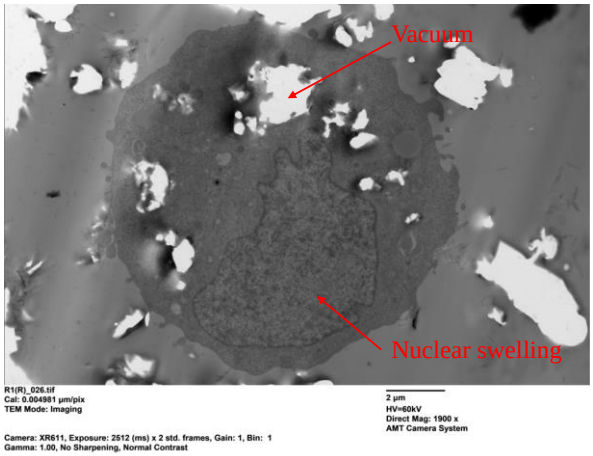

(E) MBECs treated with rock

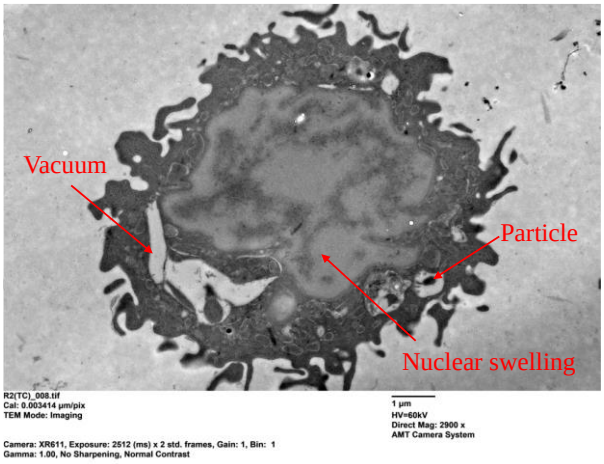

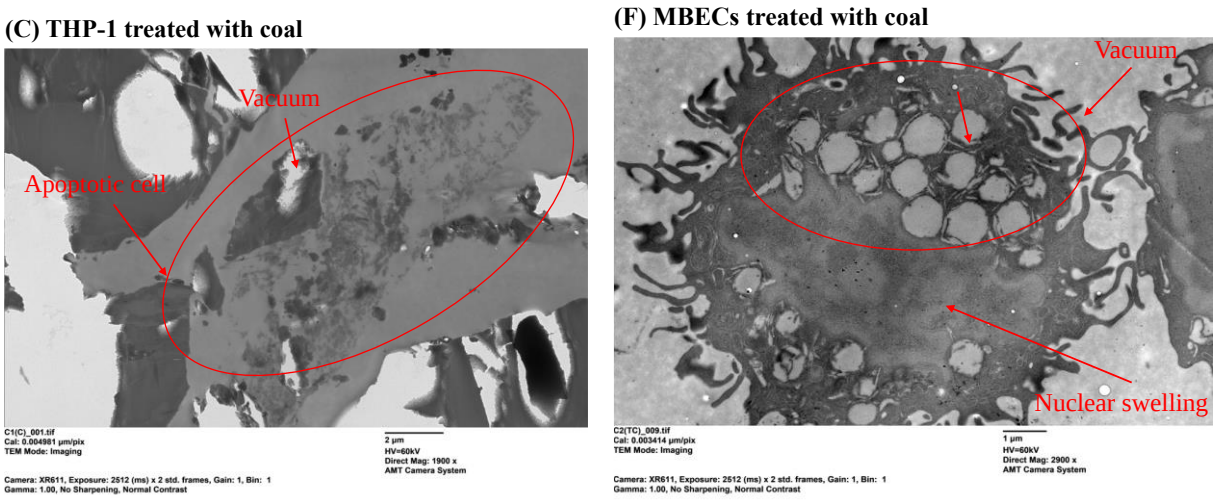

Figure 13. TEM images present the shape, structure, form, and size of (A) THP-1 cells and (D) MBECs changed following uptake of (B and E) rock or (C and F) coal treatments.

Finding summary: The TEM images showed the coal mine dust particle cellular localization and uptake and confirmed that the particles were uptaken in the THP-1 cells and MBECs. The mine dust exposure can stimulate the toxicity effect in different levels from coal and rock dust. The coal particles significantly induced more serious cellular damage than rock dusts, supporting by nuclear swelling and cell death displaying on TEM images. The results are supported by our following cytotoxicity findings.

C. Cytotoxicity and oxidative stress

a.1 MTS Assays (HBECs) –

To determine mitochondrial activity as an indirect measurement of cytotoxicity, MTS was used and cells were assayed at 1,3, and 24 h (1- and 3-hour results are not included due to little variation between sample types). As seen in Fig. 14a-d there was no significant increase in mitochondrial activity at 24 hours for any of the coal sizes or doses. There was a trend towards higher MTS at the top exposure levels, especially 500 µg/ml top coal.

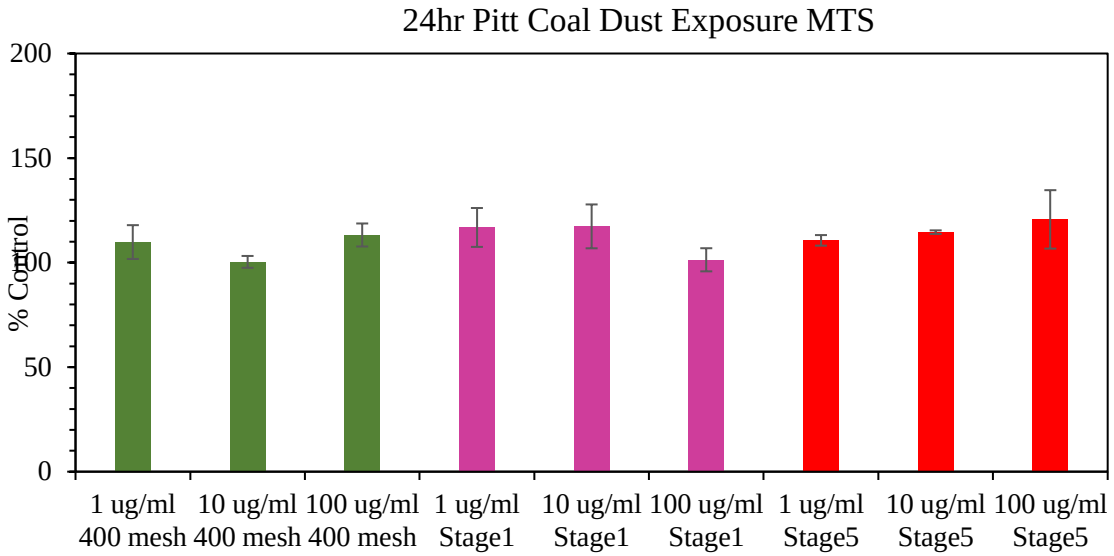

Figure 14a. 24 Hour MTS Results – Various concentrations of 400 mesh, Stage 1 and Stage 5 Pitt Coal

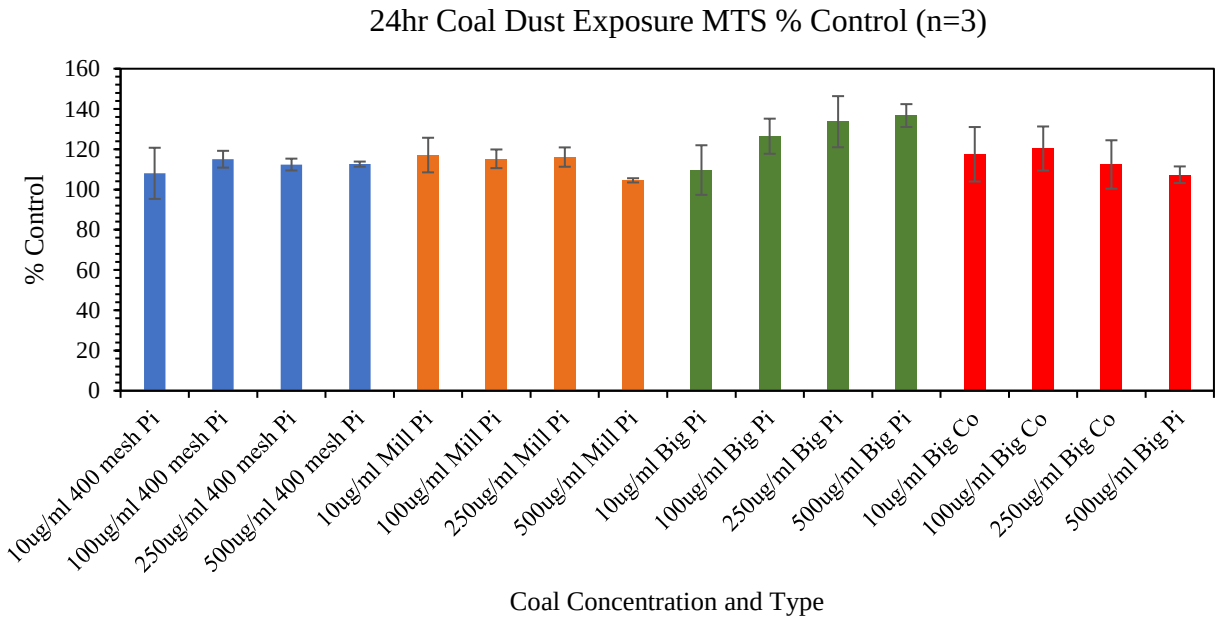

Figure 14b. 24 Hour MTS Results – Various concentrations of 400 mesh, Milled, Big Pitt and Big Colorado Coal.

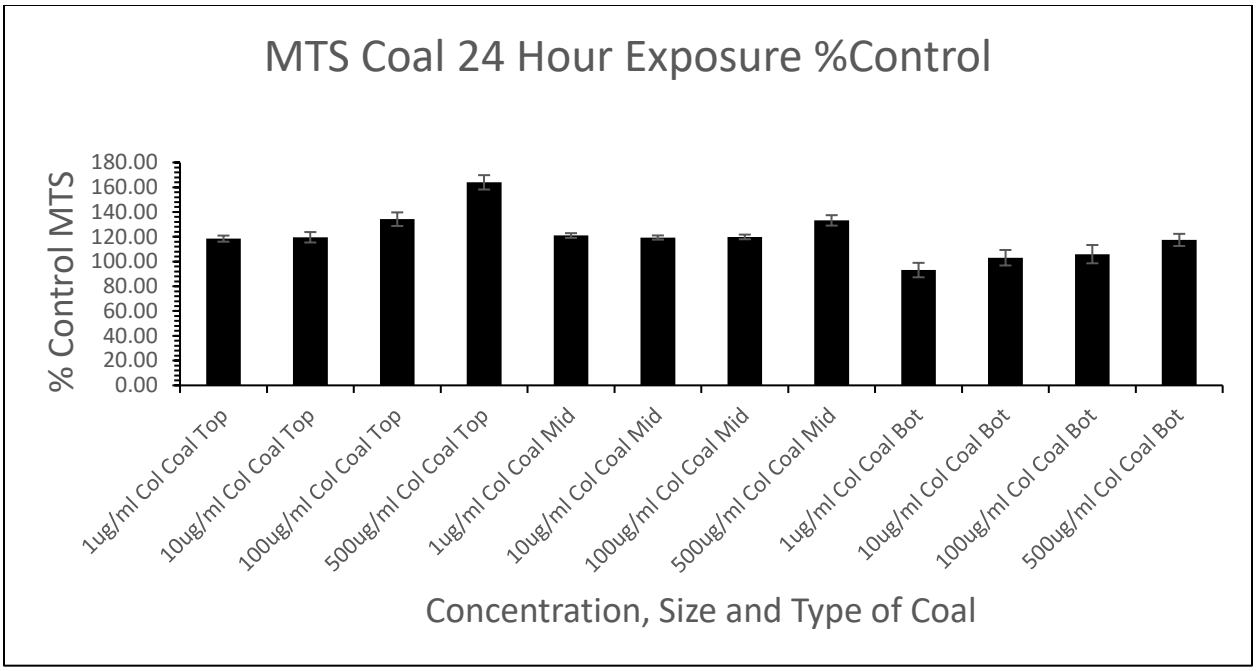

Figure 14c. 24 Hour MTS Results – Various concentrations of Top, Middle and Bottom Colorado Coal.

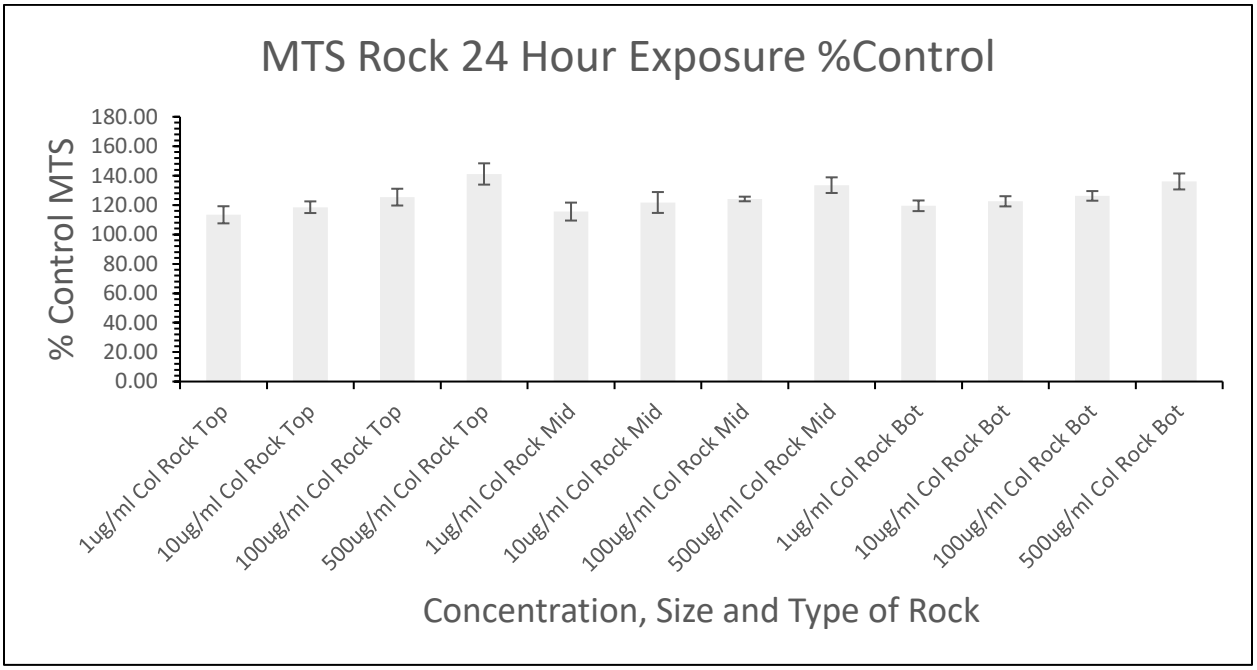

Figure 14d. 24 Hour MTS Results – Various concentrations of Top, Middle and Bottom Colorado Rock.

a.2 MTS Assays (Summary) –

Cell viability determined by MTS assay. There was no significant difference in viability as determined by MTS for THP-1 cells or HBECs treated with any rock or coal size or concentrations (Fig. 15).

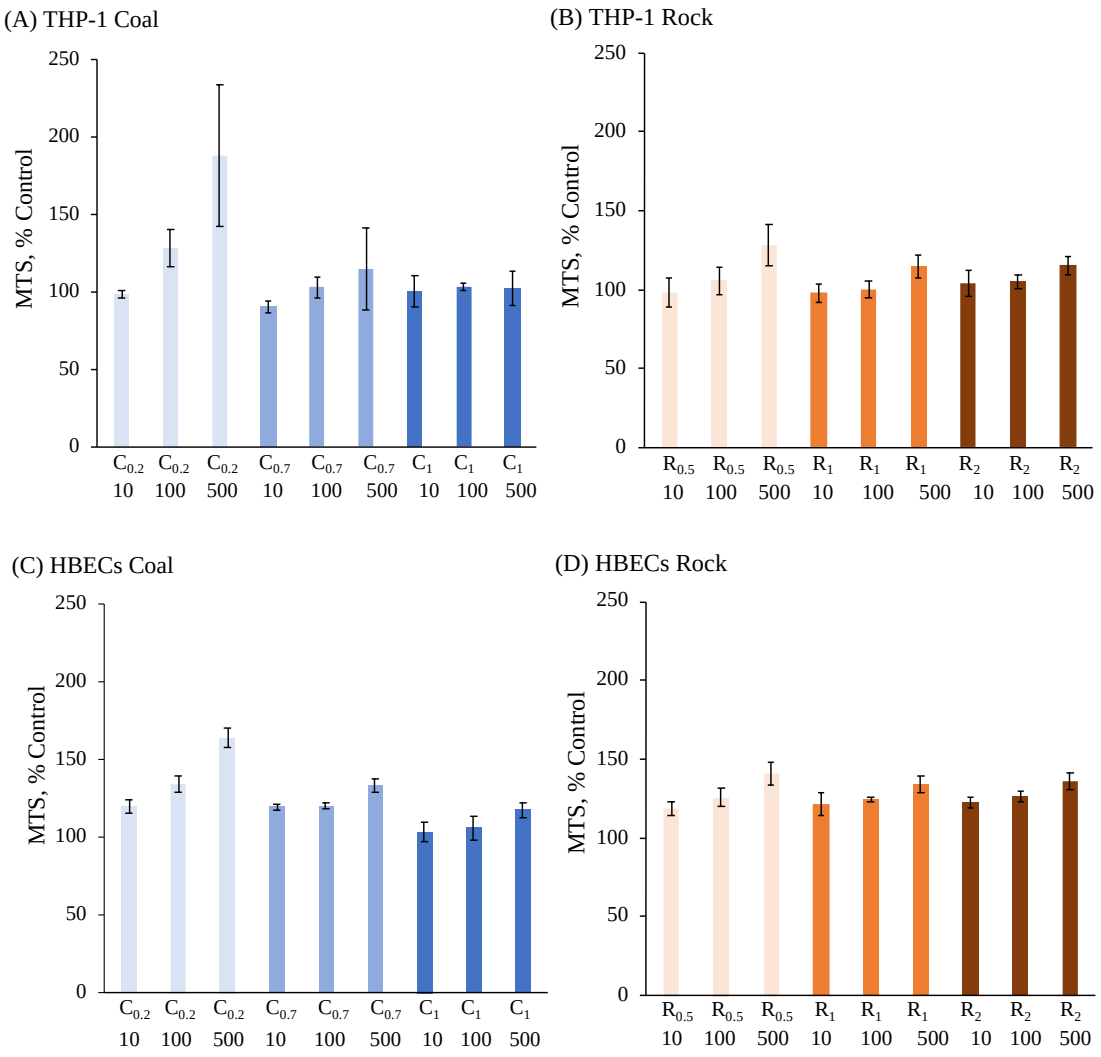

Figure 15. MTS analysis for (A)-(B) THP-1 cells and (C)-(D) HBECs of various coal and rock treatments (10, 100, 500 µg/ml).

Finding summary: MTS assays showed that varying the size of the coal and rock particles did not impact mitochondrial activity. Concentration of particles was the only variable that appeared to affect mitochondrial activity though this finding was not significant.

b. LDH Assays –

As seen in Fig. 16a-d, LDH results for coal and rock dust were similar. LDH release, which is used to determine cell viability, was assessed at 1, 3 and 24 hrs following coal dust exposure at concentrations ranging from 1 – 100 µg/mL (1- and 3-hour results were not included due to little variation between sample types). Fig. 16a-d show there were no significant changes in LDH release at any coal processing type and any dose. There was a trend towards higher LDH release at the top exposure levels, especially at 500 µg/ml.

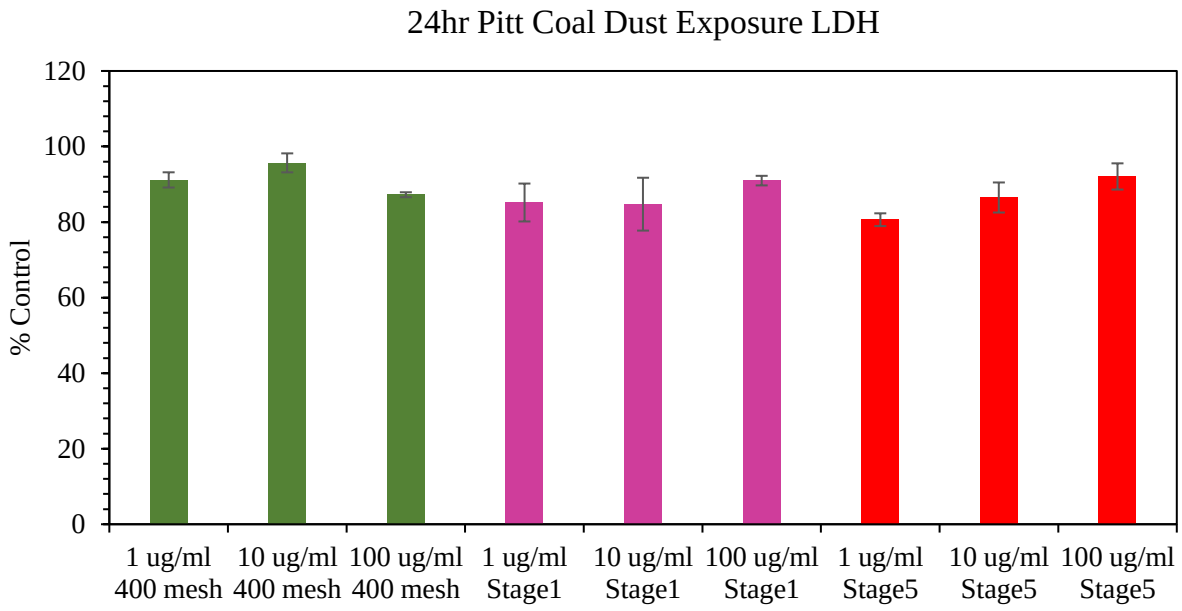

Figure 16a. 24 Hour LDH Results – Various concentrations of 400 mesh, Stage 1 and Stage 5 Pitt Coal

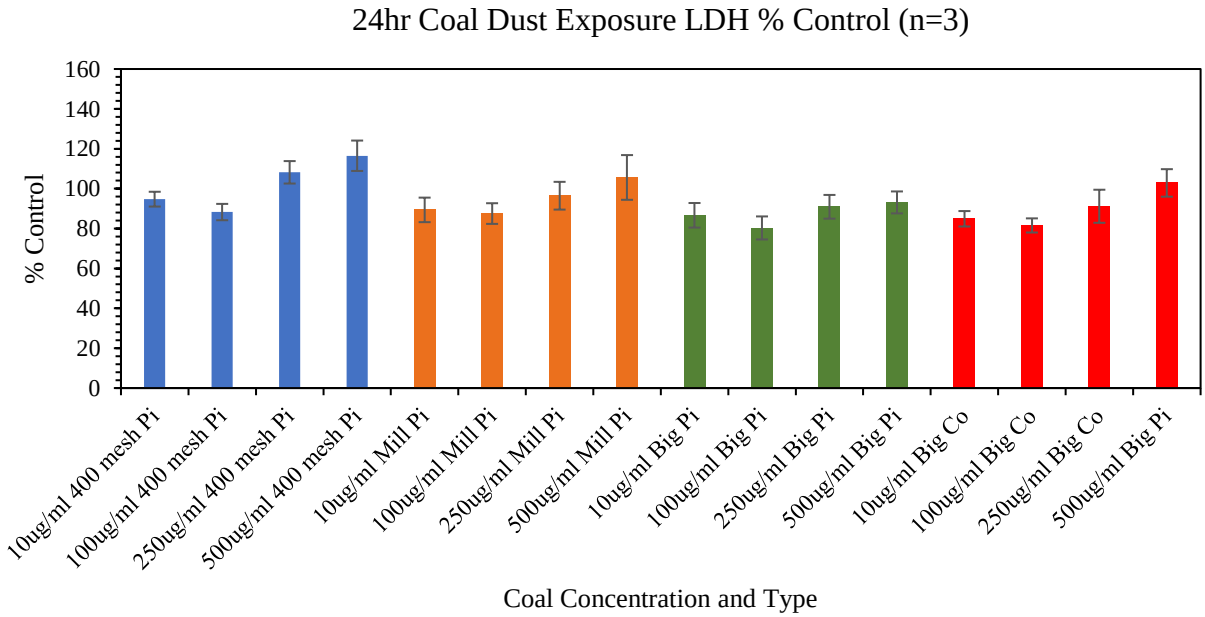

Figure 16b. 24 Hour LDH Results – Various concentrations of 400 Mesh Pitt , Milled Pitt, Big Pitt and Big Colorado Coal.

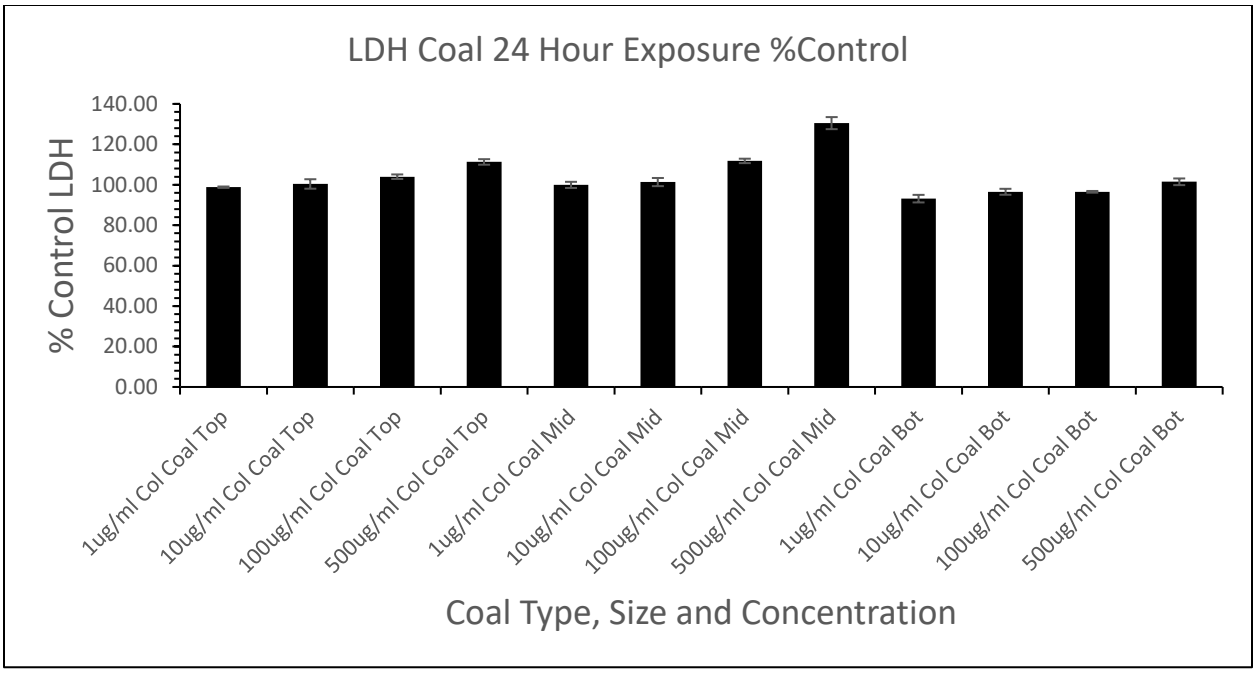

Figure 16c. 24 Hour LDH Results – Various concentrations of Top, Middle and Bottom Colorado Coal.

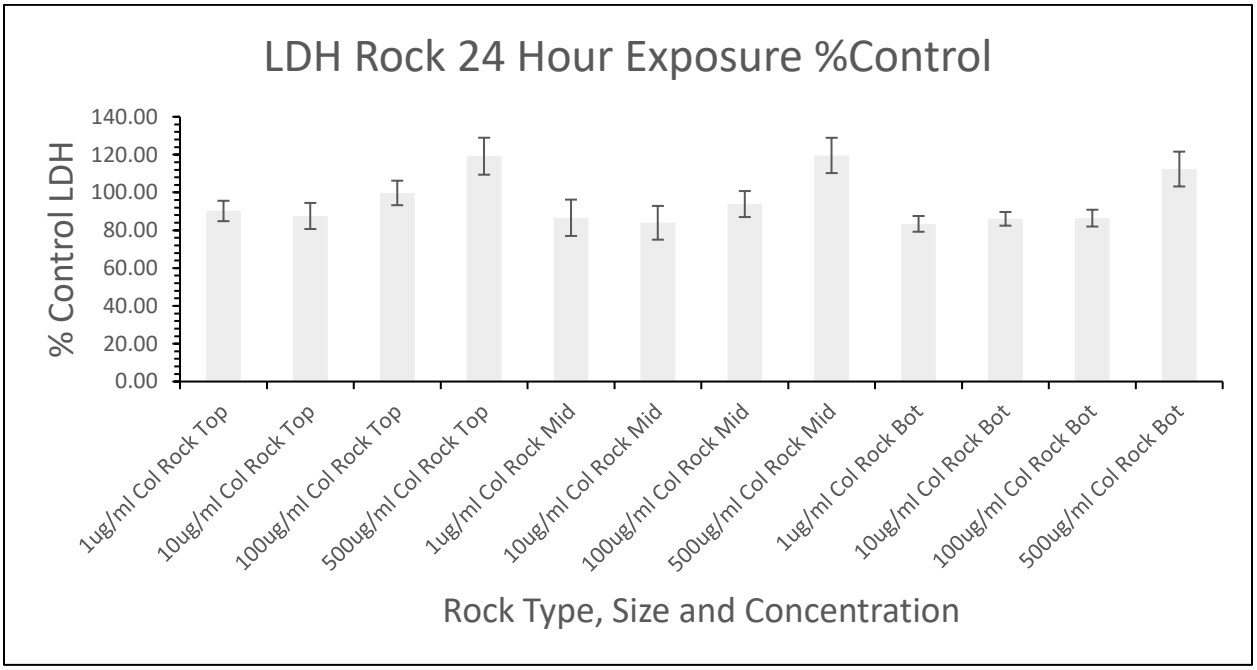

Figure 16d. 24 Hour LDH Results – Various concentrations of Top, Middle and Bottom Colorado Rock.

Finding summary: LDH assays showed that varying the size of the coal and rock particles did not significantly impact cell viability. Overall, the cytotoxicity studies (both MTS and LDH assays) suggest that an acute exposure to the varying size of coal and rock dust was largely not cytotoxic.

c. Seahorse Assays –

a) Experiment One - As shown in Fig. 17, coal and rock exposure leads to increased basal respiration, ATP production and proton leak at higher coal/rock levels. Generally, rock dust tends to cause slightly larger increases than coal dust, which is an indication that the rock dust is putting HBEC cells under more stress than coal. After consulting with the Agilent representative, we believe the 500 µg/ml wells for small coal and middle coal were due to cell damage. It is normal to see an increase in these parameters with increased stress and then a drop in these parameters as damage/toxicity occurs, and the cell becomes overwhelmed. Maximal respiration and spare respiratory capacity, shown in Fig. 18, give an idea of how much the cells can ramp up energy production to deal with stress. These results indicate that rock dust treated cells have a higher capacity to respond to stress than the cells treated with coal dust. As shown in Fig. 19, non-mitochondrial oxygen consumption is greatly increased in the rock dust treated cells but only a little in the coal dust treated cells. Finally, coupling efficiency, which indicates how much of the ATP produced is linked to basal respiration remains high and constant across all treatments.

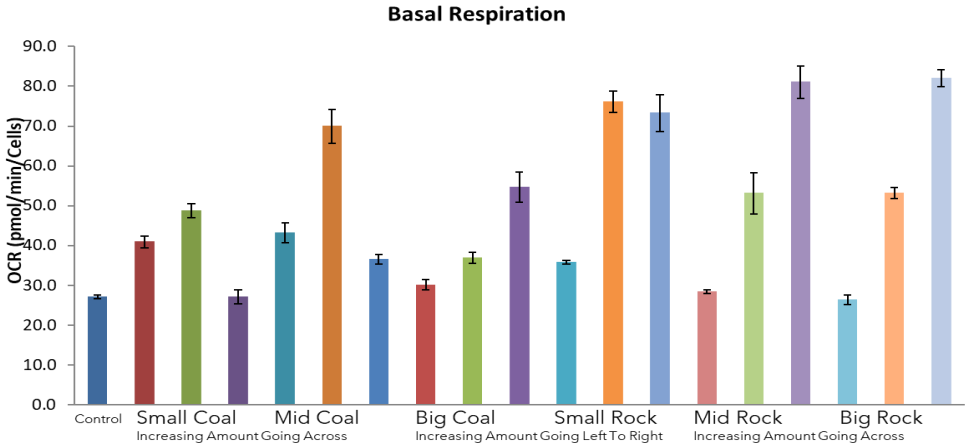

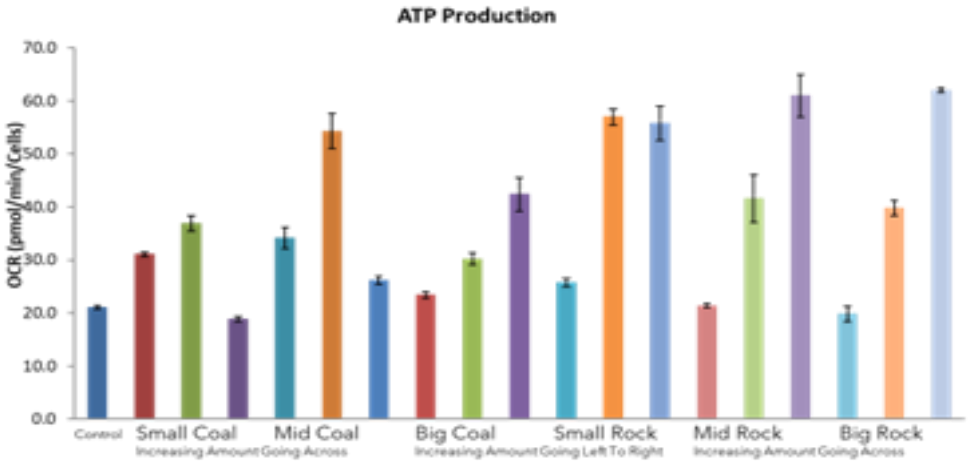

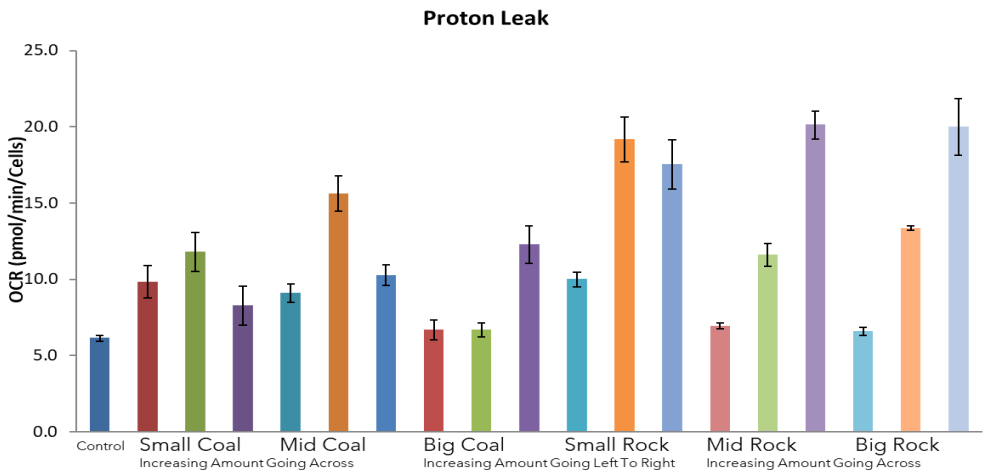

Figure 17. Basal respiration, ATP production and proton leak results of 3 different sized coal and rock particle exposure.

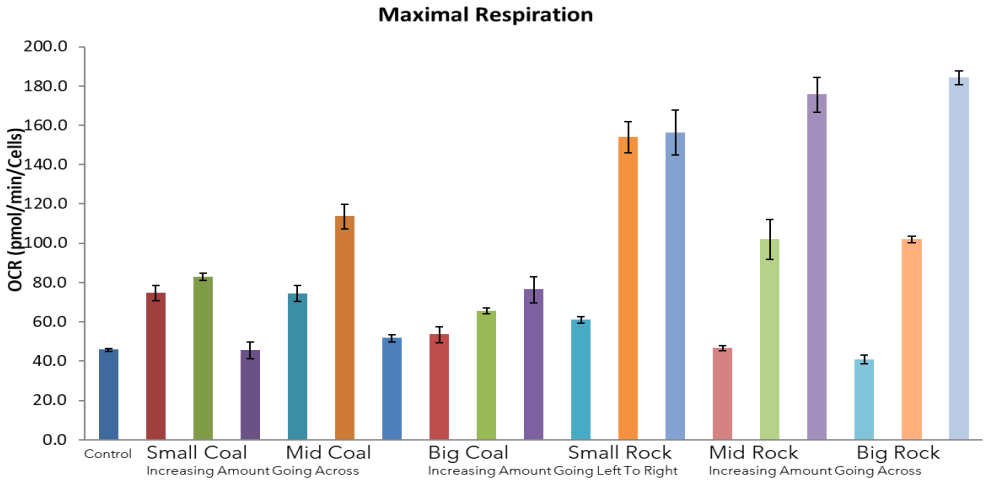

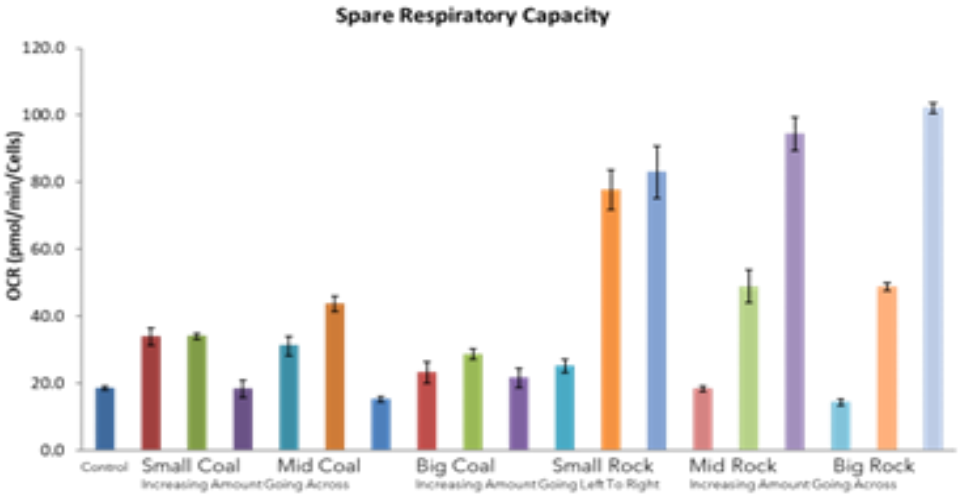

Figure 18. Maximal respiration and spare respiratory capacity of 3 different sized coal and rock particle exposure.

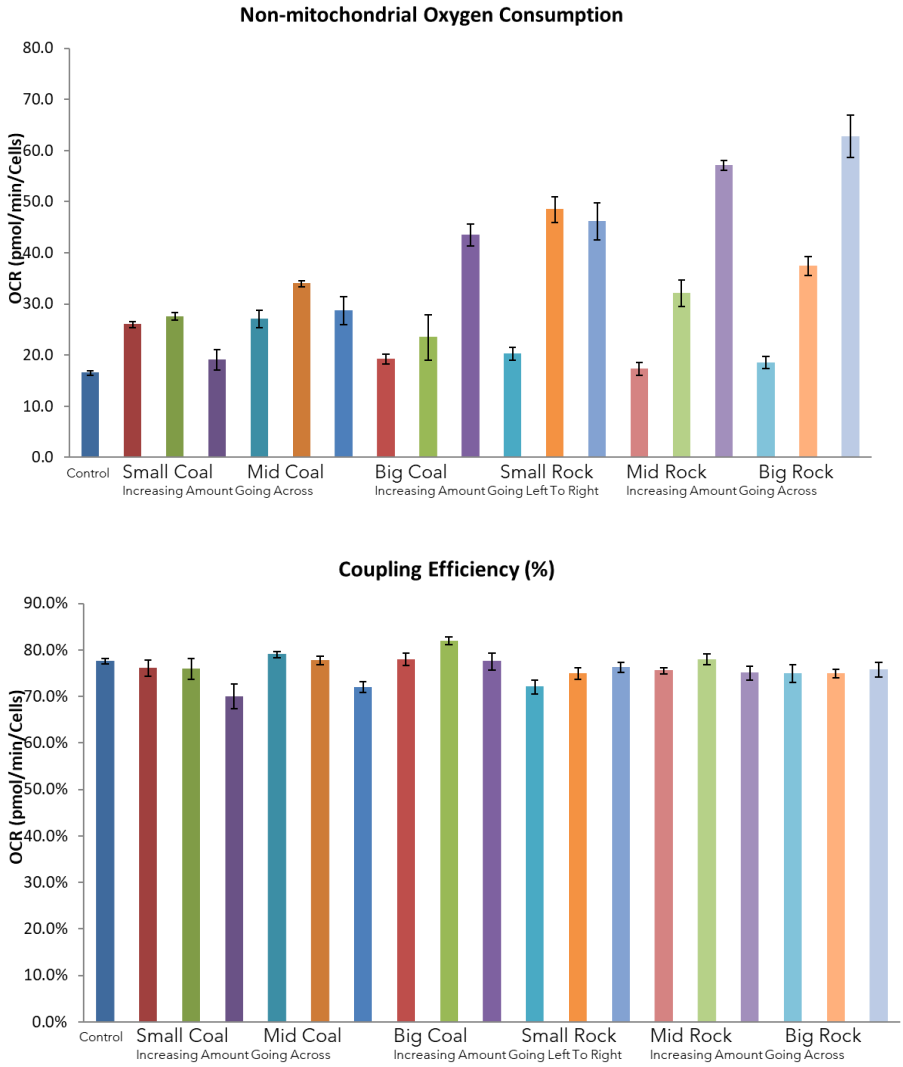

Figure 19. non-mitochondrial oxygen consumption and coupling efficiency of 3 different sized coal and rock particle exposure.

b) Seahorse Experiment Two - As shown in Fig. 20, and in previous experiments, coal and rock exposure leads to increased basal respiration and ATP production at higher coal/rock levels. As in the last experiments, the rock dust heavy mixture caused a slightly larger increase than coal dust heavy mixture at 100ug/ml, which is an indication that the rock dust is putting HBEC cells under more stress than coal. Maximal respiration and spare respiratory capacity, shown in Fig. 21, give an idea of how much the cells can ramp up energy production to deal with stress. These results indicate that HBEC cells treated with mixtures containing more rock dust have a higher capacity to respond to stress than the cells treated with more coal dust. Results for the East South and South mine samples look similar to

the higher rock sample. As shown in Fig. 22, coupling efficiency, which indicates how much of the ATP produced, is linked to basal respiration remains high and constant across all treatments.

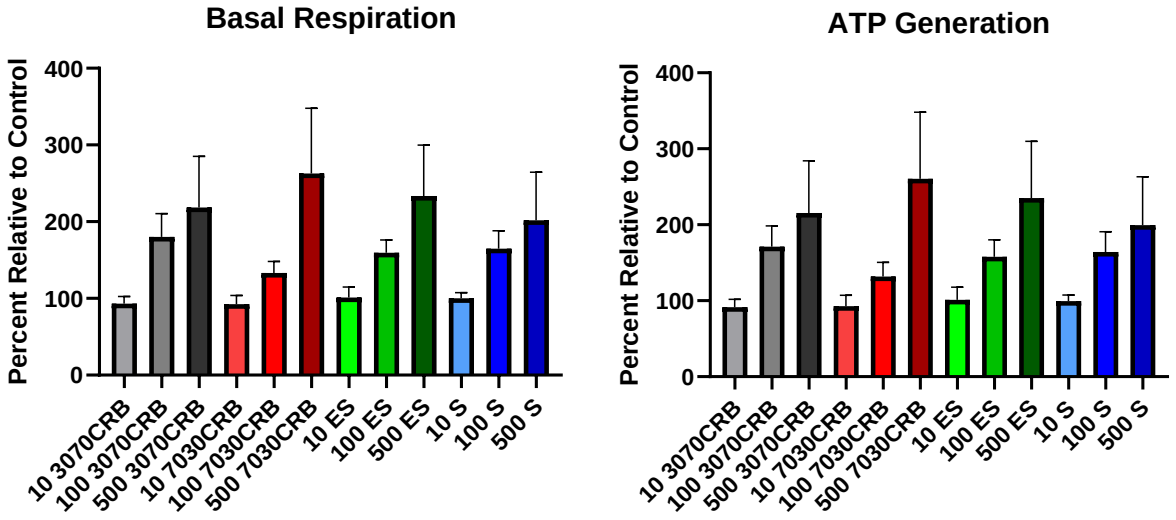

Figure 20. Basal respiration and ATP production results for the 4 treatment groups (East South Mine, Sunset mine, and the 70/30 and 30/70 Colorado Bottom coal and rock mixtures)

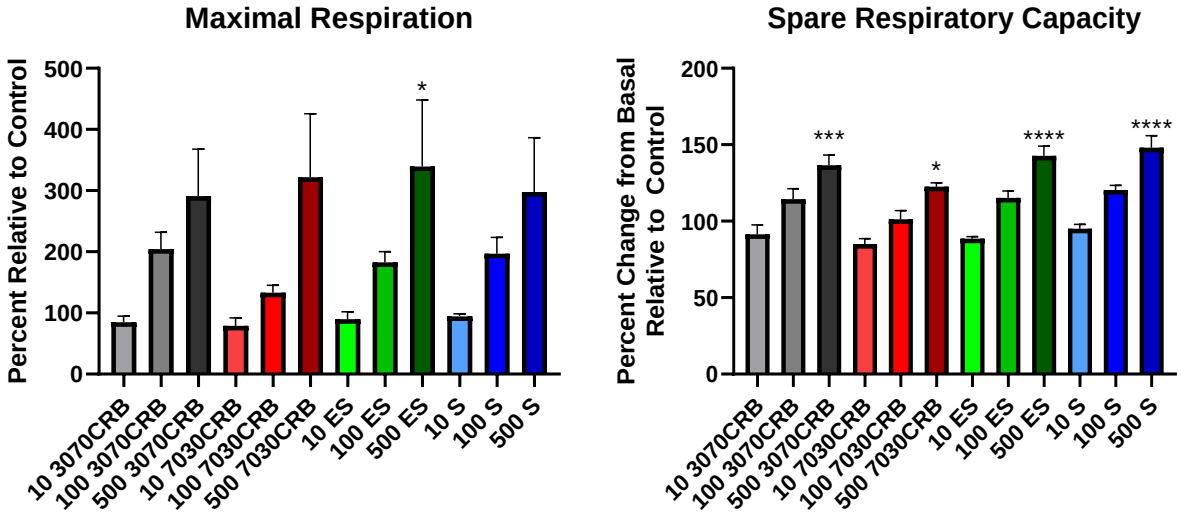

Figure 21. Maximal respiration and spare respiratory capacity results for the 4 treatment groups (East South M2ne, Sunset mine, and the 70/30 and 30/70 Colorado Bottom coal and rock mixtures).

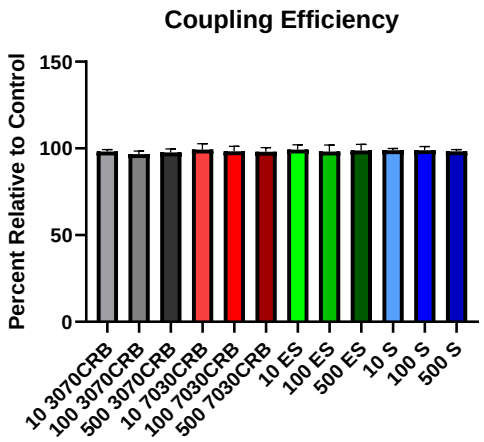

Figure 22. Coupling efficiency results for the 4 treatment groups (East South Mine, Sunset mine, and the 70/30 and 30/70 Colorado Bottom coal and rock mixtures).

Finding summary: Overall, these results demonstrate the exposure of human bronchial epithelial cells to coal and rock dust induces cellular metabolic changes. These metabolic changes are indicative of cellular stress which is a precursor to cellular toxicity and inflammatory responses. Since we did not observe and significant cell toxicity, it appears the cells were able to adapt to the cellular stress. Similar changes to cellular metabolism are also observed in other fibrotic lung diseases. In addition, cellular stress can lead to inflammatory responses and as noted in our cytokine analysis section, we did observe some inflammatory responses in the absence of direct toxicity.

d. 1 ATP Light Assays (HBECs) -

As seen in Fig. 23 the ATP levels were reduced in all coal 500 ug/ml treatments. It is notable that none of the larger coal fractions significantly reduced HBECs ATP at 10 or 100 μg/ml. The ATP levels after rock treatment of HBECs showed no significant differences. These results suggest that the coal is causing a stress response leading to reduced ATP levels as the cell attempts to adapt.

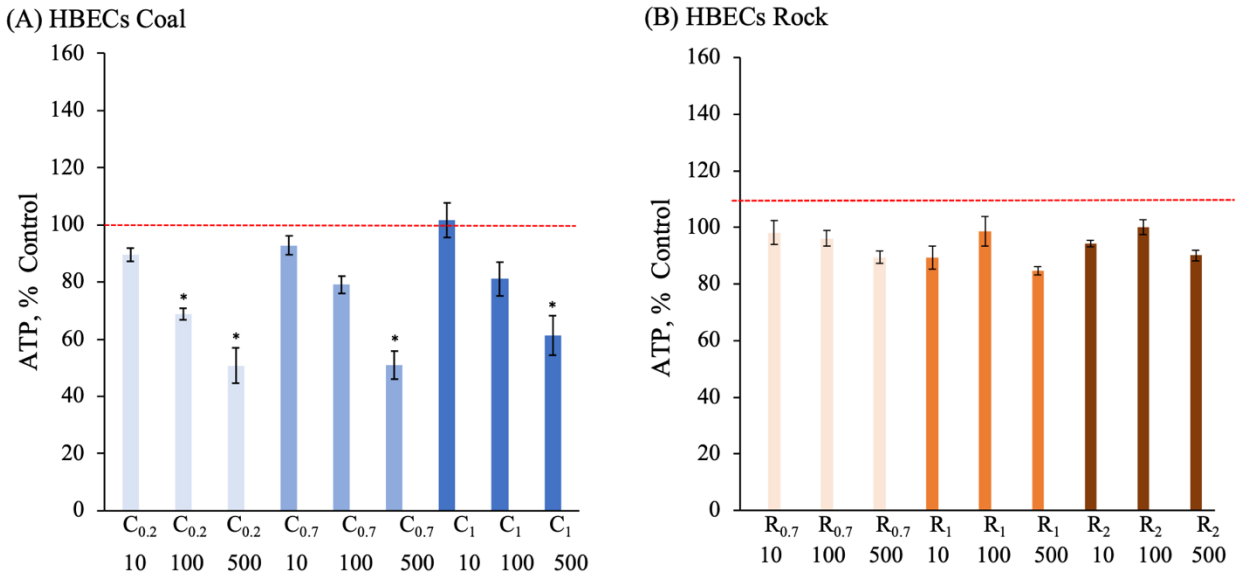

Figure 23. ATP Light assay results for top coal ($C_{0.2}$), middle coal ($C_{0.7}$), bottom coal (C_1), top rock ($R_{0.7}$), (R_1) and (R_2).

d. 2 <u>ATP Light Assays (HBECs)</u> -

ATP levels displayed a decrease in coal-treated THP-1 cells and were significantly lower in the cells treated with fine coal particles at the highest concentration ($C_{0.2,\ 500}$) as compared to untreated cells ($p<0.05$) (Fig. 24 (A)).

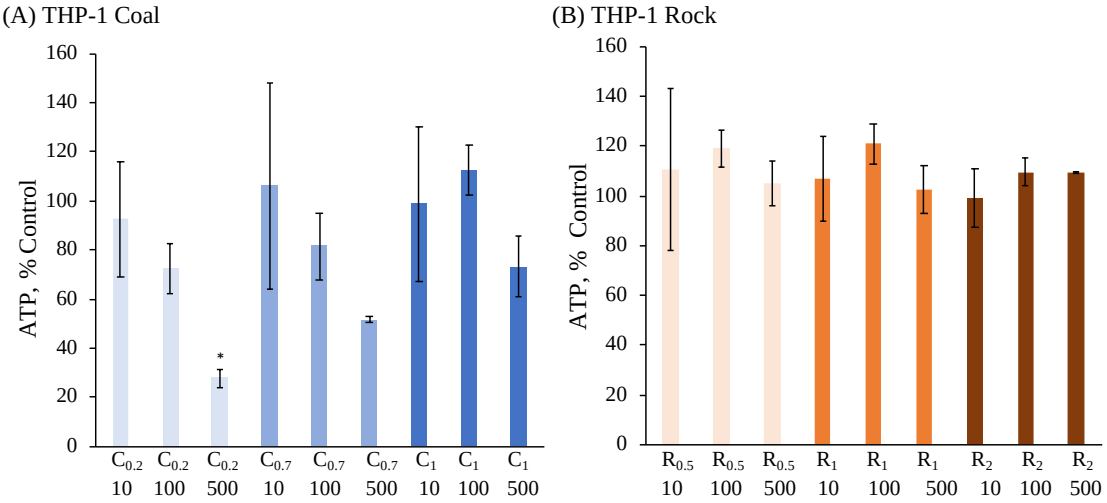

Figure 24. (A)-(B): ATP analysis for THP-1 cells of various coal and rock treatments (10, 100, 500 µg/ml).

Finding summary: Overall, these results demonstrate the exposure of human bronchial epithelial cells to coal and rock dust induces cellular metabolic changes as indicated by decreased ATP levels. As we observed with the Seahorse results previously, these metabolic changes are indicative of cellular stress but the cells seemed to be able to adapt to this stress as we did not observe toxicity.

D. Inflammation measurements

a. Cytokine PCR Assays (HBECs) -

As shown in Table 2a-c, cytokine levels increased with increasing coal exposure (24 hours). The results created a concern about possible endotoxin exposure which is addressed in the next section.

Table 2a. TNF Results

Treatment	Average fold change TNF	sd	n
No Treatment 1	1	0	3
1ug/ml pitt 400 mesh	2.41	2.28	3
10ug/ml pitt 400 mesh	2.10	1.44	3
100ug/ml pitt 400 mesh	10.30	12.23	3
500ug/ml pitt 400 mesh	23.66	21.79	3
1000ug/ml pitt 400 mesh	24.22		1
Treatment	Average fold change TNF	sd	n
No Treatment 2	1	0	3
1ug/ml pitt big	0.94	0.58	3
10ug/ml pitt big	2.51	2.29	3
100ug/ml pitt big	4.09	2.51	3
500ug/ml pitt big	11.28	1.74	3
1000ug/ml pitt big	8.15	5.88	3

Table 2b. IL-1B Results

Treatment	Average fold change IL1B	sd	n
No Treatment 1	1	0	3
1ug/ml pitt 400 mesh	1.28	0.24	3
10ug/ml pitt 400 mesh	1.75	0.95	3
100ug/ml pitt 400 mesh	4.21	3.31	3
500ug/ml pitt 400 mesh	7.80	10.22	2
1000ug/ml pitt 400 mesh	0.60		1
Treatment	Average fold change IL1B	sd	n
No Treatment 2	1.00	0.00	3
1ug/ml pitt big	1.34	0.67	3
10ug/ml pitt big	1.15	1.00	3

100ug/ml pitt big	2.54	0.98	3
500ug/ml pitt big	7.12	4.87	3
1000ug/ml pitt big	7.88	3.44	3

Table 2c. IL-6 Results

Treatment	Average fold change IL6	sd	n
No Treatment 1	1.00	0	2
1ug/ml pitt 400 mesh	1.94	0.43	2
10ug/ml pitt 400 mesh	2.29	1.29	2
100ug/ml pitt 400 mesh	48.20	40.02	2
500ug/ml pitt 400 mesh	218.78	303.58	2
1000ug/ml pitt 400 mesh			1
Treatment	Average fold change IL6	sd	n
No Treatment 2	1.00	0.00	2
1ug/ml pitt big	1.04	0.64	2
10ug/ml pitt big	1.42	0.84	2
100ug/ml pitt big	4.56	1.35	2
500ug/ml pitt big	17.40	1.65	2
1000ug/ml pitt big	1434.00	0.56	2

Finding summary: We saw that 24 hours of treatment with 400 mesh (smaller) coal created more TNF and IL-6 than larger coal particles, while IL-1 remained unchanged with exposure to different sized coal particles. This result is common with endotoxin contamination which led us to test our samples for endotoxin.

b. Endotoxin Testing –

The results of this initial coal testing on the Pitt coal showed the media, Colorado coal and less processed Big Pittsburg coal samples were not contaminated with endotoxin. In contrast, the 400 mesh Pittsburg coal samples showed endotoxin contamination near the top of the assay curve. As seen in Fig. 25 the Top, Middle and Bottom Pittsburg coal samples were also contaminated with endotoxin and the rock samples were not; therefore, it was decided to size fractionate and use Colorado coal samples, that were previously determined to be uncontaminated with endotoxin, for further experiments.

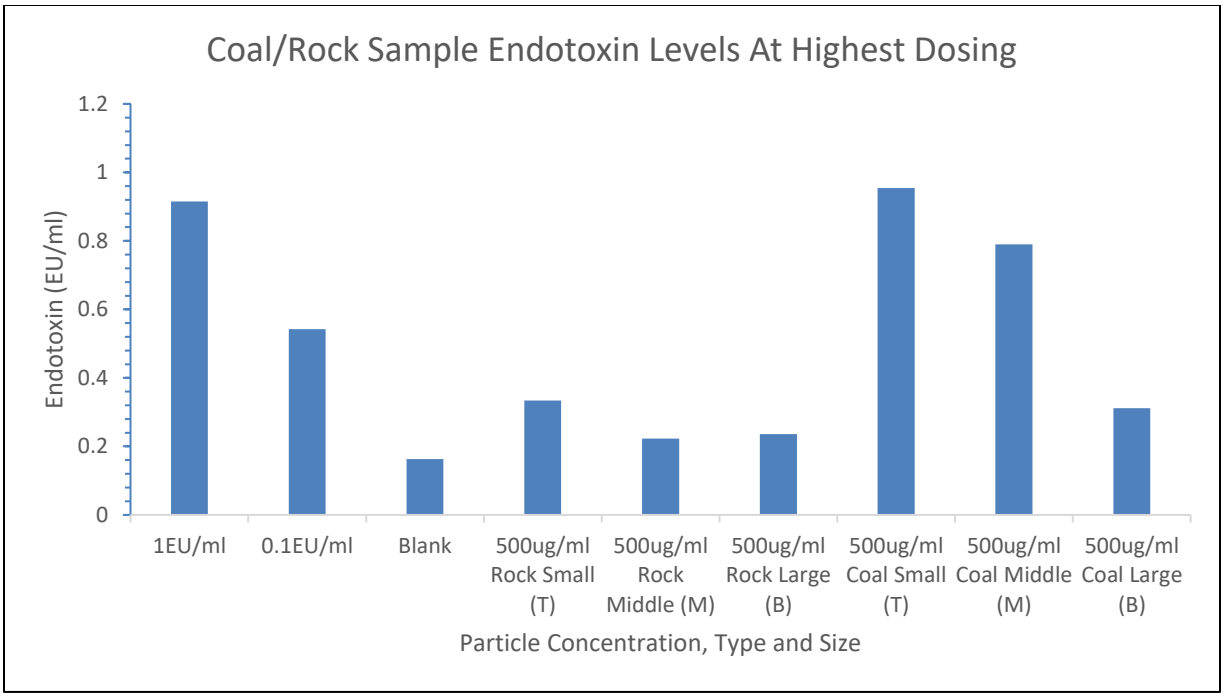

Figure 25. Endotoxin testing of Rock and Pitt Coal samples.
Finding summary: Endotoxin was found in our 400 mesh Pitt coal samples and samples prepared from the 400 mesh Pitt coal samples. Our response was to size differentiate the uncontaminated Colorado coal and use the top, middle and bottom separations in subsequent experiments.

c. Cytokine PCR Assays (THP-1) –

Fig. 26 show the inflammation markers for THP-1 cells following treatment with coal and rock dust. The expression of cytokines was all upregulated exposure concentration increased. More interesting than the relationship of higher inflammation with concentration, is its dependence on size.
Smaller size fractions consistently induced higher cytokine release across both cell lines.THP-1 cells exposed to $C_{0.2}$ generated significantly higher interleukin-1β (IL-1β) and TNF-α levels than the control, $C_{0.7}$ and C_1 groups at the highest concentration (500 μg/ml) (Fig. 26 (A) and 26 (C)). THP-1 IL-1β levels induced by rock show the same trend: $R_{0.5}$ induced significantly higher IL-1β and TNF-α expression than the larger-sized R_1 and R_2 treatments (Fig. 26 (B) and 26 (D)). In fact, when treatment concentration is controlled for, size alone is correlated with these responses. Size has a negative correlation with TNF-α expression in both rock and coal at 10 and 500 μg/ml, as well as with IL-1β in all coal treatments and 100 and 500 μg/ml rock treatments (Table 3 and Fig. 27).

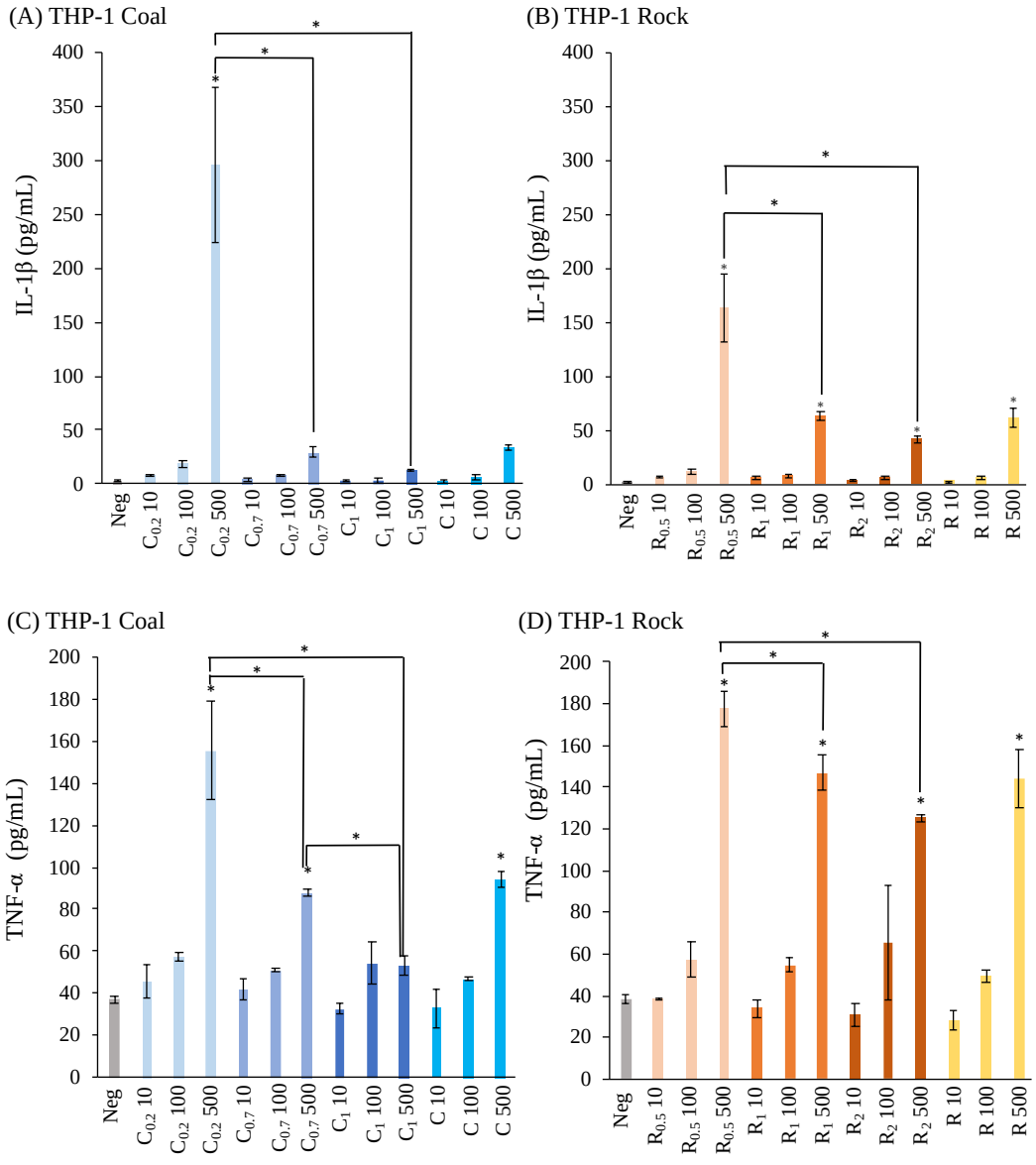

Figure 26. Inflammatory cytokines expressions for THP-1 cells of various coal and rock dust treatment (10, 100, 500 µg/ml): (A)-(B) IL-1β; (C)-(D) TNF-α.

Table 3. Pearson's correlation of inflammation cytokines (TNF-α, IL-1β, and IL-6) between sized-mining dusts of three exposure concentration (10, 100, 500 μg/ml).
The mining dusts are ranked as following in the analysis: the smallest size of dust particles ($C_{0.2}$ and $R_{0.5}$)=1, the middle size of dust particles ($C_{0.7}$ and R_1) =2, and the biggest size of dust particles (C_1 and R_2).

Concentration (μg/ml)	Mining dust	THP-1 TNF-α		THP-1 IL-1β		HBECs IL-6	
		Coefficient, r	*p*-Value	Coefficient, r	*p*-Value	Coefficient, r	*p*-Value
10	Coal	-0.791	0.011*	-0.900	0.0011*	-0.685	0.042*
	Rock	-0.791	0.011*	-0.580	0.1322	-0.580	0.102
100	Coal	-0.474	0.197	-0.949	0.0001***	-0.527	0.145
	Rock	-0.053	0.893	-0.791	0.0112*	-0.211	0.586
500	Coal	-0.949	0.0001***	-0.949	0.0001***	-0.316	0.407
	Rock	-0.949	0.0001***	-0.949	0.0001***	-0.474	0.197

* $p < 0.05$; ** $p < 0.01$; *** $p < 0.0001$

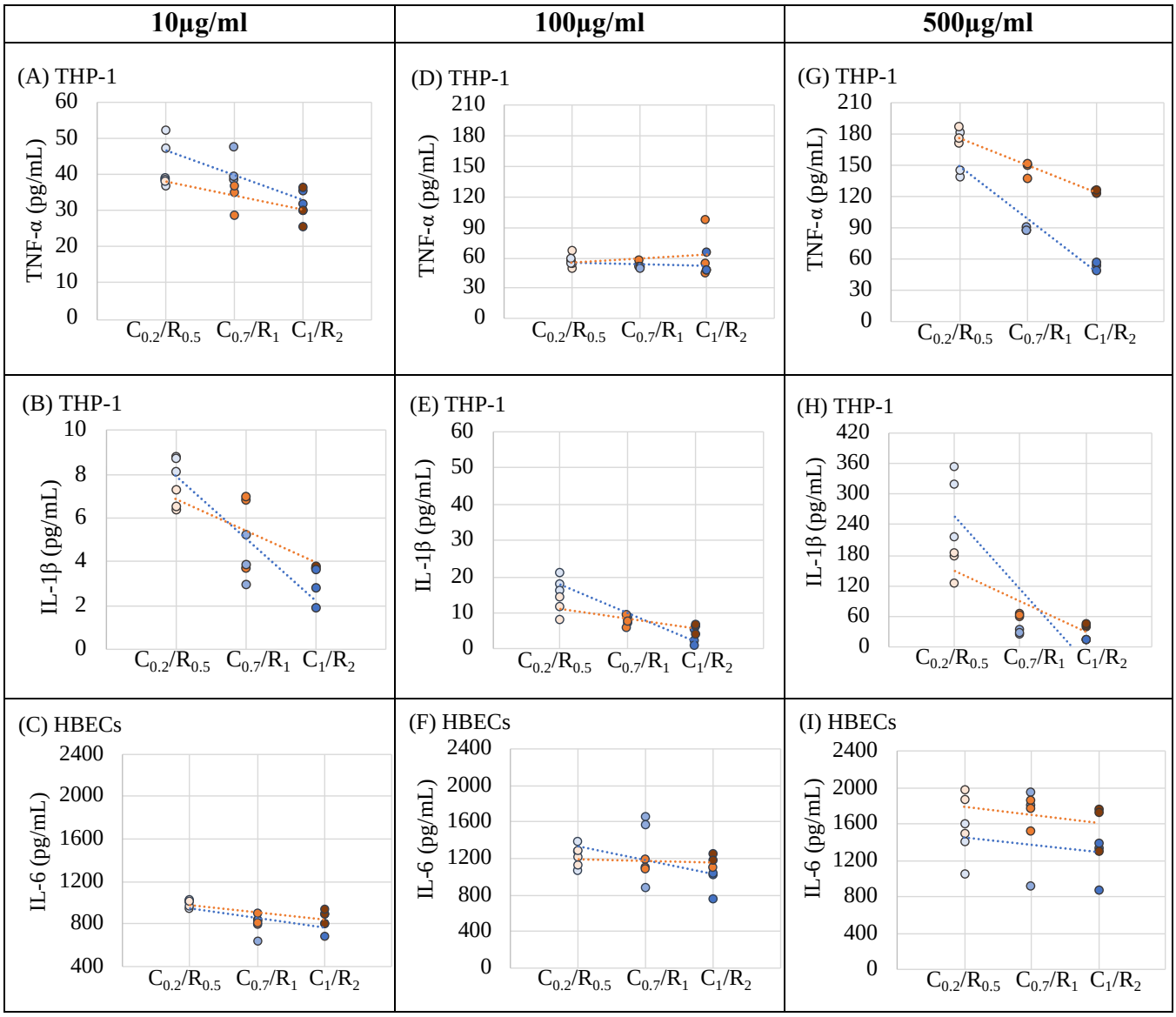

Figure 27. The correlation of inflammation cytokines (TNF-α, IL-1β, IL-6) between sized-mining dusts of three exposure concentration (10, 100, 500 µg/ml). Blue dot line is Coal; Red dot line is Rock.

Finding summary: As noted above, we observed that coal and rock dust induced cellular stress but did not result in cell toxicity. However, it appears that the cell response largely consists of inflammatory cytokine responses as shown in the HBEC and THP1 cells. Overall, we saw a dose response like relationship with the increasing particle number resulting in higher cytokine production and release. But more importantly, we show that the smaller coal dust results in a greater amount of cytokine production. This could be related to the amount of particles being taken up into the cell or a greater number of particles per mass in the smaller fraction of coal dust. Overall, it is clear that the smaller particles do induce a greater inflammatory response despite no direct toxicity. We would predict based on these data that long-

term exposure to smaller particles would lead to greater inflammation of lungs of coal miners which would ultimately suggest greater lung disease.

E. Dust characterization and dose-response effect analysis: including animal study

a. DLS Sizing of Coal and Rock Particles -

DLS sizing of Coal and Rock Particles – Overall results showed that the coal and rock particles agglomerated quickly after sonication so DLS results were not optimal.

a) DLS Experiment #1 - Table 4a shows that we saw similar results when comparing coal dust to the previous rock dust results. The average size of particles measured in the 400 mesh and ball milled samples in media was generally in the 500-650 nm range at the 1:100 dilution while the more refined Anderson cascade samples appeared to be bigger due to agglomeration. We conclude that the Z-average numbers for the less processed coal particles were lower due to the larger particles falling out of solution which was a visible phenomenon.

Table 4a. Particle characterization using DLS method for coal and rock dust.

DLS Results Hand-Sonication Method (1/100)					
Sample	Z-Ave d.nm	SD	PdI	SD	~ Primary Peak Number (different reads) nm
400MeshPitt	558.2	125.1	0.5	0.1	180, 240, 270
400MeshColo	499.3	152.8	0.5	0.2	120, 180, 200
400 Mesh Rock	614.3	165.4	0.6	0.1	168, 149, 264
Ball Milled Pitt	519.0	242.3	0.5	0.2	115, 250, 290
Ball Milled Rock	639.5	83.9	0.6	0.2	173, 214, 259
Stage1 Pitt	1026.4	232.4	0.7	0.1	187, 210, 289
Stage 1 Rock	1005.7	174.7	0.9	0.2	129, 161, 198
Stage3 Pitt	737.4	60.3	0.5	0.1	470, 500, 720
Stage 3 Rock	887.4	184.5	0.7	0.1	270, 409, 406
Stage4 Pitt	570.2	28.8	0.5	0.5	170, 517, 433
Stage 4 Rock	1044.4	131.2	0.8	0.1	210, 304, 289
Stage5 Pitt	700.8	9.2	0.5	0.0	455, 625, 699
Stage 5 Rock	658.5	152.3	0.6	0.1	312, 397, 527
Less Processed Colorado Coal	441.3	412.3	0.5	0.2	222, 222, 211
Less Processed Pitt Coal	216.0	11.5	0.3	0.0	243,220, 187

b) Experiment #2 – Water Bath Sonication – Table 4b shows the results of water bath sonicating the samples for 5, 10, 15 and 30 minutes instead of hand sonicating. We found some improvement in standard deviation between DLS reads but no improvement in agglomeration.

Table 4b. DLS analysis hand sonication vs water bath sonication of 400 mesh particles.

DLS Analysis Hand Sonication vs Water Bath Sonication of 400 Mesh Particles					
Sample	Z-Ave d.mn	SD	PdI	SD	~ Primary Peak Number (different reads)
Hand Sonication	558.2	125.1	0.51	0.1	180, 240, 270
5 Minute WBS	567.6	100.5	0.55	0.04	205, 237, 440
15 Minute WBS	444.2	17.7	0.47	0.05	257, 427, 313
30 Minute WBS	489.2	149.1	0.54	0.06	220, 311, 285

Finding summary: DLS sizing of coal and rock samples was difficult because DLS works better with standard sized particles and the coal and rock samples were not consistent in size due to particle agglomeration. DLS did give us a general idea of particle sizes. Once we realized DLS did not work well with our coal and rock particles we chose to use TEM to measure particle sizes.

b. Animal Experiment (Murine) –

The initial instillation/lavage experiment looked at 10, 50 and 100ug doses of 400 mesh coal to determine which dose would give a readable response with minimal toxicity. None of the doses appeared to be toxic nor was there a difference in the dose response (e.g., measuring inflammatory cell infiltration into the lung) in the mice so 100ug was chosen for the dose in the final experiment. For the final experiment we treated groups of 4 C57BL/6 mice per group with PBS, Bottom Rock (largest size fraction), Top Rock (Smallest size fraction), Bottom Coal (largest size fraction), and Top Coal (Smallest size fraction). After 72 hours mice were euthanized with CO2, had their blood collected with a cardiac draw and were lavaged as described in the methods section. Lavage was successful for 17 of the mice (4 PBS, 2 Bottom Rock, 3 Top Rock, 4 Bottom Coal and 4 Top Coal). Lung lavage numbers are shown in Fig. 28. 300 cells were counted on each cytospin slide. Top Rock and Bottom Coal showed some minimal cellular infiltration compared to other treatments. Bottom coal showed some very minor neutrophilic infiltration whereas no other treatments did. Top rock had trends with increased lymphocytes, epithelial, and monocyte cells compared to other treatments along with increased total cell counts but these were not significant. Bottom Rock showed significantly fewer total cells with drastically increased RBC numbers (not shown) compared to every other treatment. Overall, the animal studies did not show any biologically meaningful differences between size of coal or rock dust in cellular infiltration. These studies were designed to use neutrophil influx as a measure of inflammation and to determine a NOAEL and LOAEL, but that generally negative data obtained prevented us from being able to establish these parameters. Future studies would likely investigate long-term exposure as coal miners lung is a chronic disease that may have not been captured with the acute exposures that we performed in the animal model.

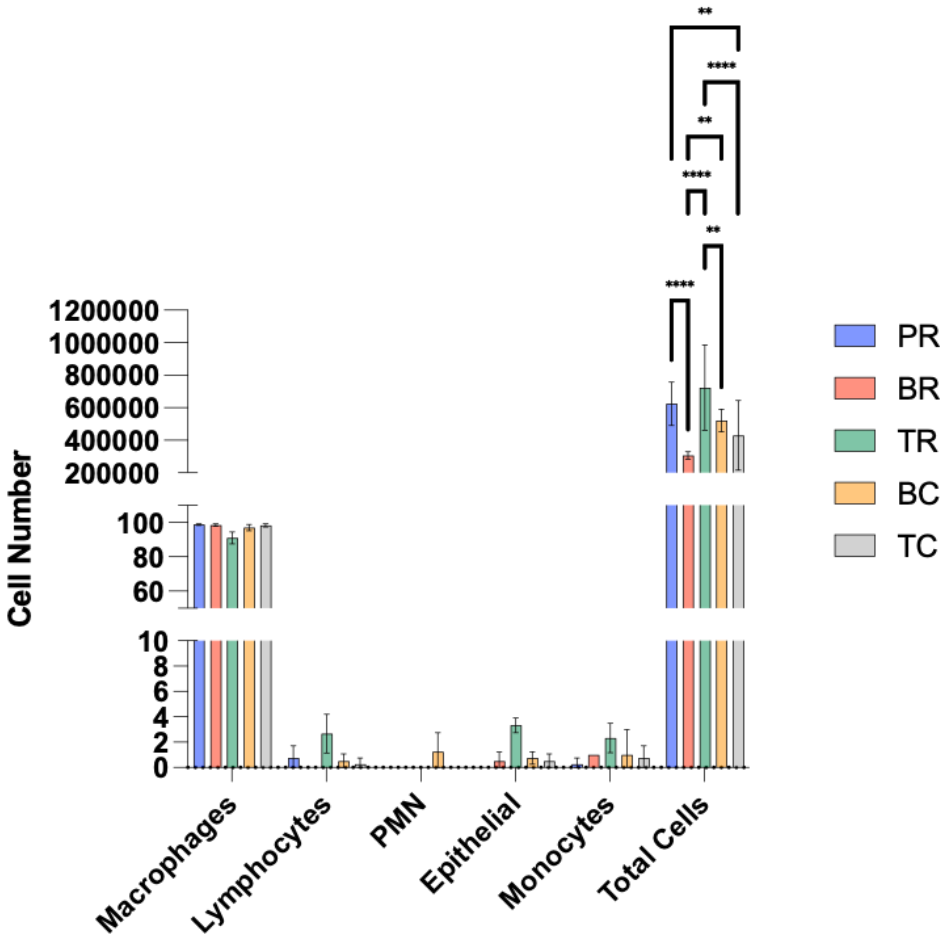

Figure 28. Cell numbers from murine lavage experiment * = P ≤ 0.05 ** = P ≤ 0.01 *** = P ≤ 0.001 **** = P ≤ 0.0001.

Finding summary: While we saw changes in cell numbers based on animal study, we did not see many neutrophils in our lavage samples. Coal does not seem to elicit much of a response with one treatment.

a. <u>Centrifugation separation-</u>

Separation by centrifugation method of Colorado coal has hydrodynamic size peaks for Colorado coal top layer ($C_{0.2}$) at 188 and 1130 nm and for Colorado coal middle layer ($C_{0.7}$) at 838 nm as measured by DLS (Fig. 29). Visibly large Colorado coal bottom layer (C_1) particles settled to the bottom of the DLS cuvette quickly, resulting in measurement with 500 nm peak. C_1 size determined by TEM had particle sizes ranging from 1000 to 3000 nm (Fig. 30). TEM images are shown in Fig. 30 and 31for Pittsburg $C_{0.2}$ and C_1. A comparison of the Colorado separated particles in 2 mg/mL water solution are shown in Fig. 32.

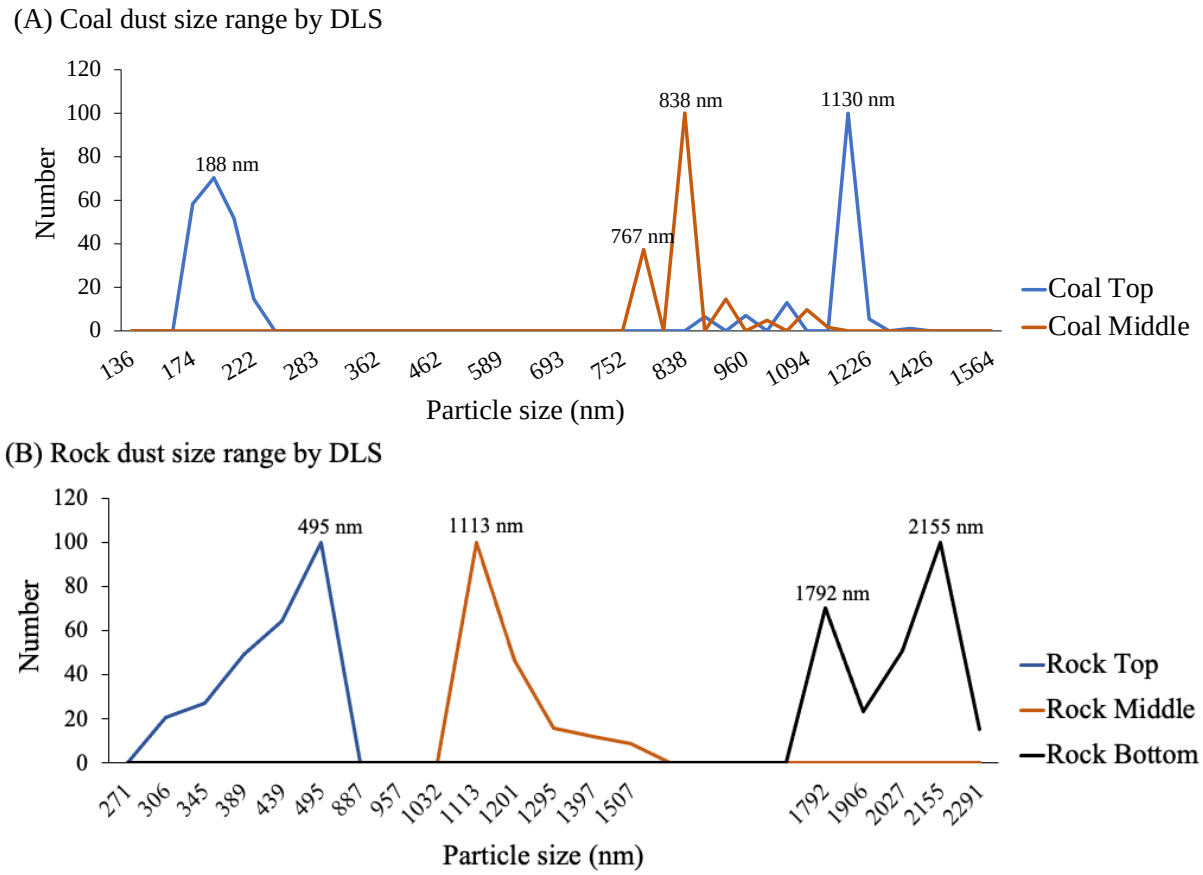

Figure 29. Hydrodynamic size by count of (A) Coal and (B) Rock samples in water from top, middle, and bottom layers.

The top layer has a mix of small and large particle, indicated by two size peaks, but generally has more of a small particle fraction (~200 nm) than the middle and bottom layers. *Bottom layer size was determined by TEM because of the measurement limitation by DLS cuvette.

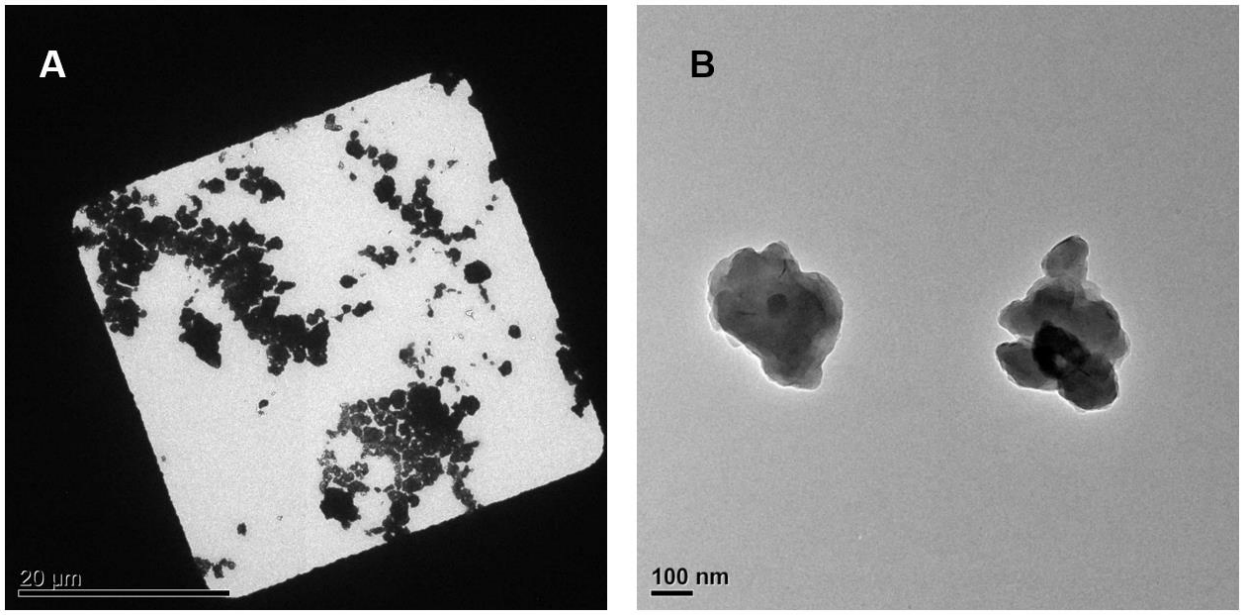

Figure 30. Coal top (CT) layer small particles (A) square view and (B) individual particles sized around 200 nm (Table 1)

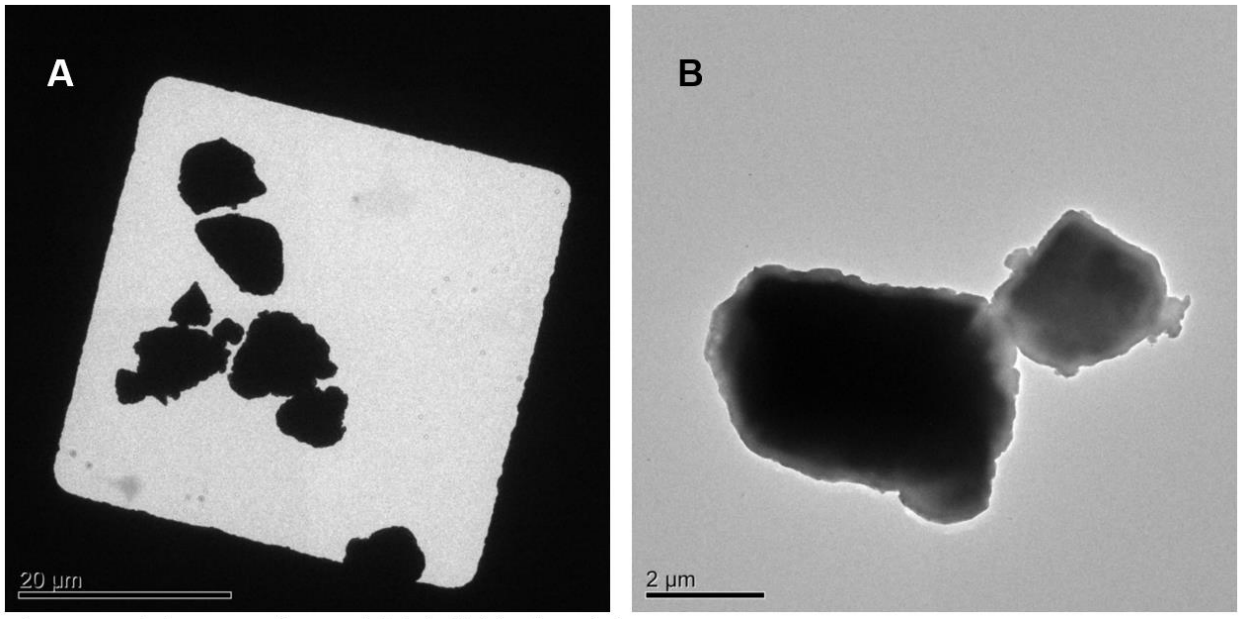

Figure 31. Coal bottom (CB) layer large particles (A) square view and (B) individual particles sized at 1000+ nm (Table 5).

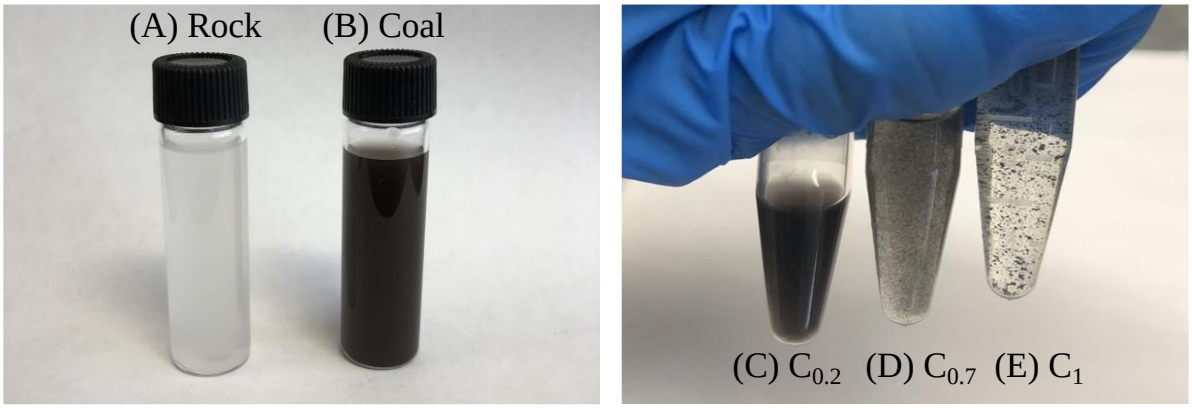

Figure 32. The dispersibility of 1 mg/ml (A) Rock; and (B) Coal suspensions. 2 mg/mL size-separated coal in water solution following dispersion by vortex. (C) C0.2, (D) C0.7, and (E) C1 represent sizes of fine, mixed, and coarse coal particles from top, middle, and bottom layers after separation.

The centrifugation method of rock has peaks for the top layer at 495 nm ($R_{0.5}$); for the rock middle layer at 1110 nm (R_1); and for the rock bottom layer at 1790 nm and 2160 nm (R_2) as measured by DLS. TEM images are shown in Fig. 33-35. Individual particles are less discernable and have more aggregation than the coal images.

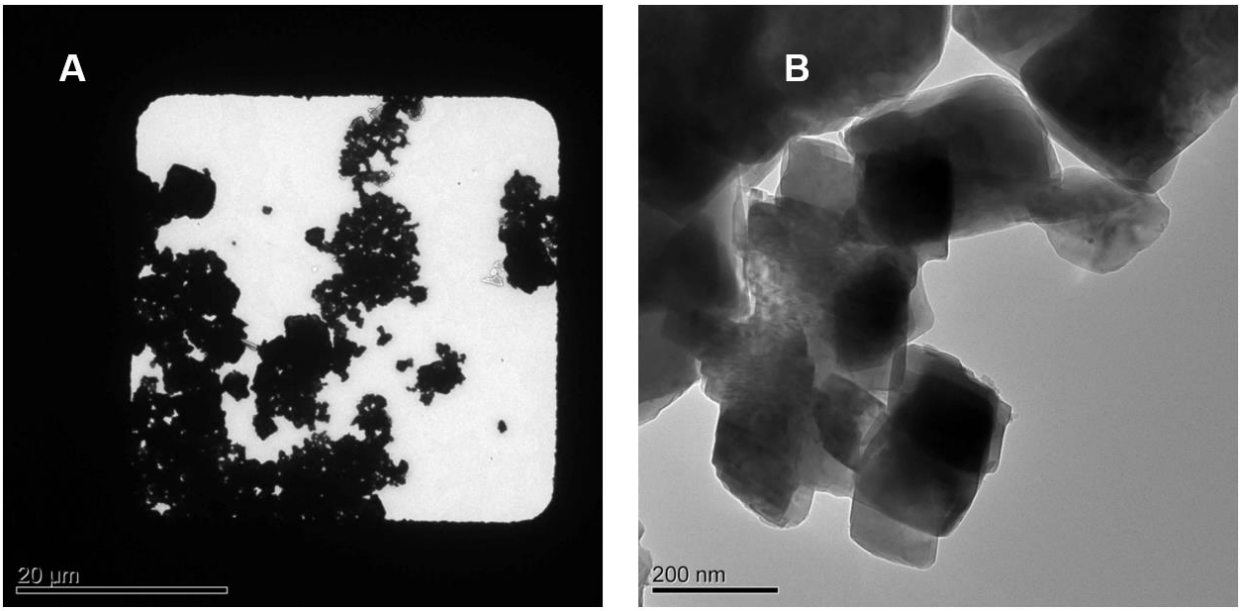

Figure 33. Rock top layer (RT) (A) square view and (B) individual particles sized around 500 nm by DLS (Table 5).

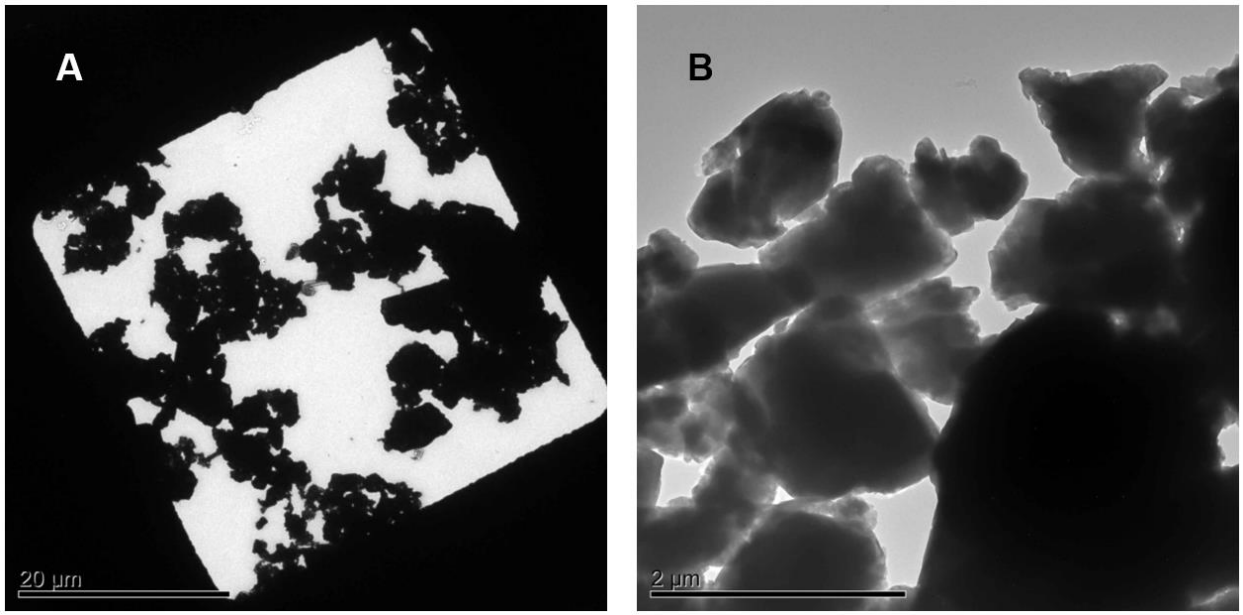

Figure 34. Rock middle layer (RM) (A) square view and (B) individual particles sized around 1000 nm (Table 5).

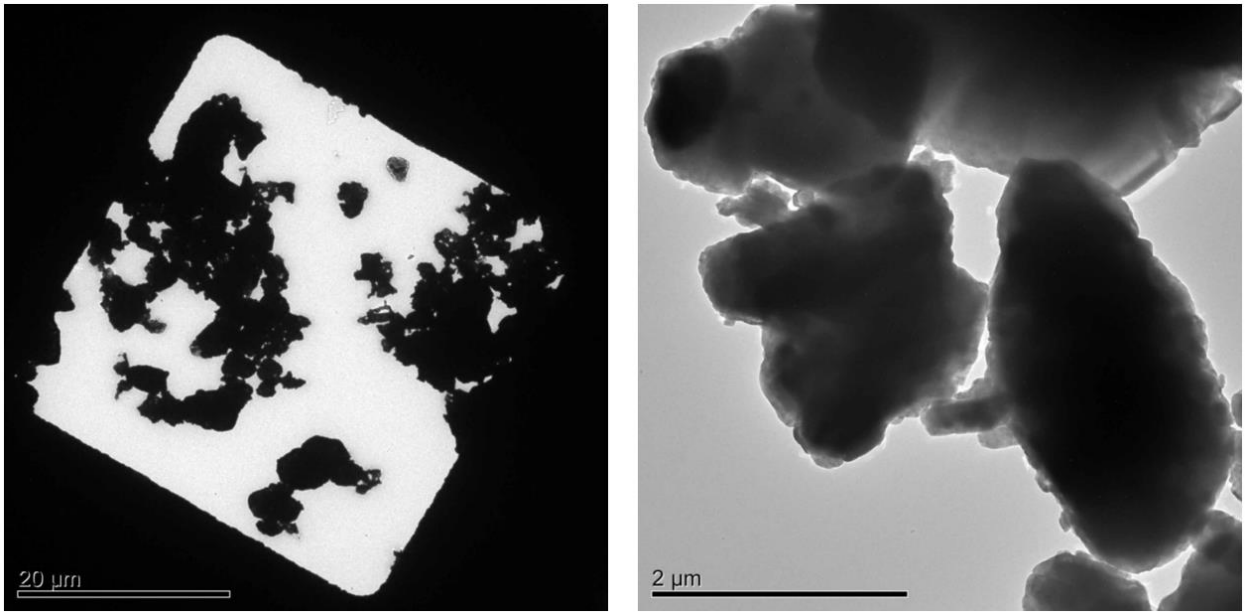

Figure 35. Rock bottom layer (RB) (A) square view and (B) individual particles sized around 2000 nm (Table 5).

b. Characteristics of mining dust-

Table 5 displays the summary of respirable mining dust particles characteristics.

Dispersibility, size range, and morphology of dust samples: 1mg/ml rock and coal dust solutions in water showed visually different dispersibility in suspension (Fig. 32). After 10 min water bath sonication, the rock particles quickly deposited at the bottom and the coal particles remained suspended in the solution.

Coal has hydrodynamic size peaks for the top layer at 188 nm and 1130 nm ($C_{0.2}$), and for the coal middle layer at 767 and 838 nm ($C_{0.7}$) as measured by DLS. Visibly large coal bottom layer particles settled to the bottom of the DLS cuvette quickly. Due to the limitation, the size of coal particles from the bottom layer was determined by transmission electron microscopy (TEM) to range from 1000 nm to 3000nm (C_1). The centrifugation method of rock has peaks for the top layer at 495 nm ($R_{0.5}$); for the rock middle layer at 1110 nm (R_1); and for the rock bottom layer at 1790 nm and 2160 nm (R_2) as measured by DLS.

The high-magnification microscopy images showed the morphology of dust particles and confirmed successful size separation as shown in Fig. 30-31 and 33-35. For the raw unseparated coal and rock dust images, both samples included particles smaller than 200 nm and coarse particles around 600 nm, consistent with the hydrodynamic size distribution measured by DLS. Identically, the coal particles in the top layer were around 200-300 nm in the TEM images, which were finer than the rock dust. The size difference between the middle and bottom layers is apparent. The coal particles were rounder than the rock, which were sharp in the images. In summary, the dispersibility and morphology results differ between coal and rock dust.

Surface features of raw coal and rock dust: The contact angle is related to the hydrophobicity of a substance. After a drop of water, the contact angle of raw coal and rock dust was measured immediately. The contact angle of raw coal dust was around 86 ± 5° (Fig. 36), which is more hydrophobic than that of rock. In contrast, a contact angle could not be determined for rock because the droplet immediately dispersed over the surface of the rock pellet, indicating higher hydrophilicity. The contact angle measurement shows surface feature differences between rock and coal dusts.

Elemental composition for raw coal and rock dusts: Elemental composition percentages from scanning transmission electron microscope with energy dispersive X-ray (STEM w/ EDX) are shown in Table 5 and the spectrum map is displayed in Fig.37. The spectrum showed that the rock dust consisted of carbon (C; 61.4%), oxygen (O; 14.5%), calcium (Ca; 13.5%), and copper (Cu; 9.5%). Silicon (Si; 12.7%), platinum (Pt; 3.7%), iron (Fe; 2.3%), aluminum (Al; 1.4%), and cobalt (Co; 1.2%) were detected in the coal dust samples. For comparison, the elemental composition of rock dust was more monotonous than coal dust.

Functional groups for raw coal and rock dusts: Functional groups were determined using fourier-transform infrared spectroscopy (FTIR). While both dusts contain structures like hydroxyl and aliphatic groups, coal's hydrophobic CH_3 and CH_2 groups indicated in the blue 2850-293 cm^{-1} region have a stronger signal compared to coal's hydrophilic -OH stretching indicated in the red 3200-3600 cm^{-1} region compared to that of rock. Rock has less prominent CH_3 and CH_2 strength relative to the corresponding OH stretching. Furthermore, as seen in Fig. 38, a C=C peak at 1600 cm^{-1} is present in coal but not in rock. The zeta potential given in Table 5 ranges from -38.70 to -7.83 mV. Bulk rock appeared to be more stable as determined by zeta potential compared to size fraction rock.

(A) (B)

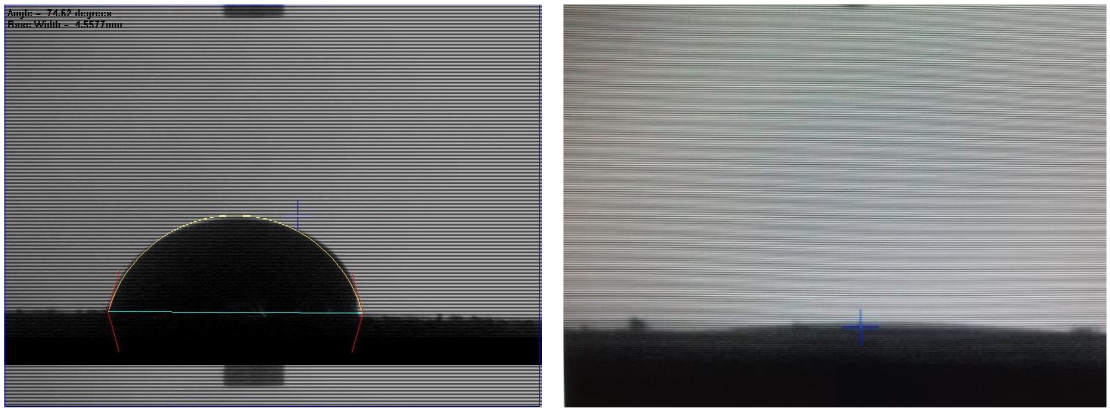

Figure 36. (A) Immediate contact angle of coal dust was 86° ± 5 averaged for 3 pellets; (B) Water contact angle for rock pellets was immediately dispersed.

(A)

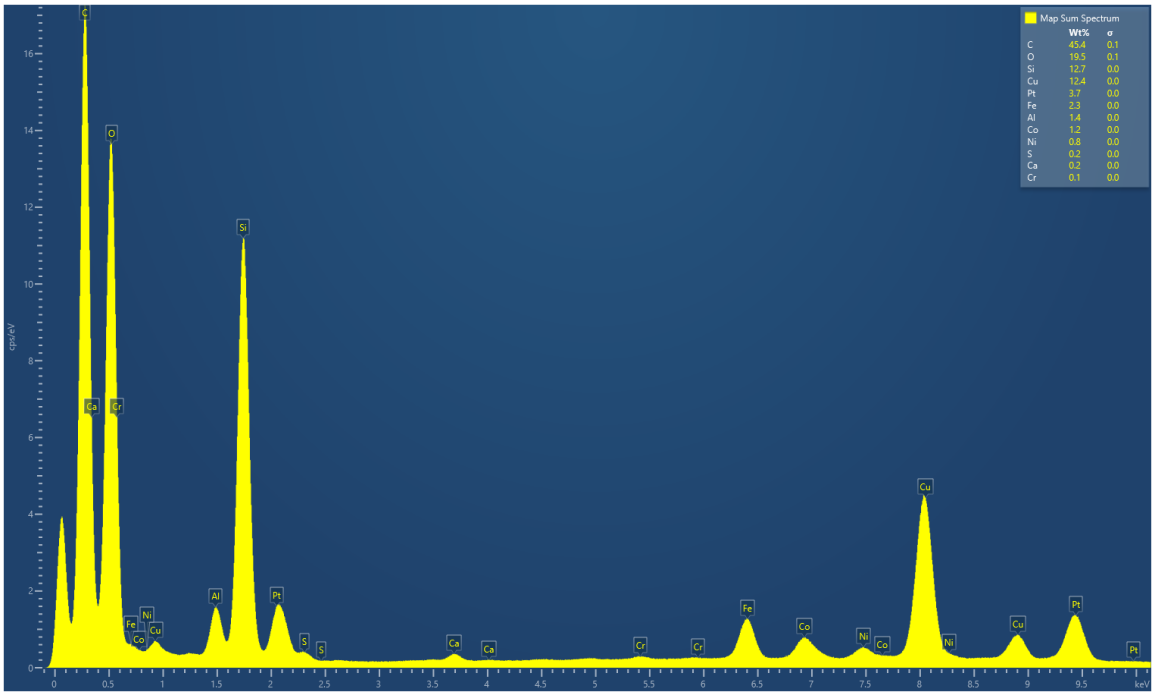

(B)

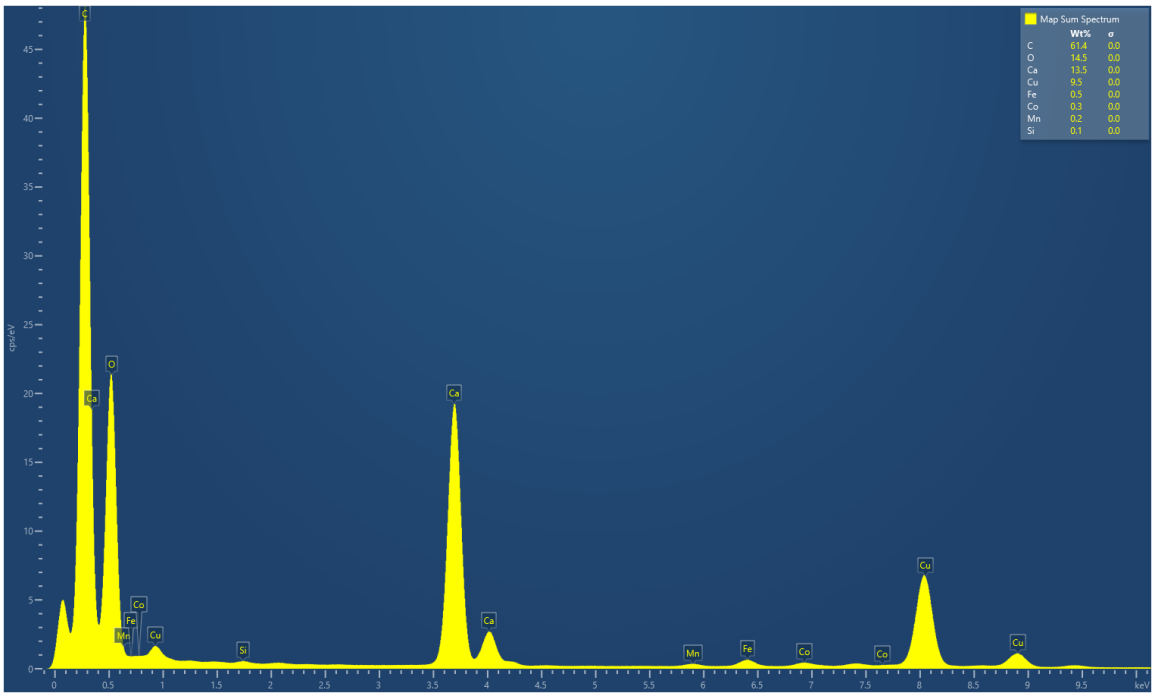

Figure 37. The spectrum map from STEM w/ EDX indicate the elements composition for (A) Coal and (B) Rock dust particles.

A previous unpublished field sampling study concluded that miners were primarily exposed to coarse particles based on the coal particle size distribution ranging from 38 μm to 850 μm. However, exposures to respirable and sub-micron sized coal particles were also found. Area particle concentration measurements conducted at the coal mine field by us with a NanoScan SMPS to measure particle sizes 10-420 nm and OPS to measure 0.3-10 μm found that peak particle number count was roughly 100 nm measured by SMPS and 300 nm measured by OPS. Our separated sizes ($C_{0.2}$ ~ 200 nm; $R_{0.5}$ ~ 495 nm) reflect those of particles in mining dusts. Novel sampling equipment in recent studies revealed that the workers might also be exposed to nanometer-sized particles due to the use of newer technology in mining equipment creating smaller respirable particles in modern mine environments (Duarte, DaBoit et al. 2019, Liu and Liu 2020). A survey conducted in 2007 investigated the coal dust size in a US underground mine, showing that the size of coal dust within airways was finer than the size characterized in the 1920s. The significant change of size distribution in coal dust might be related to the highly mechanized nature of modern coal mining that has increased coal production rates (Sapko, Cashdollar et al. 2007, Petsonk, Rose et al. 2013). An occupational safety-based assessment reported the considerable increase in productivity was due to the introduction of new mining technology. For example, a Russian coal mining company had its productivity jump from 2270 to 7950 thousand m^3/year. However, these economic benefits come at the cost of various health effects and safety problems due to the high amount of respirable dust particles generated. The small size fraction characterized in the present study further points to CMDLD being of continuing and growing concern, as toxicity increases with the smaller size particles and greater doses seen in modern mines. The dust particles suspensions in this present study have the tendency to aggregate, forming larger hydrodynamic diameters, despite precautions taken before exposure including sonication

of the dust suspensions before treatment and vibration of the cell plate after the particle treatment. The aggregation might underestimate the cell toxicity corresponding to the size-toxicity effect.

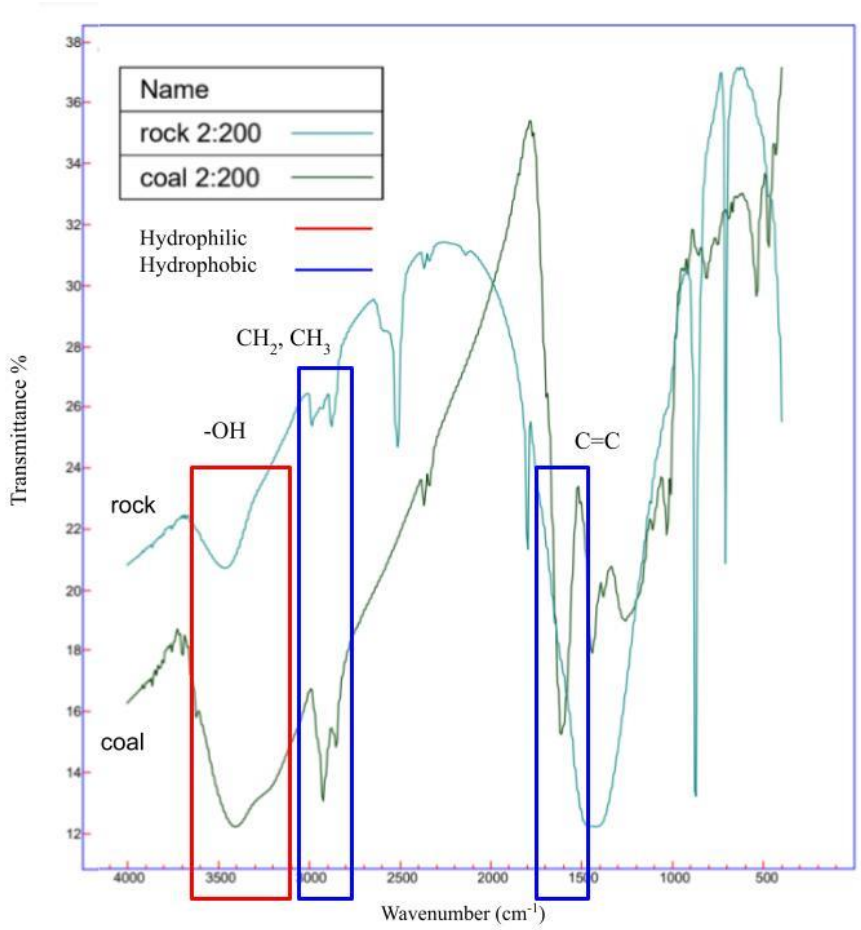

Figure 38. FTIR spectra of coal showed that it has a relatively stronger aliphatic signal compared to its hydroxyl signal, as well as a C=C bend that is not present in rock. This suggests that coal contains more C-containing groups than O-containing groups which contribute to its hydrophobicity.

Table 5. Summary of respirable mining dust particles characteristics.

Sample	Z Potential in water (mV)	Hydrodynamic size peak (nm)	Elements (Wt%)[1]	Functional groups present	Contact angle (degree)
Coal	-17.10 ± 1.23	570	C (45.4%), O (19.5%), Si (12.7%), Cu (12.4%), Pt (3.7%), Fe (2.3%), Al (1.4%), Co (1.2%)	-OH, CH, C=O, C=C	86° ± 5
$C_{0.2}$	-21.70 ± 1.92	188, 1130			
$C_{0.7}$	-25.03 ± 0.21	767, 838			
C_1	-24.50 ± 0.53	1000-3000			
Rock	-38.70 ± 1.94	520	C (61.4%), O (14.5%), Ca (13.5%), Cu (9.5%)	-OH, CH, pyran ring	NA
$R_{0.5}$	-19.40 ± 0.54	495			
R_1	-14.60 ± 0.30	1110			
R_2	-7.83 ± 1.06	1792, 2155			

[1] Elements shown in the table were detected > 1% in the dust suspension.

c. Aerosolization of mining dust

The elemental composition analysis detected the presence of Si, Al, Fe, Ba, Cl, K and Pt in the coal dust in our study (Table 1), which might contribute to the higher cell toxicity observed in coal compared to the rock dust particles. The relationship between elemental composition and cell toxicity has been researched, but a comprehensive understanding for the mechanism is still lacking and the precise role of individual elements in biological alterations is still debated. Si, C, and Fe detected in our coal suspension samples are known to cause pulmonary toxicity (Pinot, Kreps et al. 2000, Huang, Gordon et al. 2006, Sambandam, Palanisami et al. 2014). Among these elements, silica-induced toxicity has been widely discussed for decades. However, there is variability in *in-vitro* and *in-vivo* responses from numerous studies, such as reactive oxygen species generation and macrophage activation (Fubini and Hubbard 2003). This makes it difficult to definitively identify what characteristics of silica contribute to the toxicity mechanism and clarify all interactions at the molecular level to result in lung function impairment. The present study did not directly demonstrate how hydrophobicity affects cell toxicity. However, in terms of

carbon, coal's hydrophobic nano-sized aromatic carbon particles might modify the air-liquid interfacial properties, surface tension, and behavior of pulmonary surfactants (PS) in the alveolus. The reshaping is because solubilization of phospholipids in PS increases with the degree of hydrophobicity (Zhao, Li et al. 2019). This suggests that the particles that can penetrate through the surfactant linings induce intercellular reactions, including inflammation, oxidative stress, and cytotoxicity(Zhao, Li et al. 2019, Wang, Liu et al. 2020).

In addition to silica, scientists have considered the role of iron. The interaction between heavy metals and PS is crucial when discussing metal-associated lung toxicity. Studies have illustrated a negative correlation between cell viability and iron content of dust in both alveolar macrophages and human lung epithelial cells (Ghio, Pavlisko et al. 2015, Sun, Kinsela et al. 2022), and a systematic review summarized that iron-related genes altered mitochondrial function and levels of cytochrome oxidase, leading to mitochondrial dysfunction and the development of COPD (Zhang, Nemeth et al. 2019). The bioavailability of heavy metals, particularly solubility, strongly influences particle-induced pulmonary toxicity (Manousakas, Papaefthymiou et al. 2014, Dean, Elom et al. 2017). The leachable fraction of iron in the coal particles might potentially stimulate an increase of PS, enhancing its bioavailability and strengthening pulmonary toxicity. Interestingly, a previous biochemistry study provided evidence to support that heavy metal-rich particles might change the solubility of heavy metals in particles because of the protein component in PS (Fang, Zhao et al. 2020).

To estimate the anticipated "airborne" particle concentrations which resulted in the exposure concentrations in liquid medium applied to the 2D cell exposure study, we aerosolized the coal and rock dust in Dr. Tsai's lab to perform the calibration with both mass and particle number concentrations. Fig. 39 shows the mass and number concentrations of the mine particles in airborne from aerosolization for calibration and in cell medium for *in-vitro* treatment. The "mass concentrations" showed that the respirable coal particles had a concentration which was approximately 2 times higher than the amount of rock during the same aerosolization rate and duration (Fig. 39A1). The particle "number concentrations" monitored by SMPS (10-420 nm) and OPS (0.3-10 μm) during aerosolization showed that coal dust produced much finer airborne particle with a much higher number concentrations monitored by SMPS (4000-6000 particles/cm^3) than the OPS (<500 particles/cm^3) generated from the stirring/aerosolization process (Fig. 39B1). The finding indicated that more fine particles (<500 nm) were produced from coal than rock with an identical aerosolization method (Fig. 39B1). In the cell medium with average size of 500 nm particles (Fig. 39B2), we also notice that the coal particles presented a 1.4 times higher number concentration in the medium suspension than the rock particles under the identical *in-vitro* environment.

In addition, when we compare the aerosolized mass concentrations to the measured concentration in the underground coal mine, we found that the average mass concentrations of aerosolized rock (9×10^{-4}μg/ml) and coal dust (20×10^{-4}μg/ml) in Fig. 39 A1 demonstrated that the mass concentration levels in our aerosolization study were similar to the real-word mine dust exposure, in a range from 5.4 to 15.6×10^{-4} μg/ml (seen in Table 1b and Fig. 6A), collected at the underground mine.

Fig. 39B2 presents the equivalent airborne particle number concentrations based on the mass concentration of the coal or rock in the cell medium for *in-vitro* dust particle exposure. The equivalent particle number concentrations of our cell study, 470,970 particles/cm^3 for rock and 340,550 particles/cm^3

for coal, seen in Fig. 39B2 were similar to the peak number concentrations found in our measurements at the mine site showing 487,540 particles/cm^3 from the SMPS measuring a respirable size range (10-420nm).

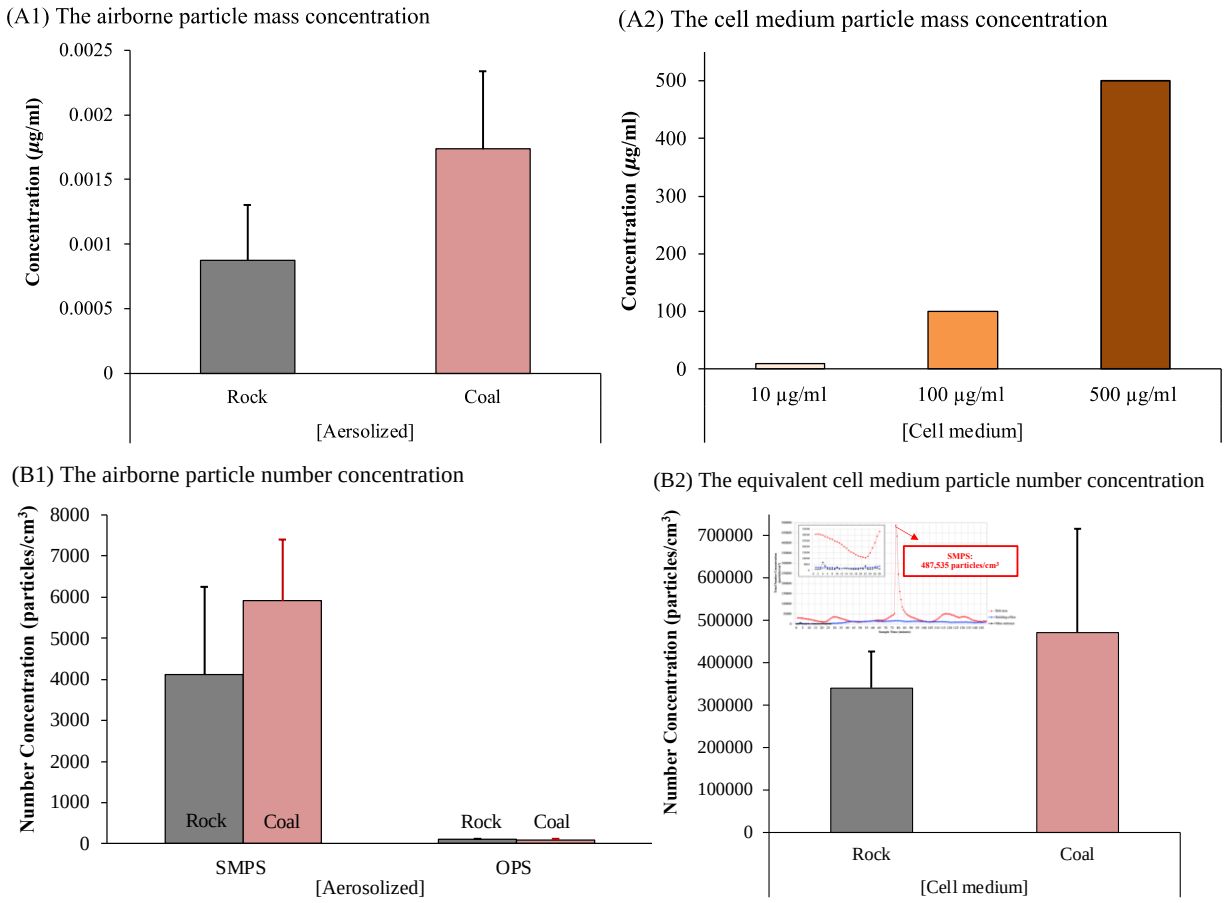

Figure 39. The concentrations of mine particles from the aerosolization experiment and in cell medium for in-vitro dust particle exposure. A1 and A2 are mass concentrations; B1 and B2 are number concentrations.

Regarding size analysis of exposed coal and rock particles, based on all particle size measurements and SEM/TEM analysis on particle morphology and sizes as seen in Figure 7 showing particles found in underground mine, and Figures 30-31 and 33-35 showing particles in cell medium (570 nm for coal and 520 for rock), we also see the consistent particle sizes on lab aerosolized coal and rock particles (550 nm for coal and 460 nm for rock) as seen in Figure 40.

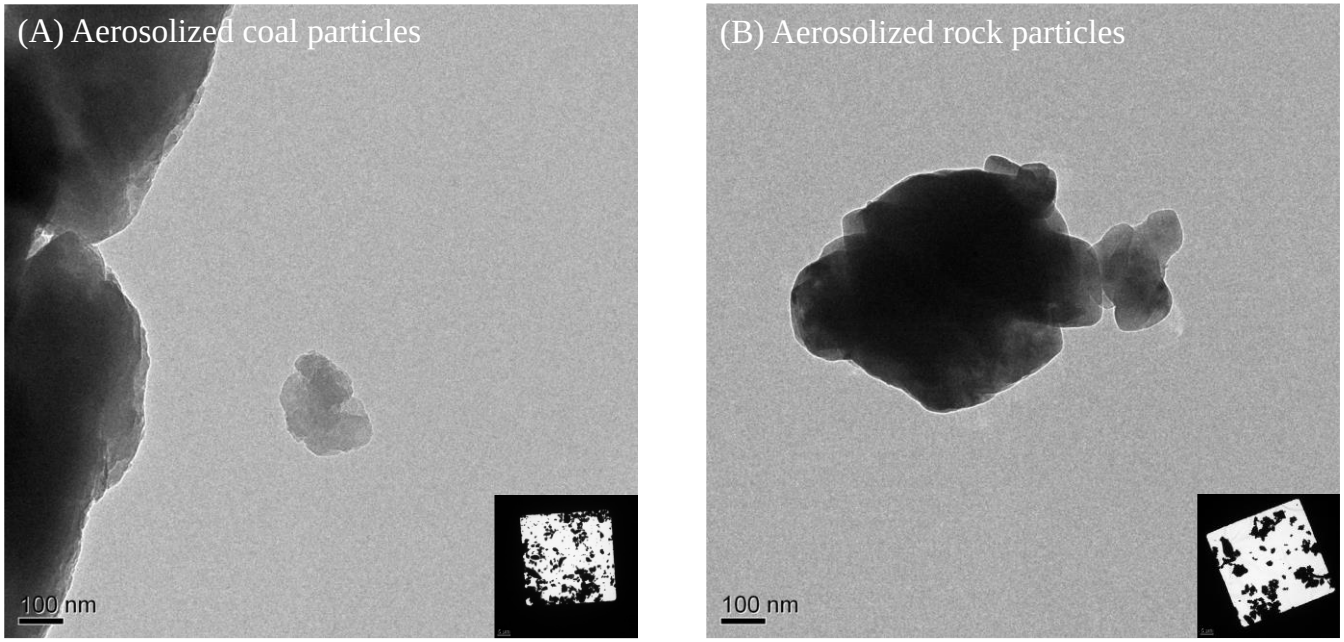

Figure 40. The TEM images for aerosolized (A) coal and (B) rock dust particles.

5.0 Publication Record and Dissemination Efforts

The results of this project have been published in one peer-reviewed journal and presented in six podium presentations in scientific conferences including the annual conference of Society for Mining, Metallurgy & Exploration (SME) and American Industrial Hygiene Conference and Exposition (AIHCE). We plan to further analyze some of the results to present in conference next year and hopefully produce another manuscript for publication in peer-reviewed journal.

Journal Publications:

1. Chen, Y.H, Nguyen, D., Brindley, S., Ma, T., Xia, T., Brune, J., Browne, J. **Tsai, C.S.J.*,** The dependence of particle size on cell toxicity for modern mining dust, Scientific Report, 2023, 13, 5101. [Impact factor: 5.516] https://doi.org/10.1038/s41598-023-31215-5

Scientific Conference Presentations:

1. Chen, Y., Nguyen, D., Brindley, S., Ma, T., Xia, T., Brune, J., Brown, J., **Tsai, C.*,** Understanding the primary particle characteristics affecting dust-induced pulmonary toxicity in the modern mine environment, American Industrial Hygiene Conference and Exposition (AIHCE), Phoenix, AZ, May 22-24, 2023.
2. Chen, Y., Nguyen, D., Brindley, S., Ma, T., Xia, T., Brune, J., Brown, J., **Tsai, C.*,** Size effects of nano and submicron coal and rock particles and physico-chemical property characteristics, Society for Mining, Metallurgy & Exploration (SME) Auunal Conference & EXPO, Denver, Colorado, Feb 26.-Mar. 1, 2023.
3. Angulo, J-P., Brune, J., **Tsai, C.S.J.*,** Potential determinants of increased incidence of pneumoconiosis in central Appalachian underground coal miners, podium, American Industrial Hygiene Conference and Exposition (AIHCE), Nashville, Tennessee, May 23-25, 2022.
4. Angulo, J-P., Brune, J., **Tsai, C.S.J.*,** Potential determinants of increased incidence of pneumoconiosis in central Appalachian underground coal miners, Southen California Educational Research Center (SCERC) Clinical Case Conference, virtual, Mar. 4, 2022.
5. **Tsai, CSJ*,** Brune, J., Duzgun, S., Resuspension of Airborne Submicrometer- and Nanometer-Sized Particles at the Underground Coal Mine Associated with Common Work Practices, Society for Mining, Metallurgy & Exploration (SME) Auunal Conference & EXPO, Salt Lake City, Utah, Feb. 27-Mar. 2, 2022.
6. **Tsai, CSJ*,** Invited Seminar, Measuring and sending submicron mining particles with emerging technology, Society for Mining, Metallurgy & Exploration (SME), Sept. 23, 2021.

6.0 Conclusions and Impact Assessment

The results clearly showed that submicron sized coal particles were found at all locations where we collected samples including the office building, entrance and underground belt area during transporting mined coal. The belt area exhibited the highest concentration across all size fractions compared to the building office and entrance and has significantly higher concentrations in submicron and nano-sizes. Coal and rock particles were found on both personal and area samples collected at the belt area. Mass concentrations obtained from filter sampling and PDM showed a few samples exceeded the current PEL of 1.5 mg/m^3. The particles found in the personal samples at the belt area carry more metal elements than those found in the bulk coal or rock dust and those sampled in office and at entrance. The higher level of metal elements including Pt, Co, Mg, Na and Ni may anticipate in leading to stimulate toxicity after entering respiratory tracks and the deposited organisms.

Although the exposed dosage in mass concentration applied for *in-vitro* studies were higher than the common coal exposure concentration at a mine site in our study, we found that the equivalent airborne particle number concentrations of submicron particles were similar to the peak concentration measured at the underground coal mine. The size dependent dose-response effect was explicit from our study that indicated the potential damage to the lung after a long-term exposure to coal or rock dust especially to the particles smaller than submicron (<500nm). The cumulative exposure to such small particles when accumulated to a level comparable to our *in-vitro* study dosage is expected to show a sign of symptom leading to disease development.

Based on our characterizations of airborne mine particles, a high level of small particles, approximately half million (5×10^5 particles/cm^3) of submicron particles per cubic centimeters, found at the underground mine contributed a very small portion of the mass concentration detected, below PEL. That indicated an extremely high number of submicron particles would be in the air with a mass concentration below PEL. The cell uptake analysis using bioTEM clearly showed the uptake of small coal particles and the damage to the cells. Our study presented the importance of characterizing particle sizes, morphology and composition especially when the exposed mass concentration is low. As a result, the appropriate method for measuring the most harmful portions of respirable coal/rock dust needs to incorporate size, particle count, and composition analysis to control and reduce exposure.

In summary, the present study explored the finer fraction of approximately 200 nm in coal dust particles from an underground modern mine. Our *in-vitro* findings support that fine particle fractions explicitly induced stronger toxicity than their coarser sizes in coal dusts. The reaction difference between coal and rock might be related to surface hydrophobicity and elemental composition. Macrophages are more sensitive to particle-induced toxicity than epithelial cells.

The exploration of particle size effect, related physio-chemical characterization of respirable ground modern mining dusts and molecular toxicity can be utilized in future lung disease risk reassessment. Additionally, the particle characterization results in this study emphasized the importance of dust properties which would affect particle-induced cell reactions. Although this study found no significant differences in pulmonary cell viability, the difference in inflammatory endpoints induced by dust particles is still explored in the *in-vitro* study. This is consistent with toxicity studies showing marginal differences

in viability despite substantial stress responses , as well as epidemiological evidence of sustained stress response and disease.

Based on various endpoints, our results demonstrate consistent inflammatory endpoints and cellular stress responses induced by the smaller sized dust particles explored in the *in-vitro* study suggest that long-term exposure to smaller particles would result in an increase in relevant pulmonary diseases such as CWP, as well as other chronic obstructive pulmonary diseases.

In conclusion, this occupational-based research explored the impact of particle physicochemical properties on dust-induced pulmonary toxicity, cell uptakes and provided data based on endpoints and dose response to aid in future work for estimating no-observed-adverse-effect-level (NOAEL) and lowest-observed-adverse-effect-level (LOAEL) values for exposure to the small-sized dust portion.

7.0 Recommendations for Future Work

Several suggestions can be applied in future studies to elucidate the molecular mechanism causing occupational pulmonary toxicity and determine a dose-response correlation for the respirable mining dusts in the modern mine workplace. Future studies can extend the treatment duration to better resemble the long-term chronic mine dust exposure in the practical workplace. Considering the *in-vitro* study, although it is useful to initially explore the relationship between particle exposure and cell reactions, an animal study with *chronic exposure* has been indicated as a more appropriate environment that can imitate the *cause-response relationship*. While we saw changes in cell numbers based on current animal study, we did not see many neutrophils in our lavage samples. Coal does not seem to elicit much of a response with one treatment in an animal. The actual intracellular dose and localization of animal exposure analyzed using bio-TEM or histological stains like hematoxylin and eosin stain (H&E stain) need to be further explored to identify the particles entering through the cell membranes and their behavior inside the cells.

8.0 References

NIOSH, (2011). "Coal mine dust exposures and associated health outcomes, a review of information published since 1995." Department of Health and Human Services, Centers for Disease Control and Prevention Current Intelligence Bulletin 64(DHHS (NIOSH) Publication No. 2011-172).

Blackley, D. J., J. B. Crum, C. N. Halldin, E. Storey and A. S. Laney (2016). "Resurgence of Progressive Massive Fibrosis in Coal Miners- Eastern Kentucky " MMWR Morb Mortal Wkly Rep 65: 1385-1389.

Brown, J. H., K. M. Cook, F. G. Ney and T. Hatch (1950). "Influence of particle size upon the retention of particulate matter in the human lung." Am J Public Health Nations Health 40(4): 450-458.

Chen, Y. H., D. Nguyen, S. Brindley, T. Ma, T. Xia, J. Brune, J. Brown and C. Tsai (2023). "The dependence of particle size on cell toxicity for modern mining dust." Scientific Report, Nature Research Journal Under review.

Dean, J. R., N. I. Elom and J. A. Entwistle (2017). "Use of simulated epithelial lung fluid in assessing the human health risk of Pb in urban street dust." Science of the Total Environment 579: 387-395.

Drinker, P. and T. Hatch (1936). Industrial dust - hygienic significance, measurement and control. New York, McGraw-Hill Book Company, Inc.

Duarte, A. L., K. DaBoit, M. L. Oliveira, E. C. Teixeira, I. L. Schneider and L. F. Silva (2019). "Hazardous elements and amorphous nanoparticles in historical estuary coal mining area." Geoscience Frontiers 10(3): 927-939.

Elsaesser, A. and C. V. Howard (2012). "Toxicology of nanoparticles." Advanced Drug Delivery Reviews 64(2): 129-137.

Fang, Q., Q. Zhao, X. Chai, Y. Li and S. Tian (2020). "Interaction of industrial smelting soot particles with pulmonary surfactant: Pulmonary toxicity of heavy metal-rich particles." Chemosphere 246: 125702.

Fubini, B. and A. Hubbard (2003). "Reactive oxygen species (ROS) and reactive nitrogen species (RNS) generation by silica in inflammation and fibrosis." Free Radical Biology and Medicine 34(12): 1507-1516.

Ghio, A. J., E. N. Pavlisko and V. L. Roggli (2015). "Iron and iron-related proteins in asbestosis." Journal of Environmental Pathology, Toxicology and Oncology 34(4).

Glover, D. and K. Cram (1997). "Respirable airborne dust exposure levels in the New South Wales Coal Mining industry." Appl Occup Environ Hyg 12(12): 980-987.

Grove, T., T. Van Dyk, A. Franken and J. Plessis (2014). "The evaluation and quantification of respirable coal and silica dust concentrations: a task-based approach." J Occup Environ Hyg 11: 406-414.

Huang, X., T. Gordon, W. N. Rom and R. B. Finkelman (2006). "Interaction of iron and calcium minerals in coals and their roles in coal dust-induced health and environmental problems." Reviews in mineralogy and geochemistry 64(1): 153-178.

ICRP (1994). "Human respiratory tract model for radiological protection." Ann. ICRP 24(1-3): 1-482.

Liu, T. and S. Liu (2020). "The impacts of coal dust on miners' health: A review." Environmental Research 190: 109849.

Manousakas, M., H. Papaefthymiou, K. Eleftheriadis and K. Katsanou (2014). "Determination of water-soluble and insoluble elements in PM2. 5 by ICP-MS." Science of the total environment 493: 694-700.

Naidoo, R., N. Seixas and T. Robin (2006). "Estimation of respirable dust exposure among coal miners in South Africa." J Occup Environ Hyg 3: 293-300.

National Academies (2018). "Monitoring and Sampling Approaches to Assess Undereground Coal Mine Dust Exposures." The National Academies Press The National Academies of Sciences, Engineering, Medicine.

Oberdorster, G., A. Maynard, K. Donaldson, V. Castranova, J. Fitzpatrick, K. Ausman, J. Carter, B. Karn, W. Kreyling, D. Lai, S. Olin, N. A. Monteiro-Riviere, D. B. Warheit and H. Yang (2005). "Principles for characterizing the potential human health effects from exposure to nanomaterials: elements of a screening strategy." Particle and Fibre Toxicology 2(8): 1-35.

Petsonk, E. L., C. Rose and R. Cohen (2013). "Coal mine dust lung disease. New lessons from an old exposure." American journal of respiratory and critical care medicine 187(11): 1178-1185.

Pinot, F., S. E. Kreps, M. Bachelet, P. Hainaut, M. Bakonyi and B. S. Polla (2000). "Cadmium in the environment: sources, mechanisms of biotoxicity, and biomarkers." Reviews on environmental health 15(3): 299-324.

Sambandam, B., E. Palanisami, R. Abbugounder, B. Prakhya and D. Thiyagarajan (2014). "Characterizations of coal fly ash nanoparticles and induced in vitro toxicity in cell lines." Journal of nanoparticle research 16: 1-9.

Sapko, M. J., K. L. Cashdollar and G. M. Green (2007). "Coal dust particle size survey of US mines." Journal of Loss Prevention in the Process Industries 20(4-6): 616-620.

Sun, Y., A. S. Kinsela, X. Cen, S. Sun, R. N. Collins, D. I. Cliff, Y. Wu and T. D. Waite (2022). "Impact of reactive iron in coal mine dust on oxidant generation and epithelial lung cell viability." Science of the Total Environment 810: 152277.

Tomb, T., R. Peluso, A. Gero and J. Seiler (1998). "Study to assess respirable dust exposures in underground U.S. coal mines." Appl Occup Environ Hyg 13(1): 62-72.

Wang, F., J. Liu and H. Zeng (2020). "Interactions of particulate matter and pulmonary surfactant: Implications for human health." Advances in colloid and interface science 284: 102244.

Yaroshevsky, A. (2006). "Abundances of chemical elements in the Earth's crust." Geochemistry International 44: 48-55.

Zhang, V., E. Nemeth and A. Kim (2019). "Iron in lung pathology." Pharmaceuticals 12(1): 30.

Zhao, Q., Y. Li, X. Chai, L. Zhang, L. Xu, J. Huang, P. Ning and S. Tian (2019). "Interaction of nano carbon particles and anthracene with pulmonary surfactant: The potential hazards of inhaled nanoparticles." Chemosphere 215: 746-752.

9.0 Appendices

N/A